

Review

Research progress and future perspectives on electromagnetic wave absorption of fibrous materials

Yuzhang Du,¹ Yichen Liu,¹ Aoao Wang,¹ and Jie Kong^{1,*}

SUMMARY

Electromagnetic waves have caused great harm to military safety, high-frequency electronic components, and precision instruments, and so forth, which urgently requires the development of lightweight, high-efficiency, broadband electromagnetic waves (EMW) absorbing materials for protection. As the basic fibrous materials, carbon fibers (CFs) and SiC fibers (SiC_f) have been widely applied in EMW absorption due to their intrinsic characteristics of low density, high mechanical properties, high conductivity, and dielectric loss mechanism. Nevertheless, it has remained a great challenge to develop lightweight EMW-absorbing fibrous materials with strong absorption capability and broad frequency range. In this review, the fundamental electromagnetic attenuation mechanisms are firstly introduced. Furthermore, the preparation, structure, morphology, and absorbing performance of CFs and SiC_f-based EMW absorbing composites are summarized. In addition, prospective research opportunities are highlighted toward the development of fibrous absorbing materials with the excellent absorption performance.

INTRODUCTION

Electromagnetic wave (EMW) within the gigahertz range is increasingly applied in the military field, wireless technology, high-frequency electronic components, communication instruments, and others. The needs of stealth performance for moving targets and constructions under radar detection, less interference for high precision wireless equipment, and health-care for people in daily life urgently require the development of highly effective microwave absorption (MA) materials.^{1–4} In the field of EMW absorption, material with the unique characteristics of thin thickness, light weight, wide bandwidth, and strong absorption is the goal always pursued by many scholars.^{5–7} For the MA materials, the traditional metals have inherent limitations such as impedance mismatching, large size, high density and lack of corrosion resistance, such as Fe, Co, Ni,⁸ and Fe₃O₄^{9–12} hinder their practical application. Recently, fibrous materials, e.g., carbon fibers^{13,14} and silicon carbide fibers^{15,16} have attracted extensive attentions and show a great potential in MA beneficial from light weight, high conductivity, good mechanical properties, as well as the structural featured with large specific surface area easy to compound with other materials.

Carbon fiber is a carbon-based fiber material, mainly made from raw materials such as polyacrylonitrile (PAN) fiber, viscose fiber, and pitch-based fiber. There are many ways to prepare carbon fiber. Generally, some carbon-containing organic fibers such as nylon, acrylic fiber, rayon, and other raw materials are used. The organic fibers and plastic resin are combined together and placed in a rare gas environment. After a certain time of pre-oxidation, carbonization, graphitization, and other strong thermal treatments, carbon fibers can be made under certain tension, temperature, and pressure conditions. Among traditional methods, carbonization and pyrolysis are mainly techniques for preparing carbon fibers.^{15–17} By taking advantages of their low specific mass, large specific surface area, high conductivity, good chemical stability and superior mechanical strength, CFs have attracted extensive attentions in the field of EMW absorption. In addition, relatively low price and ease of use make CFs as a promising candidate absorber compared with other carbon-based materials for this application. As we well-known that CFs have outstanding dielectric loss properties attributed from the electrical conductivity. Nevertheless, the contribution of fibrous structure to the magnetic loss is usually overlooked.^{18–20} Qi et al.²¹ demonstrated that the graphite defects can be introduced in CFs when the amorphous carbon or graphite carbon fiber carbonized in high temperature. They determined the type of graphite defects by the intensity ratio of the D and D' peaks in the Raman spectra, and analyzed detailedly the contribution of different defect types to electromagnetic wave absorption. Their work indicated CFs with predominantly boundary-type graphite defects have excellent EMW absorption. Although the magnetic loss mechanism induced by the graphite defects in CFs has been demonstrated, the dielectric loss is the main attenuation mechanism of CFs that is widely accepted. Good electrical conductivity is beneficial to dielectric loss, however, the high conductivity of carbon materials especially for CFs ($\sim 10^7$ S/m)²² causes the lower impedance matching between air and the surface of CFs, which results in a huge portion of reflection of the incident microwave and leads to poor EMW absorption performance.^{22,23} Therefore, combining CFs with

¹Shaanxi Key Laboratory of Macromolecular Science and Technology, School of Chemistry and Chemical Engineering, Northwestern Polytechnical University, Xi'an 710072, China

*Correspondence: kongjie@nwpu.edu.cn
<https://doi.org/10.1016/j.isci.2023.107873>



other dielectric loss and/or magnetic loss materials (e.g., CNTs, conductive polymers, transition metal oxides, ferrites, magnetic metals, and metallic alloys) to prepare CFs-based composites is considered as a promising approach for refining impedance matching and improving EMW absorbing properties.

Generally, graphene and carbon nanotube, as representative lightweight carbon-based absorbers, exhibit superior EMW absorption performance at room temperature due to the excellent dielectric loss. However, their poor oxidation and corrosion resistance are not suitable for practical applications at high temperatures and/or under harsh working conditions. Silicon carbide (SiC) is one of the representatives of wide band gap semiconductor and is regarded as an attractive candidate in the field of MA due to its designable dielectric properties combined with outstanding thermal stability, chemical stability, high tension strength, and low density.^{24–28} There are several methods to prepare silicon carbide fibers, including precursor conversion, chemical vapor deposition, ultrafine powder sintering, and activated carbon fiber conversion. Among these methods, precursor conversion is a commonly used method. The basic steps of precursor conversion including: synthesizing organic precursors containing silicon, carbon, oxygen, and other elements such as polycarbosilane and polysiloxane. The precursor is then fused and spun to obtain continuous organic fibers. Next, the organic fiber is pyrolyzed at high temperature in an inert atmosphere to gradually volatilize the oxygen atoms in the precursor molecules and form amorphous ceramic fibers containing carbon and silicon. Finally, the amorphous ceramic fibers are crystallized into silicon carbide fibers by high-temperature heat treatment in an inert or reducing atmosphere. This method has the advantage of producing high-strength, high-modulus, and high-temperature-resistant silicon carbide fibers that can be controlled by adjusting the composition and structure of the precursor.^{24,27}

Compared with bulk SiC and SiC particles, one-dimensional (1D) SiC materials including of fibers (SiC_f), nanowires, and whiskers with better EMW absorbing property has been demonstrated and developed.^{29–31} In addition, one-dimensional (1D) carbon and 1D silicon carbide fibrous materials have higher specific surface area, which can provide more surface reaction active sites for material modification. Flexibility and plasticity are others advantages for the better application in flexible electronic devices and wearable devices.^{16,20,26–29} However, low conductivity and single polarization (intrinsic electric dipolar polarization) of the intrinsic SiC prevents them from becoming an excellent absorber. So, the improvements of EMW absorbing performance of these 1D SiC materials are highly desirable, and much approaches such as introducing the multiple interfacial polarization and enhancing dielectric loss have been conducted in this respect. Among the efforts, compositing dielectric and/or magnetic loss materials with 1D SiC has attracted considerable attention in recent years.^{32–36} According to the energy dissipation mechanism, it is well known that EMW can be dissipated via eliminating the energy of electric or magnetic fields, high performance in EMW absorption can be achieved when the absorbing materials possess both of magnetic and dielectric loss mechanisms together. Consequently, the fabrication of CFs or SiC_f-based EMW absorbing composites that are decorated with dielectric and/or magnetic materials is an effective way to enhance the impedance matching and promote the EMW attenuation.

Based on energy dissipation mechanisms, EMW absorbing materials can be classified into dielectric loss and magnetic loss types. The conductivity and polarization originating from the defects, interfaces, and functional groups are the main reasons for the dielectric losses. For magnetic loss materials, the loss mechanisms are mainly based on eddy current loss, natural resonance, domain-wall resonance, and exchange resonance. Recently, EMW absorbing performance of magnetic materials has been summarized by Kong and co-workers.³⁷ EMW absorption performance of conductive polymers and carbon-based composites has been reviewed by different researchers.^{23,38–42} However, there is no comprehensive review article focusing on fibrous materials for EMW absorption applications in general. Therefore, this review highlights the recent progress of CFs and SiC_f-based EMW absorbing composites by evaluating their vital EMW absorption parameters. First, the fundamentals of MA are introduced, followed by the effects of chemical composition on the EMW absorbing performance and associated mechanisms. Also, the recent research progresses in EMW absorption performances concerning fibrous composites including of fiber/CNTs, fiber/conductive polymers, fiber/MXene, fiber/nonmagnetic oxides, fiber/Fe₃O₄, fiber/cobalt derivatives, and fiber/MOFs derivatives are summarized. The effect of components, structure, and morphology on the minimum reflection loss (RL_{min}) and effective absorption bandwidth (EAB) of the resultant composites are discussed in detail. Finally, the research direction of fibrous absorbing materials has been prospected.

FUNDAMENTALS OF EMW ABSORPTION

Microwave is a radiation with the interaction of the magnetic field (H) and an electric field (E) in the frequency range of 300 MHz–300 GHz. Maxwell's equations are undoubtedly the most basic and universal theory about the relationship between electric fields and magnetic fields, as well as the interaction law between magnetic/electric fields and absorbing materials using mathematical methods, but the complex interaction mechanisms make Maxwell's equations powerless.^{43–47} Therefore, scholars have developed many mathematical theories and methods for explaining the interaction between EMW and materials based on Maxwell's equations. At present, transmission line theory is a widely used analysis method with easy understanding, convenient calculation, and high precision characteristics.^{48,49} So, the evaluation of absorbing properties in this review is also based on transmission line theory.

Schematic in Figure 1A shows the interaction process when the EM wave propagates in space and reaches the surface of EMW absorbing materials based on transmission line theory, including reflection on the material surface, multiple reflection inside the material, absorption, and transmission. In order to achieve perfect EMW absorption, developers hope that EMW can be absorbed maximum and dissipated almost without reflection and transmission, which depends on the impedance matching between EMW in free space and EMW absorbing materials.^{50,51} If the impedance is mismatched, most of the incident EMW will be reflected on the surface of absorbing materials, even though they exhibit excellent absorption capabilities. Therefore, good impedance matching is the prerequisite for highly effective EMW absorbers.

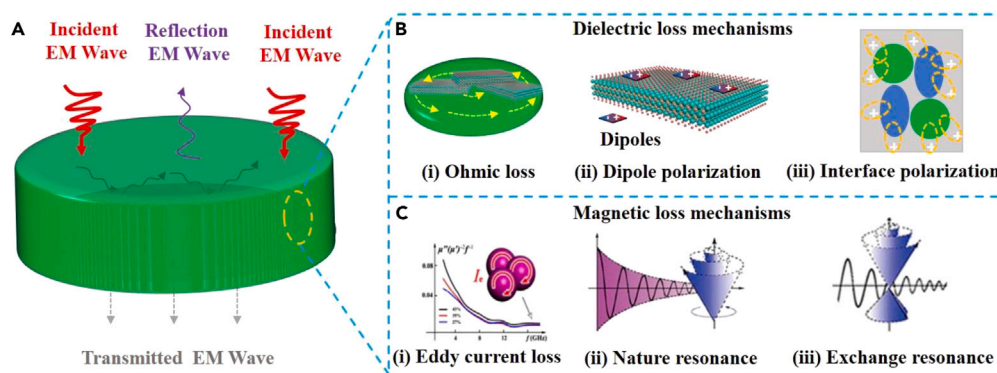


Figure 1. Schematic of the EMW absorption mechanisms

(A) The interaction relationship between EMW and EMW absorbing materials.

(B) Main types of dielectric loss including ohmic loss, dipole polarization, and interface polarization. Reproduced with permission from Kong et al.,⁵² Copyright 2022, ELSEVIER.

(C) Eddy current loss, nature resonance, and exchange resonance are the dominant factors for magnetic loss. Reproduced with permission from Cao et al.,⁵³ Copyright 2018, Springer.

Impedance matching

For EMW absorption, the EMW enters and interacts with the absorbing material, converting the electromagnetic energy into electrical energy, heat energy and mechanical energy. Therefore, the prerequisite for excellent absorption is that maximum EMW enters the material. However, when EM wave propagates through the air and meets the material, if the impedance of the absorbing material does not match that of the free space (or air), the EMW will reflect and transmits at the interface between the air and the material. So, the key to the absorption is the impedance matching between the absorbing material and the free space. The reflection coefficient (R) of the single-layer absorbing material meets the follows:

$$R = \frac{Z_0 - Z_{in}}{Z_0 + Z_{in}} \quad (\text{Equation 1})$$

$$Z_0 = \sqrt{\frac{\mu_0}{\epsilon_0}}, Z_{in} = \sqrt{\frac{\mu_r}{\epsilon_r}} \quad (\text{Equation 2})$$

$$\epsilon = \epsilon' - j\epsilon'', \mu = \mu' - j\mu'' \quad (\text{Equation 3})$$

Where Z_{in} stands the normalized input impedance of the absorber, Z_0 is impedance of free space. ϵ_r and μ_r are the relative complex permittivity and permeability, ϵ_0 (8.854×10^{-12} F/m) and μ_0 ($4\pi \times 10^{-7}$ H/m) are the permittivity and permeability constant of EMW in free space, respectively. ϵ' and μ' are the real part of permittivity and permeability, which represent the storage capability of electric and magnetic energy, respectively. ϵ'' and μ'' are the imaginary part of permittivity and permeability, which describe the energy dissipation capability of the materials during the interaction with EMW.⁵⁴⁻⁵⁶

When the impedance of absorbing material completely matches with that of the EM wave in free space, zero reflection on the surface can be achieved:

$$R = \frac{Z_0 - Z_{in}}{Z_0 + Z_{in}} = 0 \Rightarrow Z_0 - Z_{in} = 0 \Rightarrow \frac{\mu_0}{\epsilon_0} - \frac{\mu_r}{\epsilon_r} = 0 \quad (\text{Equation 4})$$

However, if the absorbing material with zero reflection on the surface, this characteristic is consistent with the feature of wave transmitting material, which is not conducive to strong the absorption efficiency of EMW absorbing material. Therefore, the values of impedance mismatch degree are close to zero ($|\Delta| < 0.4$) that is regarded as a good impedance matching as follows.

$$|\Delta| = |Z_0 - Z_{in}| = \left| \sqrt{\frac{\mu_0}{\epsilon_0}} - \sqrt{\frac{\mu_r}{\epsilon_r}} \right| < 0.4 \quad (\text{Equation 5})$$

Many scholars have deduced many mathematical theories and methods to describe the interaction between EMW and materials to improve the related quantitative calculation more precisely. Among the reported mathematical theories and methods, Steffensen acceleration method is the most widely recognized. When the energy loss is realized on the surface of the absorbing material, the reflection loss (RL) can be calculated according to Equations 6 and 7:⁵⁷⁻⁵⁹

$$RL(\text{dB}) = 20 \lg \left| \frac{Z_{\text{in}} - Z_0}{Z_{\text{in}} + Z_0} \right| \quad (\text{Equation 6})$$

$$Z_{\text{in}} = Z_0 \sqrt{\frac{\mu_r}{\epsilon_r}} \tanh \left[j \left(\frac{2\pi f d}{c} \right) \sqrt{\mu_r \epsilon_r} \right] \quad (\text{Equation 7})$$

Where f represents the frequency of the EMW, d is the thickness of the tested material, and c is the propagation velocity of EMW in vacuum condition. According to the above equations, based on the ϵ' and ϵ'' of complex permittivity, as well as μ' and μ'' of complex permeability, the reflection loss of materials to EMW can be calculated indirectly. Generally, a material with RL less than -10 dB can be regarded as qualified absorbing material, it can be considered that more than 90% of the EMW is absorbed, and the frequency range that meets this condition is called effective absorption bandwidth (EAB).^{36,60–62}

Electromagnetic wave attenuation mechanisms

As mentioned before, EMW consists of electric and magnetic fields, and EMW absorbing materials can be divided into dielectric loss and magnetic loss types. The absorbing capability of EMW absorbing materials can be understood by calculating attenuation constant (α) based on the evaluation of dielectric properties and magnetic properties of materials according to Equation 8.^{63–65}

$$\alpha = \frac{\sqrt{2\pi f}}{c} \sqrt{(\mu' \epsilon' - \mu'' \epsilon'') + \sqrt{(\mu' \epsilon' - \mu'' \epsilon'')^2 + (\mu' \epsilon'' + \mu'' \epsilon')^2}} \quad (\text{Equation 8})$$

Dielectric loss mechanisms

Dielectric loss is mainly determined by ohmic loss and polarization loss,^{66–68} and the polarization loss can be caused by electron polarization, ion polarization, dipole polarization, and interfacial polarization. In general, electron polarization and ion polarization can be easily excluded from microwave absorption because they usually occur in the higher frequency region of 10^3 – 10^6 GHz.⁶⁹ Therefore, the EMW loss mechanisms for dielectric loss materials are mainly attributed to dipole polarization, interfacial polarization, and conduction loss,⁵² as shown in Figure 1B. Dipolar or dipole polarization refers to the motion of a dipole in a polar or non-polar molecule under the changing electromagnetic field. For non-polar molecules, dipole polarization is also displacement polarization because this phenomenon is induced by the displacement of positive and negative charges owing to no intrinsic dipoles in the material. With respect to polar molecules, the rearrangement of intrinsic dipoles will occur under an external electromagnetic field, thus is also known as orientation polarization usually related to defects and residual groups of material. The dipoles reorient repeatedly depleting the EMW energy effectively. Due to the restriction of defects and residual groups, the dipoles cannot reorient timely in response to the high-frequency alternating electric field, and the polarization relaxation phenomenon appears. According to Debye's dipole relaxation theory, the relationship between ϵ' and ϵ'' can be described according to Equation 9.^{70–72}

$$\left(\epsilon' + \frac{\epsilon_s + \epsilon_\infty}{2} \right)^2 + (\epsilon'')^2 = \left(\frac{\epsilon_0 - \epsilon_\infty}{2} \right)^2 \quad (\text{Equation 9})$$

Where ϵ_s , ϵ_∞ represent the static permittivity and the relative dielectric permittivity at the high frequency limit, respectively. Interfacial polarization effect has been widely applied in absorbing materials to enhance their EMW attenuation capacity. The differences in dielectric characteristics and electrical conductivities of different components cause the accumulation and unevenly distribution of charges at the interface of two different materials, which generates a macroscopic electric moment. In the process of charge separation, the rearrangement of charges depletes the EMW energy effectively. The plot of $\epsilon' - \epsilon''$ is a single semicircle related to a Debye relaxation process, which is called the Cole–Cole semicircle. For EMW absorbing composites, multiple semicircles may be detected because more than one polarization mechanisms occur. However, for highly conductive materials, semicircles may not be observed because dielectric losses are dominated by conduction loss. Conduction loss is caused by the fact that the energy of EMW being converted into an electric current as it travels through absorbers. The instinctive resistance of absorber will produce Joule heat during the current transmission process, thus consuming the electromagnetic wave energy. Recently, dielectric loss mechanisms in EMW absorbing materials have been summarized detailly by Wu's group.⁷³

Magnetic loss mechanisms

For magnetic losses, the energy of EMW in the magnetic material is irreversibly converted into thermal energy during the magnetization and re-magnetization process. Generally, magnetic losses are mainly induced by domain wall resonance loss, hysteresis loss, eddy current loss, natural resonance, and exchange resonance loss. Among these mechanisms, the domain wall resonance loss usually occurs in the lower frequency range (1–100 MHz). Hysteresis loss consumes the energy by overcoming the coercive force during magnetization, and with increase of the coercive force of material the more energy will be consumed. However, the hysteresis loss mainly occurs in the strong electromagnetic field and can be ignored in the weak electromagnetic field. Therefore, eddy current loss and natural resonance are commonly regarded as two dominant factors that contribute to the magnetic loss (Figure 1C).⁵³ Eddy current loss is the result of Faraday's law, namely, electromotive force is induced by a changing magnetic flux in the coil of wire, so the generation of current called as eddy current in the conductor is the

way of energy attenuation under an altering magnetic field. The eddy current loss (C_0) is only related to the electrical conductivity (σ) and thickness (d) of the material, and their relation can be expressed as Equation 10.⁷⁴

$$C_0 = \mu'(\mu')^{-2}f^{-1} = \frac{2}{3}\pi\mu_0d^2\sigma \quad (\text{Equation 10})$$

According to Equation 10, C_0 should be a constant value in theory because the electrical conductivity (σ) and thickness (d) are the intrinsic parameters of the material. If the value of $\mu'(\mu')^{-2}f^{-1}$ keeps constant with the change of frequency, the eddy current loss is the only attenuation mechanism of magnetic loss. However, in many cases, the value of C_0 often changes, indicating that eddy current loss plays a minor role, while natural resonance and exchange resonance play a major role in magnetic loss.^{75,76} Moreover, Equation 10 suggests that eddy current loss could be significantly influenced by the size of material. When the thickness surpasses a critical value, the skin effect, caused by a strong eddy current, will degrade the internal magnetic field, and then reduce the relative complex permeability.^{77,78} Natural resonance is the result of shape anisotropy and magnetic crystal anisotropy, while exchange resonance is attributed to energy exchange between particles and surface anisotropy.⁷⁹ According to the natural resonance theory,⁸⁰ the natural resonance loss can be expressed by Equations 11 and 12.

$$f_r = \frac{\gamma}{2\pi}H_e \quad (\text{Equation 11})$$

$$H_e = \frac{4}{3} \frac{|k_1|}{\mu_0 M_s} \quad (\text{Equation 12})$$

Where f_r is the resonance frequency, $\frac{\gamma}{2\pi}$ represents the gyromagnetic ratio, H_e is the effective anisotropy field, k_1 is the magnetic crystalline anisotropy co-efficient for a magnetic material, M_s is the saturation magnetization. As the effective anisotropy enhanced by the small size effect and the confinement effect, decreasing the size of magnetic particles can regulate natural resonance in frequency range.⁸¹

ELECTROMAGNETIC WAVE-ABSORBING FIBROUS MATERIALS

Dielectric losses fibrous materials

Fiber/carbon nanotubes

Carbon nanotubes (CNTs), the most representative 1D nanoscale materials, can be divided into crystalline CNTs and amorphous CNTs (ACNTs) based on their crystalline structures. In the field of EMW absorption, many unique characteristics including light weight, high electrical conductivity, wide frequency bandwidth absorption, good compatibility, and excellent thermal conductivity make CNTs as an important candidate absorber.^{82–84} However, pure CNTs display an inferior EMW absorption ability because of their distinct impedance mismatch caused by the high dielectric constant.⁸⁵ So, numerous studies have focused on designing CNTs-based EMW absorbing composites with proper complex permittivity and moderate conductivity to match the required impedance for high-performance EMW absorption.^{86–88}

Although multiple methods and various matrix materials can be applied, the primary and efficient methods for the preparation of CNTs are the laser ablation^{89–91} and chemical vapor deposition (CVD),^{92–94} which requires expensive equipment and costs. By applying the induction heating method based on the CVD method, Xia et al.⁹⁵ fabricated light weight and excellent flexibility carbon nanotubes/carbon fibers (CNTs/CFs) composites, as shown in Figures 2A and 2B. Under low filling content (1%), the resultant CNTs/CFs composites exhibited excellent EMW absorbing performances characterized with strong absorption, thin absorption thickness, and wide absorption bandwidth. With increasing the mass ratio of ferrocene used as carbon source, the content of CNTs conductive network increases, the RL_{\min} value reaches -44.46 dB at 14.16 GHz with a fill ratio of 1% and a 3.0 mm matching thickness. The bandwidth of 7.44 GHz is ranging from 10.48 to 17.92 GHz, covering the entire X-band and quarter of the Ku-band. Furthermore, the EAB of samples with different thickness range of 0.5–6.0 mm is as high as 14.24 GHz. The EMW absorbing mechanisms analysis indicated that the dielectric loss is the main mechanism for the EMW dissipation, although the magnetic loss realized by the eddy current loss contributed slightly to the absorbing performance of the composite material (Figure 2C).

For EMW absorption, reflecting EMWs as little as possible in order to match the impedance matching and building rich polarization center to control the conductivity are essential for high-performance CNTs-based EMW absorbing materials. Microstructure design and composition control are generally considered as effective solution for achieving the above objects. Kong and co-workers⁹⁶ simulated the dense and regular hierarchical structure of pine branches and constructed CNTs/CFs composites with hierarchical architecture like to pine leaves in nanoscale, as shown in Figure 3. These reported CNTs/CF composites are composed of carbon nano fiber converted from bacterial cellulose (BC) and the amorphous CNTs *in situ* growth on its surface. Pine leaves-like hierarchical architecture not only improves interface polarization capability through hierarchical nano structure, but also has moderate conductivity attributed to the amorphous CNTs network, leading a well impedance mismatch. The RL_{\min} of CNTs/CFs composite with a CNTs content of 63.2 wt % and a thickness of 2.7 mm can reach -68.2 dB at frequency of 11.4 GHz, and the maximum EAB of CNTs/CFs composite is 5.4 GHz corresponding a thickness of 2.3 mm.

A single carbon material has a single absorption mechanism, and it is difficult to achieve the two requirements of impedance matching and strong EMW loss at the same time.^{97,98} Therefore, hybridizing fiber/CNTs with other dielectric and/or magnetic materials is a promising approach to significantly enhance their EMW absorption capacity. For instance, Qiu's group⁹⁹ designed and prepared Fe_3O_4 -CNTs-HPCFs

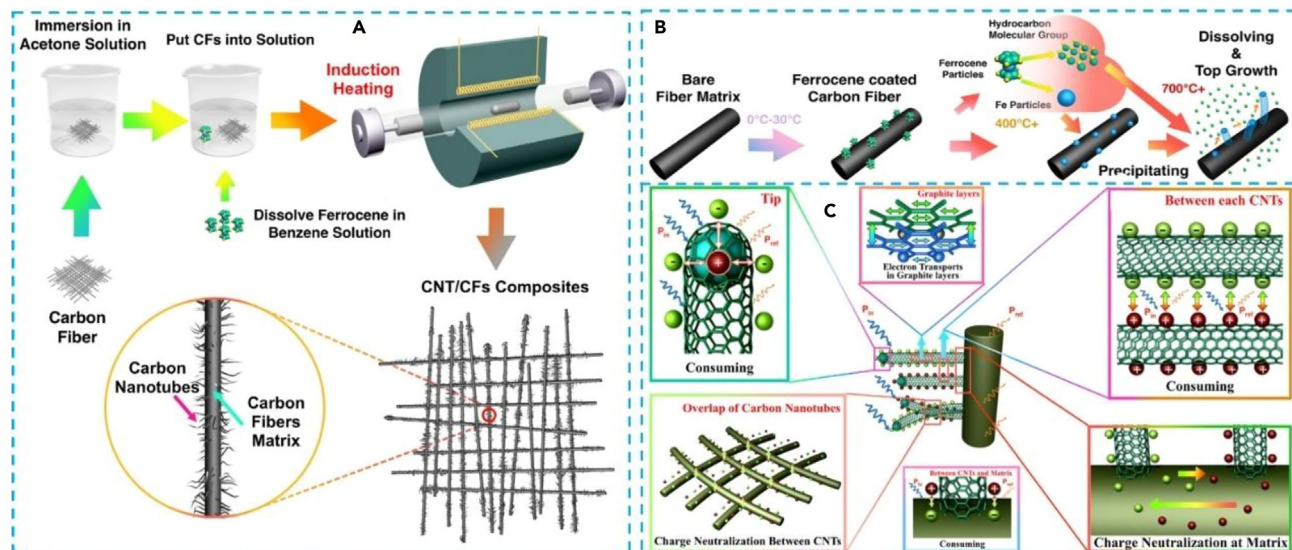


Figure 2. CNTs/CFs fibrous composites with excellent EMW absorbing performances

(A) Schematic illustration of the preparation process of the CNT/CFs composites.

(B) Schematic diagram of the growth mechanism of CNTs on the surface of CFs.

(C) The EMW absorption mechanisms the CNT/CFs composites. Reproduced with permission from Wen et al.,⁹⁵ Copyright 2021, ELSEVIER.

composites with “tree-like” structures by chemical vapor deposition technique and chemical reaction. The designed composites are composed of hollow porous carbon fibers (HPCFs) acting as “trunk”, carbon nanotubes (CNTs) as “branch” and magnetite (Fe_3O_4) nanoparticles playing the role of “fruit” structures. By taking advantages of porous structures of carbon fibers, dangling bonds of CNTs, the dielectric polarization arising from the defects and the synergetic interactions exist between Fe_3O_4 and CNTs–HPCFs, the prepared composites possessed outstanding EM wave absorbing performances. The bandwidth with a reflection loss less than -15 dB covers a wide frequency range from 10.2 to 18 GHz with the thickness of 1.5–3.0 mm, and the RL_{\min} is -50.9 dB at 14.03 GHz with a 2.5 mm thickness.

Taking advantages of the multiple interfacial polarization, constructing heterostructure with multiple components and abundant interface is an effective approach for improving attenuation coefficient and impedance matching of 1D SiC nanomaterial. Wang’s group¹⁰⁰ fabricated CNT/SiC_f composites by growing CNTs on the surface of SiC fibers based on an effective new method. In this new approach, ferrocene was utilized as both carbon source and catalyst to massively prepare the CNT/SiC_f composites, which is far more efficient than the traditional scheme, as shown in Figure 4A. CNTs with Fe particles on the tips form a unique conductive network with a mass of interfaces (Figures 4B–4D). On the one hand, the formation of conductive network is beneficial for electron transportation and conduction loss (Figure 4E), on the other hand, the interfaces between the inner walls of CNTs and Fe particles, as well as the defects in CNT walls easily generate dipoles resulting in the dipole polarization for an effective absorption of EM wave (Figures 4G and 4H). These factors together improve the impedance matching and EMW attenuation capability of CNT/SiC_f composites. The RL of paraffin composite at 4 mm with 20 wt % CNT/SiC_f filler loading reaches -62.5 dB. The broad effective absorption bandwidth is 8.8 GHz, which covers almost the entire Ku band and three-quarters X band (Figure 4I). Moreover, the EMW absorption performance can be easily tuned in a wide range by changing the mass ratio of ferrocene powder and SiC fibers.

In the past few years, biomass materials especially for biomass-derived carbon materials can be easily obtained by directly carbonization, which have been drawing increasing research attentions as low-cost sustainable raw materials for fabricating various lightweight and high performance EMW absorber.^{102–105} The natural morphology such as well-organized porous structure, hollow tube-like structure and hierarchical structure could be maintained in these biomass-derived carbon materials,^{106–108} which are very helpful for improving the EMW absorption ability and reducing composites weight. Meanwhile, defects and heteroatoms doping are easily introduced into natural structure during carbonization, leading to improve EMW dissipation capability by inducing abundant dipole polarization sites. Li and co-workers¹⁰¹ coated hierarchical hollow carbon fiber with Co/C particles and villus-like CNTs forming multicomponent composites (HCF@CZ-CNTs), as shown in Figures 4J–4L. In the preparation process, dodecahedron ZIF-67 particles were firstly grown on the surface of cotton fibers, and then cotton fibers carbonized, pyrolysis of ZIF-67 and *in situ* growth of CNTs were performed simultaneously. The resultant HCF@CZ-CNTs possesses ultra-lightweight (0.0198 g/cm³) and excellent EM wave absorption ability. RL_{\min} of -53.5 dB at 7.8 GHz with the thickness of 2.9 mm and EAB of 8.02 GHz at 2 mm are achieved (Figure 4M), which is significantly higher than pure carbonization cotton with RL_{\min} of -18.9 dB and bandwidth of 2.26 GHz. The hierarchical fibrous structure and the synergetic effect of polarization relaxation and magnetic loss contribute to the excellent broadband EMW absorption performance.

In summary, the reasonable incorporation of fiber with CNTs and other dielectric or magnetic components has proven to be an effective strategy for enhancing the EMW absorption capacity of fiber/CNTs fibrous absorbing materials. However, considering that the typical

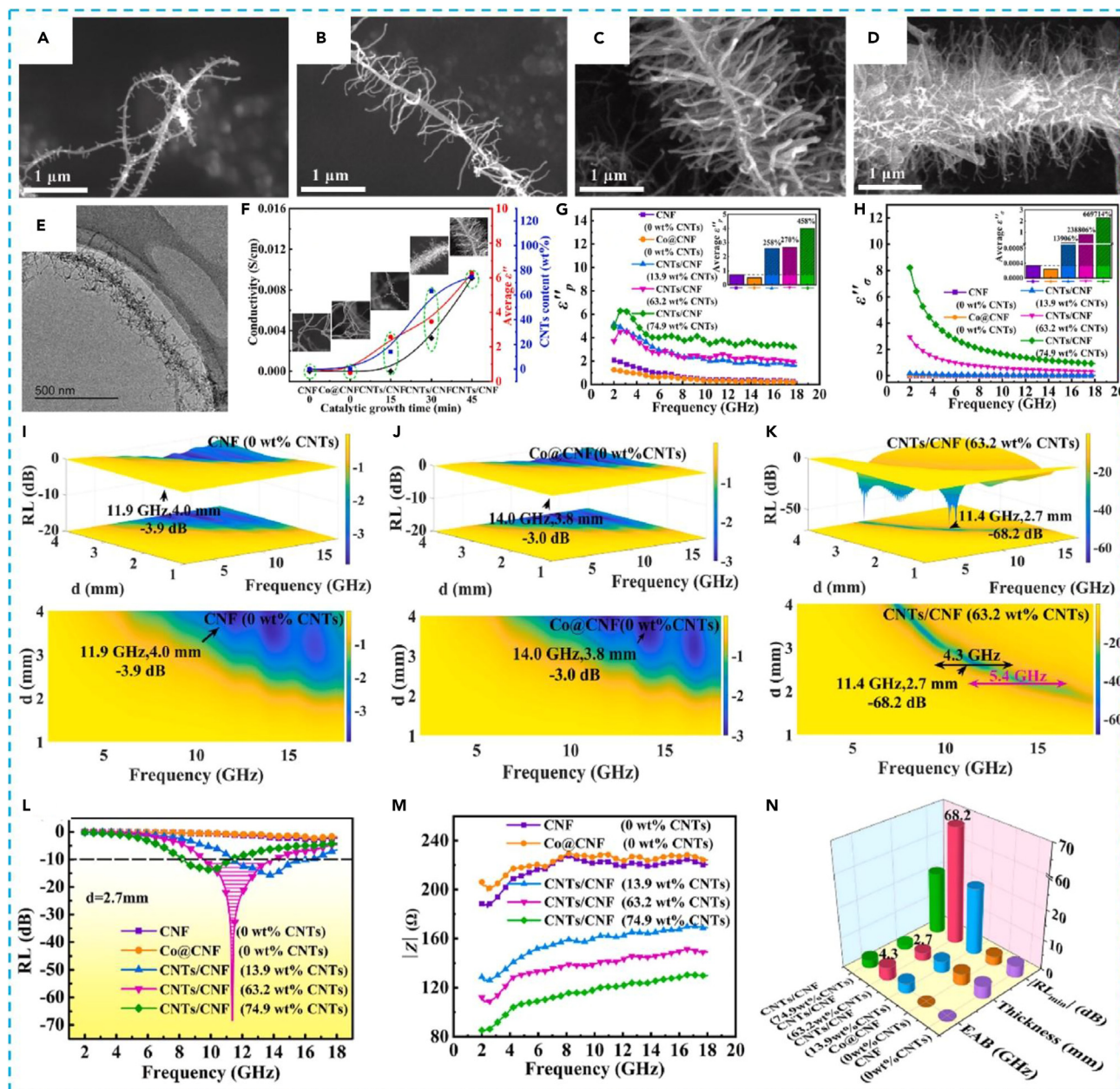


Figure 3. Hierarchical structured CNTs/CFs fibrous absorbing composites

(A–D) SEM images of CNTs/CNF obtained on different CNF matrix.

(E) TEM of CNTs/CNF-30 min.

(F–H) conductivity (F), polarization loss (G) and conductivity loss (H) of CNF, Co@CNF and CNTs/CNF with different CNTs content.

(I–K) Three-dimensional RL of CNF (I), Co@CNF (J) and CNTs/CNF (K) composite with 63.2 wt % of CNTs (20 wt % mass ratio with paraffin).

(L–N) RL of different samples with 2.7 mm (L), module of characteristic impedance of different samples (M), 3D histogram (N) for comparison of thickness, |RL_{min}| and EAB. Reproduced with permission from Huang et al.,⁹⁶ Copyright 2023, ELSEVIER.

synthesis methods for CNTs are chemical vapor deposition (CVD) and arc discharge, which require special equipment, the development of a relatively simple method for the fabrication of fiber/CNTs-based composites is greatly urgent but challenging.

Fiber/conductive polymers

As the most special class of polymer materials, conductive polymers (CPs), such as polyaniline (PANI),^{109,110} polypyrrole (PPy),^{111,112} and polythiophene (PTh), exhibit excellent potential for EMW absorption by tanking advantages of high conductivity, adjustable structure, low density,

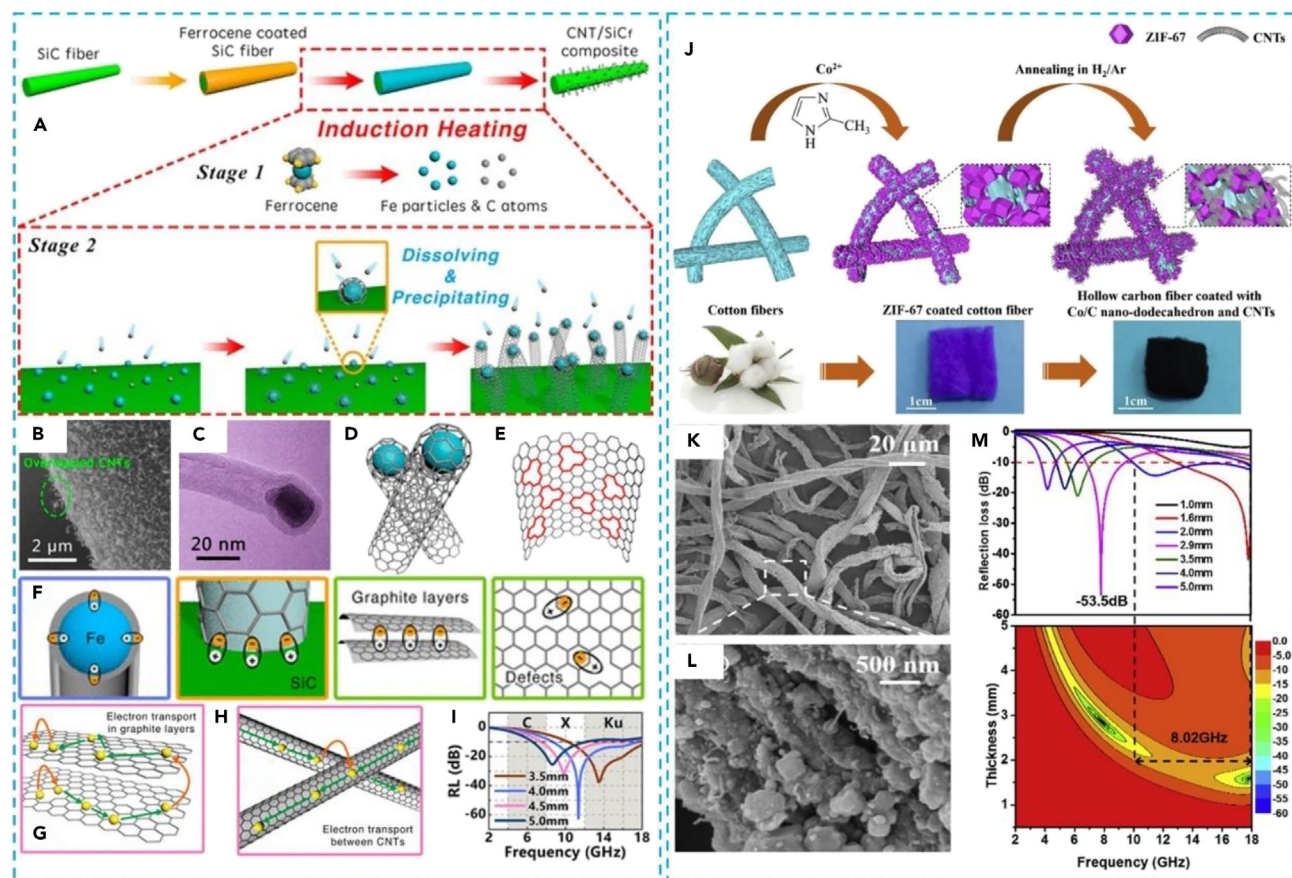


Figure 4. Multiple interfacial interactions enhanced EMW absorption properties

(A) Schematic diagram of the synthesis process of CNT/SiC_f composites by using ferrocene as both carbon source and catalyst. (B–C) SEM image (B) and TEM image (C) of CNT/SiC_f composite.

(D–E) Schematic diagrams of the overlapped CNTs (D) and the defects in graphite layer of the CNT wall (E).

(F–H) Schematic illustration of EM wave absorption mechanism for the CNT/SiC_f composite by the generation of dipoles (F) and the formation of conductive networks (G–H).

(I) RL of the 4 mm paraffin composite with 20 wt % CNT/SiC_f filler. Reproduced with permission from Wang et al.,¹⁰⁰ Copyright 2020, American Chemical Society.

(J) Schematic illustration of the synthesis procedure for HCF@CZ-CNTs composites.

(K–L) SEM images of HCF@CZ-CNTs.

(M) Reflection loss curves and the corresponding 2D contour plots of HCF@CZ-CNTs. Reproduced with permission from Li et al.,¹⁰¹ Copyright 2020, ELSEVIER.

and easy preparation.^{113,114} Among the known intrinsic CPs, the conductivity of CPs can be further improved from insulators, semiconductors to conductors through doping to meet the requirements of good conductivity. In addition, the π -conjugated chains of CPs have a delocalized electronic structure and endow extraordinary electronic performances of low ionization potential, high electron affinity, as well as energy optical transitions.^{115–117} On the other hand, the overall dielectric and/or magnetic loss capacity of fiber/CPs composites can be enhanced by introducing dielectric loss and/or magnetic loss components, which is also the focus of this review.

Polyaniline (PANI) is undoubtedly the most attractive conductive polymer as a potential candidate of absorbing materials because of their peculiar physical and chemical advantages of high conductivity, easy synthesis, and good environmental stability. In addition, employing PANI is not only expected to enhance the dielectric loss and impedance matching, but also to protect other dielectric loss and/or magnetic loss components from corrosion, and expand fiber/PANI-based composites application in harsh environments. The factors affecting the physicochemical properties of pure PANI and composites include the concentration of aniline monomer, reaction temperature and so on.^{118–120}

According to the EMW absorption mechanisms, fabrication of a novel composite composed of PANI, dielectric loss, and magnetic loss materials is expected to obtain better impedance matching and absorption performances than single components. Zhang's group¹²¹ prepared SiC_{NWS}@NiCo₂O₄@PANI one dimensional hierarchical nanocomposites through coating NiCo₂O₄ nanosheets and PANI as skin layer on the surface of SiC nanowires, as shown in Figures 5A and 5B. Due to the peculiar hierarchical microstructure, the incident EMW is firstly reflected by the networks constructed by adjacent SiC_{NWS}@NiCo₂O₄@PANI hierarchical nanocomposites and NiCo₂O₄ nanosheets. Besides, the synergistic effect of dielectric loss of the SiC nanowire, magnetic loss from the eddy loss and natural resonance of the NiCo₂O₄

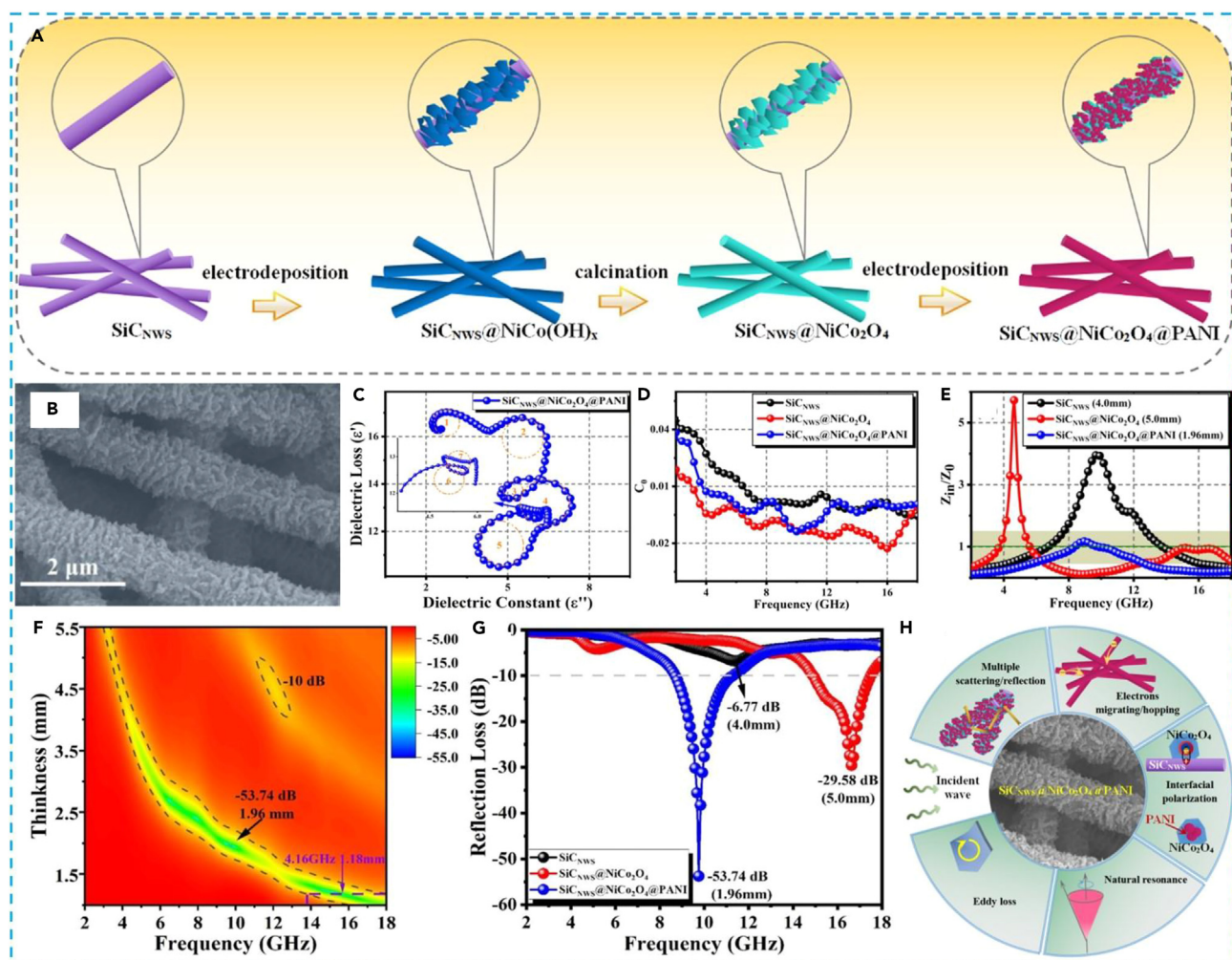


Figure 5. Hierarchical structured $\text{SiCNWS@NiCo}_2\text{O}_4\text{@PANI}$ composites

(A) Schematic illustration of the preparation process of $\text{SiCNWS@NiCo}_2\text{O}_4\text{@PANI}$ 1D hierarchical nanocomposites.

(B and C) SEM image (B) and Cole-Cole semicircles (C) of the resultant $\text{SiCNWS@NiCo}_2\text{O}_4\text{@PANI}$ hierarchical nanocomposites.

(D and E) C_0 curves (D) and impedance matching curves (E) of different samples.

(F and G) 2D RL plots (F) and the RL curves (G) of the samples at their optimum thickness. (H) Schematic illustration of the electromagnetic wave absorption mechanisms of $\text{SiCNWS@NiCo}_2\text{O}_4\text{@PANI}$ nanocomposites. Reproduced with permission from Zhang et al.,¹²¹ Copyright 2022, ELSEVIER.

nanosheets, as well as conductive loss of the PANI skin layer improve the impedance matching and EMW absorption performances (Figures 5C, 5D, and 5H). The RL_{\min} value of $\text{SiCNWS@NiCo}_2\text{O}_4\text{@PANI}$ composites with matching thickness of 1.96 mm achieves -53.74 dB, meanwhile, the EAB of 4.16 GHz corresponded ultra-thin matching thickness of 1.18 mm is obtained, as shown in Figures 5F and 5G.

Generally, a synergistic attenuation mechanism based on multiple reflection/scattering, dipole polarization, interface polarization, eddy current and magnetic resonance is usually a reasonable way for improving EMW absorption performances. Meng and co-workers¹²⁰ reported a $\text{CFs@PANI@Fe}_3\text{O}_4$ hybrid nanocomposites composed of CFs core, PANI coating and dispersed Fe_3O_4 nanoparticles. Compared with bare CFs, the systematic characterization results indicated that both PANI lay and Fe_3O_4 played positive roles in enhancing the microwave absorption properties. The resultant $\text{CFs@PANI@Fe}_3\text{O}_4$ hybrid nanocomposites exhibit remarkable microwave absorption performances owing to the combined action of CFs, PANI, and Fe_3O_4 . Its RL_{\min} value of -46.86 dB is achieved under 10 wt % filler content, and the matching thickness is 2.7 mm.

PANI can be widely used as an effective component of EMW absorbers owing to the extremely simple preparation method. In contrast, polypyrrole (PPy) is considered the other attractive candidate for EMW absorbers due to its simple synthesis, good conductivity, and stable chemical properties.¹²² In addition, the higher mass density could provide higher performance to the absorber with a smaller volume of PPy, and the better flexibility is beneficial for forming different forms easily, such as fibrous, tubular, and spherical structure. However, conductivity, thermal stability, and morphology of PPy, the key factors for excellent fiber/PPy-based absorber, are mainly affected by the polymerization methods and polymerization conditions.¹²³ In addition to the intrinsic characteristics of pure PPy and fibers, choosing the reasonable

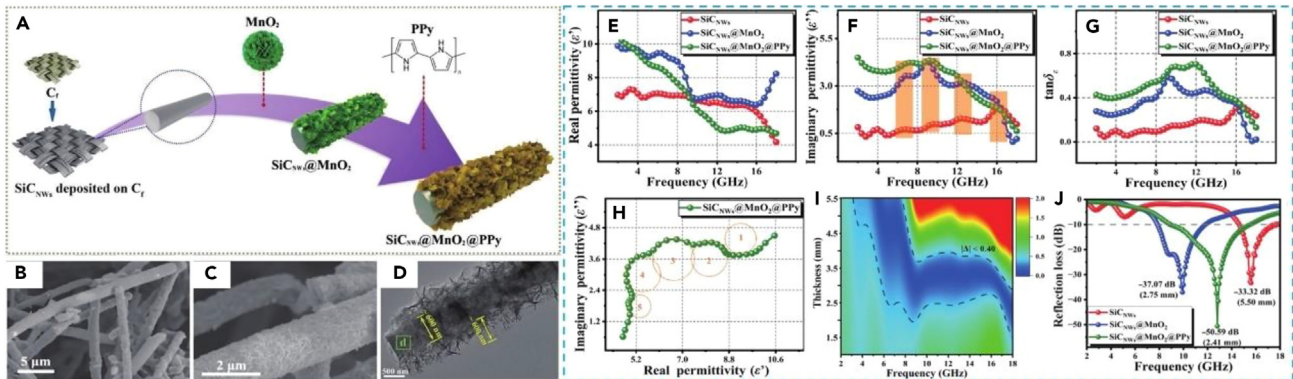


Figure 6. Core-shell structured $\text{SiC}_{\text{nws}}@MnO_2@PPy$ nanocomposites

(A) Schematic illustration of the synthesis process of $\text{SiC}_{\text{nws}}@MnO_2@PPy$ nanocomposite. (B–D) SEM images (B–C) and TEM image (D) of $\text{SiC}_{\text{nws}}@MnO_2@PPy$ nanocomposite. (E–G) The real part (E) and imaginary part (F) of the complex permittivity and the dielectric loss tangent (G) of various samples. (H–I) Cole-Cole semicircle (H) and impedance matching (I) of $\text{SiC}_{\text{nws}}@MnO_2@PPy$ nanocomposite. (J) The minimum RL values of various samples at their optical thickness. Reproduced with permission from Li et al.,¹²⁵ Copyright 2023, Springer.

components of the desirable composites is an important for refining impedance matching characteristic and excellent absorption performances. In order to get optimal impedance matching, the ideal relation between real (ϵ') and imaginary (ϵ'') parts of permittivity should be established for dielectric loss absorbing materials, which can provide reliable reference for the fabrication of high-efficiency microwave absorbing materials. Based on Material Genome Initiatives, Meng et al.¹²⁴ selected PPy and cotton non-woven fabrics (CNFs) as dielectric medium and flexible matrix, respectively, and introduced polydimethylsiloxane (PDMS) to balance the impedance matching of the produced PPy/CNFs/PDMS composites. Under the guidance of ideal $\epsilon'-\epsilon''$ relationship, the designed PPy/CNFs/PDMS composite with good impedance matching possesses outstanding absorption performance. The RL_{min} reaches -25 dB at the thickness of 4 mm and the EAB covers the whole X-band. What's more, the RL of PPy/CNFs/PDMS composite measured by arched reflecting method is consistent with the simulation result by the waveguide method.

To improve EMW absorbing property of 1D SiC-based material by enhancing impedance matching, conductive loss and interfacial polarization, Li and co-workers¹²⁵ prepared core-shell $\text{SiC}_{\text{nws}}@MnO_2@PPy$ nanocomposites by coating dielectric MnO_2 nanosheets and conductive PPy polymer on the surface of SiC nanowires (SiC_{nws}) core through chemical vapor deposition and two-step electrodeposition process, as shown Figure 6A. Introducing MnO_2 nanosheets and PPy coating results in more interfacial polarization and relaxation phenomenon generation induced by the heterogeneous interfaces between SiC nanowires, MnO_2 nanosheets, and PPy (Figures 6B–6D), which is beneficial to improve electromagnetic parameters. Therefore, the values of ϵ' , ϵ'' and $\tan\delta_e$ of $\text{SiC}_{\text{nws}}@MnO_2@PPy$ nanocomposites are higher comparing with that of SiC_{nws} and $\text{SiC}_{\text{nws}}@MnO_2$ samples (Figures 6E–6H). Besides, the $\text{SiC}_{\text{nws}}@MnO_2@PPy$ nanocomposites exhibits good impedance matching with a larger practicable area of $|\Delta| < 0.4$ (Figure 6I). By combining the synergistic effect of peculiar network structure, the intrinsic dielectric loss of various components, multiple interfacial polarization and dipole polarization, the resultant $\text{SiC}_{\text{nws}}@MnO_2@PPy$ nanocomposites displays excellent electromagnetic wave absorption performances with RL_{min} of -50.59 dB when the matching thickness of 2.41 mm, and the EAB value reaches to 6.64 GHz covering almost the entire X band and half of the Ku band at a matching thickness of 2.46 mm, as shown in Figure 6J.

As discussion above, there are mainly two ways to improve the EMW absorbing performance of fiber/CPs composites. One is focusing on the refinement of the conductivity, structure, and surface morphology of pure fiber or CPs. The other is the fabrication of composites by combining fiber/CPs with other dielectric loss materials such as graphene,^{126–131} carbon nanotubes^{132–137} and others, as well as the magnetic materials, e.g., ferrite,^{138–140} magnetic nanoparticles. The aim of these approaches is to enhance the impedance matching and EMW absorption performances by taking advantages of the synergistic effects on the dissipation of the EMW energy. However, the issues of easy oxidation and stability especially in high temperature should be concerned. Due to the length and theme, it cannot be described in detail in this review. Readers in need can refer to the relevant review and literature.^{141,142}

Fiber/MXenes

MXenes, a new and fast-growing family of two-dimensional (2D) carbides and nitrides of transition metals materials with graphene-like structure, were firstly synthesized by Naguib et al. in 2011.¹³⁴ They normally possess a formula of $M_{n+1}X_nT_x$, where M represents an early transition metal, X is the carbide and/or nitride, T refers to the terminating groups on MXenes surface such as O, OH, F and/or Cl resulted from the etching process.^{143–145} Due to the greater absorption advantages attributed to the characterizations including of high specific surface area, efficient dielectric loss from multiple polarization mechanism, and enhanced interfacial loss from unique 2D nanostructures, multilayered and/or delaminated MXenes have been extensively used in EMW absorption.

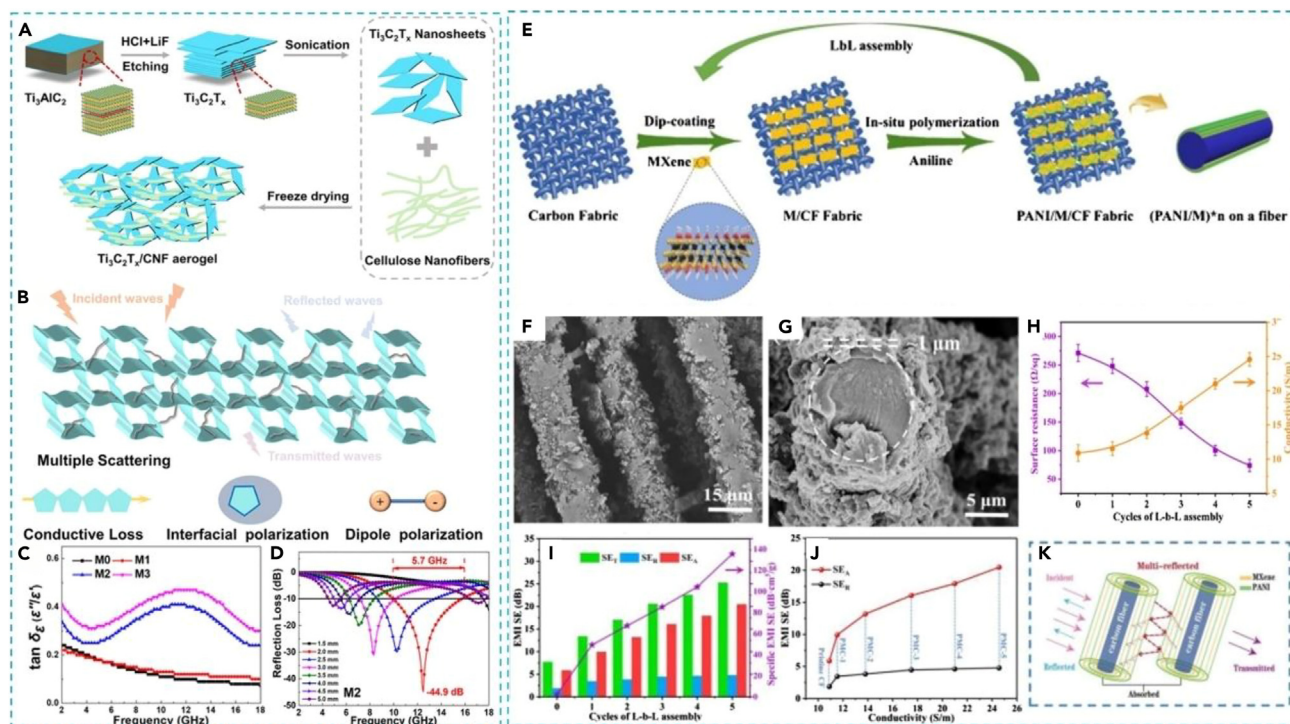


Figure 7. Fiber/MXenes absorbing composites

(A) Schematic drawing illustrating the fabrication of the $Ti_3C_2T_x/CNF$ composites.
 (B) Schematic illustration showing the mechanisms involved during the EMW absorption for the $Ti_3C_2T_x/CNF$ composites.
 (C and D) dielectric loss tangent (C) and RL (D) of $Ti_3C_2T_x/CNF$ composites with various $Ti_3C_2T_x$ mass ratios of 0, 25.0, 50.0, and 75.0 wt %, respectively. Reproduced with permission from Wu et al.,¹⁵⁰ Copyright 2022, American Chemical Society.
 (E) The schematic illustration for the manufacturing process of PANI/MXene/CF fabric via layer-by-layer (L-b-L) assembly.
 (F–G) SEM images of PANI/MXene/CF fabric after five-cycle L-b-L assembly.
 (H) The surface resistance and electrical conductivity of various samples.
 (I and J) The average values of SE_T , SE_A , SE_R and specific EMI SE values (I) and SE_A and SE_R versus the electrical conductivity (J) for PANI/MXene/CF fabrics.
 (K) Schematic drawing illustrating the shielding mechanism of PANI/MXene/CF fabric. Reproduced with permission from Yu et al.,¹⁵¹ Copyright 2020, ELSEVIER.

Fibrous absorbing composites are usually prepared by electrospinning the mixture of polymer with dielectric and/or magnetic loss materials. However, the addition of dielectric and/or magnetic loss materials will significantly influence the viscosity, electrical conductivity, stability of solution, as well as the elastic moduli, coefficients of thermal expansion, crystallization of polymer matrices, which finally determines the structure, morphology, and performance of the as-prepared fibrous absorbing composites.^{146–148} Schauer and co-workers¹⁴⁹ electrospun poly(acrylic acid) (PAA), polyethylene oxide (PEO), poly(vinyl alcohol) (PVA), and alginate/PEO with delaminated $Ti_3C_2T_x$ MXene flakes. They investigated the effect of small additions of delaminated MXene (1% w/w) on the structure and properties of the nanofibers. The results indicated that MXene has an effect on the solution properties and a greater effect on the average fiber diameter. The $Ti_3C_2T_x/PEO$ solution exhibits the largest change in viscosity and conductivity with an 11% and 73.6% increase over the initial polymer, respectively. A high degree of crystallization for $Ti_3C_2T_x/PEO$ and a slight decrease in crystallinity for $Ti_3C_2T_x/PVA$ were observed.

Combining MXene with conductive fibrous materials is an effective approach to construct conductive network and improve interface interactions for enhancing EMW absorption based on conductive loss and interfacial polarization. Wu et al.¹⁵⁰ fabricated flexible MXene/cellulose nanofibers ($Ti_3C_2T_x/CFs$) composites via selective etching and freeze-drying, as shown in Figure 7A. The addition of appropriate content of MXene formed a continuous network providing numerous conductive pathways for enhanced electron migration, which effectively regulates the dielectric constant and impedance matching, as well as enhances conductive loss. Besides, polarization relaxation including interfacial and dipole polarization between MXene and CFs also has a synergistic effect on EM wave dissipation (Figures 7B and 7C). Among these produced composites, the sample with 50.0 wt % MXene addition has optimal absorption with RL_{min} of -44.9 dB and EAB of 5.7 GHz at a thickness of 2.0 mm (Figure 7D). Importantly, compared with the performance at the natural state, after 50 cycles of bending deformation, the absorption property can be maintained due to the stress dilution by the resilient porous structure and interlayer slipping owing to the existence of $Ti_3C_2T_x$ nanosheets.

A thick coating is necessary on textile surface to shield forceful penetration of electromagnetic interference (EMI) waves, limiting their practical applications owing to the defective air permeability and flexibility. Therefore, how to achieve effective EMI shielding performance while retaining the inherent characteristics of textile substrate remains a daunting technical challenge. Yu and co-workers¹⁵¹ fabricated a

lightweight, wearable, and durable PANI/MXene/CFs fabric with exceptional electromagnetic interference shielding performance via layer-by-layer (L-b-L) assembly approach (Figure 7E). Morphologic observation exhibits the CFs is coated by PANI/MXene rough layers with a large number of particles, which made some of the narrow voids filled and construct more perfect conducting networks between interconnecting the adjacent fibers (Figures 7F and 7G). The excellent electrical conductivity higher than 1 S/m is beneficial to the highly efficient EMI shielding, a high EMI shielding effectiveness (26.0 dB) and favorable specific EMI SE ($135.5 \text{ dB cm}^3/\text{g}$) of the PANI/MXene/CF fabric with only 0.55 mm thickness can be achieved after five-cycle L-b-L assembly (Figures 7H–7K). The PANI/MXene interfaces facilitates the internal multiple reflections and interfacial polarization and attenuated EMW conductivity loss and dielectric loss.

In terms of morphology, MXene-based microwave absorbing materials are mainly two-dimensional (2D) nanosheets directly obtained after exfoliation. Spherical and 3D sponge-like MXene assemblies for microwave absorption are less reported. However, wrinkled porous microspheres have been proved to exhibit excellent microwave absorption ability due to its special surface structure.^{152,153} In order to combine the dual advantages that 1D materials form a conductive network giving dielectric loss and surface wrinkled microspheres cause multiple reflection. Zhang et al.¹⁵⁴ fabricated two kinds of MXene-based materials. One is the 1D MXene@Fe₃O₄ magnetic nanofibers with a diameter of 25 nm obtained by the self-assembly of single-layer Ti₃C₂T_x MXene nanosheets and coating Fe₃O₄ nanoparticles via thermal decomposition method. The other is the micro-scale surface wrinkled porous MXene@Fe₃O₄ composite microspheres. By blending microspheres and nanofibers with the optimal ratio of 7:3, the resultant composite shows high efficiency microwave absorbing performance. The RL_{min} of −63.3 dB and EAB of 5.2 GHz (12.8–18 GHz) are achieved at a filler content of 40% corresponding to thickness of 1.8 mm.

In summary, due to its unique physical and chemical properties, MXenes has demonstrated its enormous potential in field of microwave absorption. However, to achieve the goal of the practical application of MXene materials in the MA some problems still need to be overcome. The first one is the development of high-yield, low-cost and environmentally friendly methods for preparing high-quality MXene products. Then, the surface modification and structure construction of MXene materials with specific surface terminations should be paid more attentions. Furthermore, the understanding of the role of MXene in MA is still immature.

Fiber/nonmagnetic oxides

Zinc oxide (ZnO), as an important semiconductor material ($E_g = 3.37 \text{ eV}$), is considered as a potential EMW absorbing material due to lightweight, low cost, facile preparation and environment friendly.^{155–158} The dipole polarization and dipole moment along the polarity direction in ZnO nanocrystals are the mechanisms for EMW absorption. The interfacial polarization derived from the newly formed heterogeneous interfaces caused by the introduction of ZnO nanocrystals would also improve microwave absorption.¹⁵⁹ In addition, geometrical effect and less eddy current loss can be realized due to the formation of 3D crosslinked network of ZnO nanocrystals.^{18,160,161} Qi and co-workers¹⁶² designed and fabricated the CFs/ZnO composites with unique 3D cross-linked network based on the strategy of constructing the heterostructure interfaces, as shown in Figures 8A–8E. Results indicate that the carbonization temperature has significant influence on the absorption performances of the produced CFs/ZnO nanofiber composites, and the composites carbonized at 700°C have strong EMW absorbing properties derived from the synergy of the interface polarization, geometrical effect and the less eddy current loss. The RL_{min} of −61.91 dB at 11.44 GHz is achieved under the corresponding thickness of 2.59 mm, meanwhile, the EAB is as wide as 5.60 GHz and covers almost Ku bands (Figures 8F and 8G).

As is well known, pure CFs suffer from poor interfacial impedance matching and weak microwave absorption performance attributed to the limitations of improper electrical conductivity and extremely high complex permittivity. Forming coaxial multilayer coatings on CFs with a well-controlled, gradually increasing conductivity leading to well-matched input impedance is expected as an effective approach to improve absorption properties of CFs-based absorbers. ZnO can be doped and deposited forming a doped ZnO coating on CFs to match the impedance matching by the atomic layer deposition (ALD) method, which is the other advantage compared with nonmagnetic oxides. Qin's term¹⁶³ coated CFs using Al-doped ZnO with specifically designed gradient multilayer through ALD method to gradually increase electric conductivity. The gradient coatings composed of five layers of dielectric films serve as intermediate layers to adjust the impedance matching of CFs (Figure 8H). For all the above reasons, the obtained composites exhibit remarkably enhanced microwave absorption performance, and the RL_{min} reaches −58.5 dB at 16.2 GHz with the gradient films of rationally selected thicknesses of only 1.8 mm (Figures 8I and 8J). This reported strategy can be applied to improve the absorption properties of the dielectric loss materials by improving the impedance matching.

Similarly, TiO₂ as a semiconductor has been extensively investigated in photocatalysis, supercapacitor, biomedicine, seawater desalination and other fields owing to its chemical and thermal stability.^{164–167} For EMW absorption, benefiting from the relatively smaller real part of its permittivity value ($\epsilon' = 8$) and dipolar relaxation polarization, TiO₂ can be used as an additive phase to improve the impedance matching of the absorber and to enhance the dielectric loss of a microwave absorber. For instance, Wu's group reported¹⁶⁸ a broccoli-like composite (CFs@TiO₂) composed of short carbon fibers and TiO₂, where TiO₂ was grown vertically on the surface of short carbon fibers forming an independent broccoli-like conductive network. The unique structure is beneficial to improved impedance matching, the conduction loss, as well as strong interfacial polarization, leading to enhanced EM wave absorption capability. Besides, the eddy current loss is also found caused by the ring current produced in the conductive network, resulting in the magnetic loss mechanism. The RL_{min} of −58.63 dB at 4.56 GHz is achieved, and EAB of 3.4 GHz can be obtained even if at the ultra-thin thickness of 1.1 mm. The flower-like heterostructure is good for impedance matching, interfacial polarization, dipole polarization, conductance loss, and multi relaxation that had been demonstrated by Tang and co-workers.¹⁶⁹ The wave absorbing performance of the produced flower branch-like TiO₂@SiC/C composite nanofibers is achieved in the X and Ku bands, and the RL_{min} reaches −45.3 dB with the thickness of less than 3 mm when the composite nanofibers absorber content is 10 wt %.

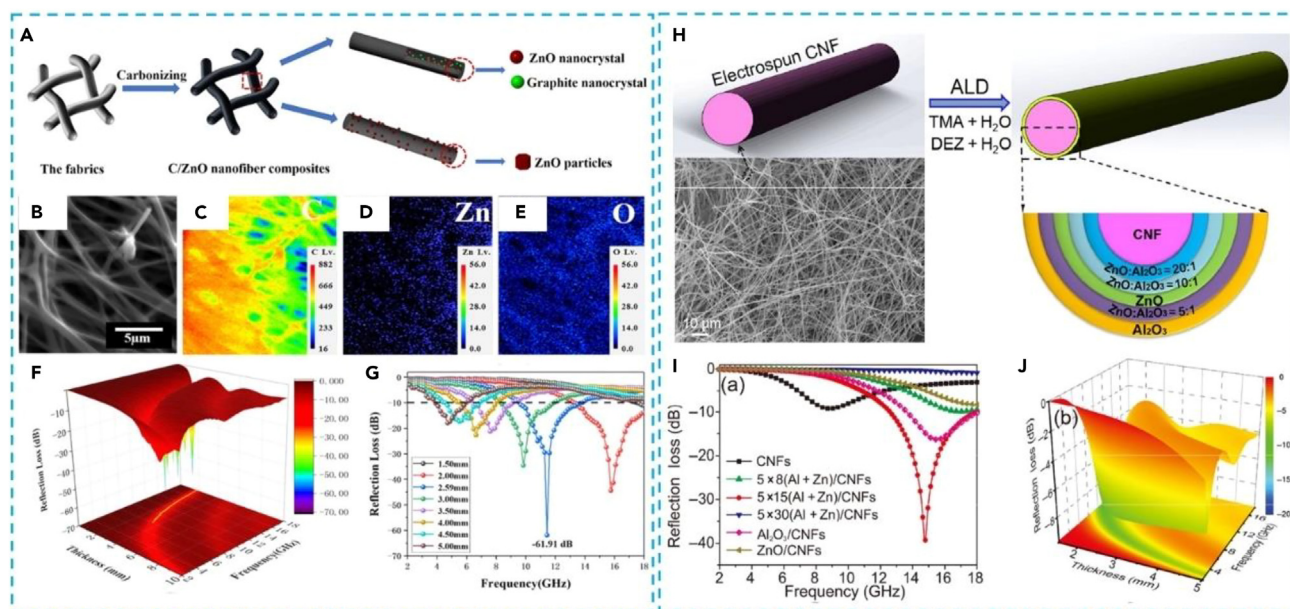


Figure 8. Fiber/nonmagnetic oxides absorbing composites

(A) The schematic illustration for the synthesis processes of the CFs/ZnO nanofiber composites.

(B) Field emission electron probe image of the CFs/ZnO nanofiber composites carbonized at 700°C.

(C–E) C, Zn, and O mapping, respectively.

(F and G) The 3D plots of RL values (F) and RL curves (G) of the CFs/ZnO nanofiber composites carbonized at 700°C. Reproduced with permission from Qi et al.,¹⁶² Copyright 2021, ELSEVIER.

(H) Schematic of the synthesis process of the gradient films/CFs via ALD.

(I) RL curves of the CFs and coated CFs with an absorbent layer thickness of 1.9 mm in the frequency range of 2–18 GHz.

(J) Three-dimensional representations of the RL curves of the coated CFs. Reproduced with permission from Qin et al.,¹⁶³ Copyright 2018, Springer.

In a word, the CFs/ZnO or CFs/TiO₂ composites with controllable size, unique morphology, and formula designability can be easily prepared by simple electrospinning technology and one-pot hydrothermal method. Besides, the raw materials are environment friendly without pollution, green, and low cost. Therefore, hybridizing CFs/ZnO or CFs/TiO₂ with other magnetic loss-based materials is a promising strategy for preparing EMW absorbers with excellent characteristics.

Combined dielectric and magnetic losses fibrous materials

Fiber/Fe₃O₄

In terms of the EMW absorbing materials, Fe₃O₄ as a traditional magnetic metal oxide has attained a special attention due to its excellent magnetic and dielectric properties,^{170,171} but in some cases, brittleness, heavy weight (about 5.18 g/cm³), and narrow bandwidth¹⁷² of a pure Fe₃O₄ significantly limit its usage as an EMW absorber.¹⁷³ Therefore, Fe₃O₄ is often used as a magnetic loss material to prepare EMW absorbing composites with carbon-based materials, such as CFs.

Generally, the temperature of Fe₃O₄ layer coating and CFs pretreatment significantly influence the compositions and morphology of the resultant CFs/Fe₃O₄ composites, leading to a great difference in EMW absorbing performances. Osouli-Bostanabad et al.¹⁷³ investigated the influence of temperature on the structure, morphology, magnetic and microwave absorption properties of the prepared composites via a multi-step cathodic method in an aqueous alkaline solution at 60°C–80°C. They found that a more homogeneous and denser Fe₃O₄ coating could be obtained by using multi-step electro-deposition method rather than the single step method, which improves the EMW absorption properties (Figures 9A–9D). The RL of the three steps coated carbon fibers (MCCFs-III) is found to be under –5 dB in the whole range of X-band. In addition, a porous flake-like layer of Fe₃O₄ can be formed uniformly under the reduction of Fe(III)–Triethanolamine complex at 60°C. While, a dense and discontinuous layer with globular nano-particles deposited on the surface of CFs when the temperature increased to 80°C, and the optimum deposition time was demonstrated by the RL of –10 dB at 12.27 GHz occurred in sample deposited for 4 min, as shown in Figures 9E and 9F. Similar work was reported by Luo and co-workers.¹⁷⁴ They also found that temperature and fiber surface pretreatment had a significant influence on the composition and morphology of Fe₃O₄ coating. Uniform and compact Fe₃O₄ layer could be prepared at 75°C, while the coating is continuous and rough when the reaction was taken at 60°C. The CFs/Fe₃O₄ composites prepared at 75°C exhibits a good absorption property with RL of lower –20 dB in wide matching thickness ranges.

Although compositing CFs with Fe₃O₄ is an attractive way in preparing EMW absorbing materials with excellent performances, the high reductivity of CFs easily reduce Fe₃O₄ to Fe₃C resulting in the increased degree of graphitization of CFs, which enhances the conductivity and

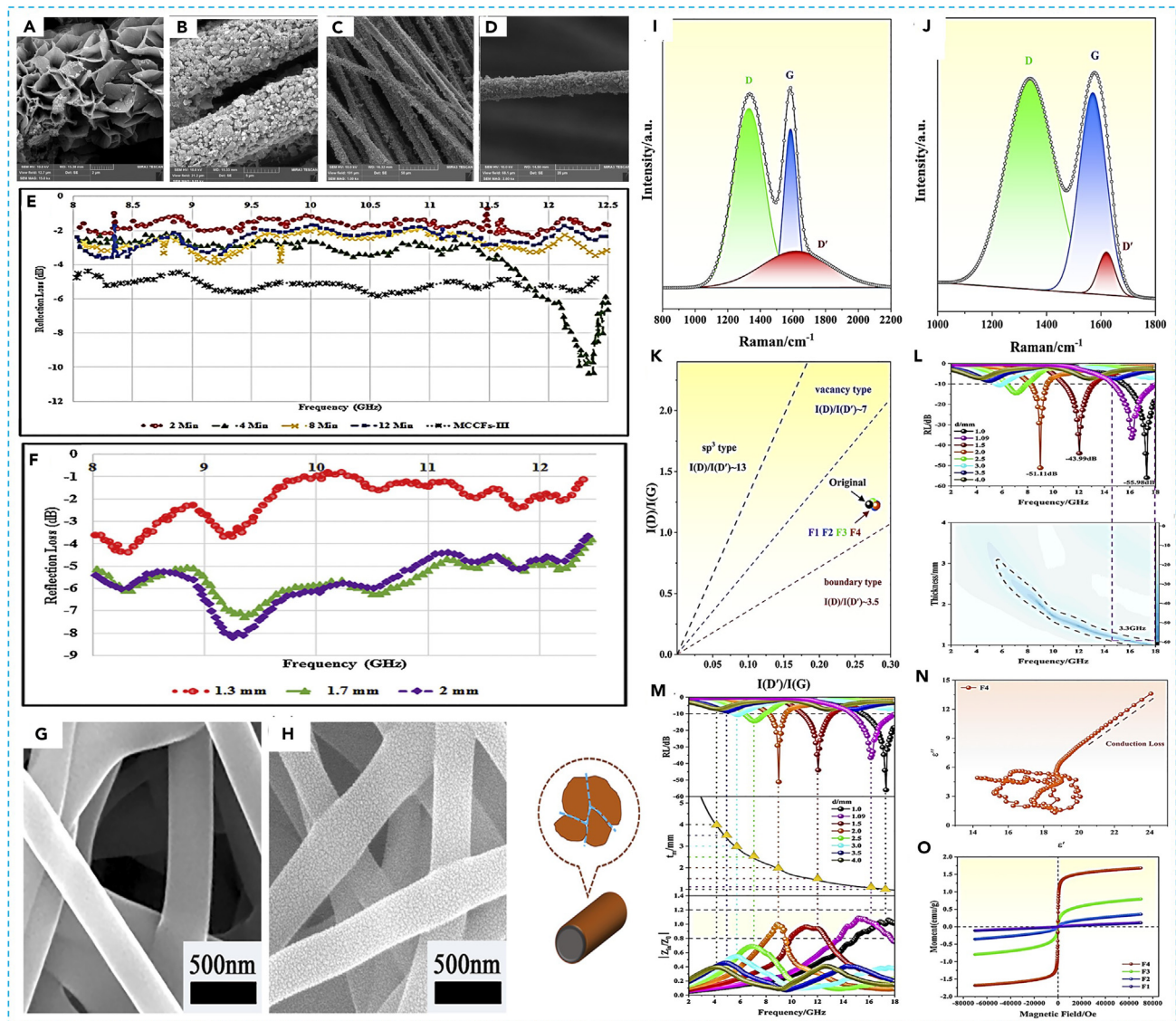


Figure 9. CFs/Fe₃O₄ absorbing composites

(A–D) SEM images of the Fe₃O₄ layer deposited on the surface of CFs at 60°C (A), 80°C (B), as well as during 4 min (C) and 4 min at 80°C (D) for three times. (E and F) RL curves of samples coated in 2–12 min with a three steps deposition process (E) and with different thickness (F). Reproduced with permission from Entezami et al.,¹⁷³ Copyright 2021, ELSEVIER. (G and H) SEM images of original CFs (G), CFs/Fe₃O₄ core–shell structure composites (H), and the corresponding schematic diagram of the designed structure. (I and J) Raman spectra of carbon nanofibers (I) and the representative CFs/Fe₃O₄ composite (J). (K) I(D)/I(G) vs. ratio I(D')/I(G) of the virus samples. (L and M) RL values at different thicknesses (L) and frequency-dependent reflection loss (M), simulations for the t_m vs. frequency subject to the $\lambda/4$ model, as well as impedance match. (N) Cole–Cole semicircles of the representative CFs/Fe₃O₄ composite. (O) Magnetic properties of the as-prepared composites. Reproduced with permission from Dai et al.,¹⁷⁵ Copyright 2022, AIP Publishing.

weakens the impedance matching and interfacial polarization. To improve the interfacial polarization and conductivity losses, Dai and co-workers¹⁷⁵ synthesized CFs/Fe₃O₄ nanocrystal core–shell composites by using an extended heterostructure interface strategy (Figures 9H and 9I). CFs as one component of the prepared composites, the cross-linked structure is beneficial to the conductive loss and macroscopic eddy current loss, besides, the heterogeneous interface formed by graphite nanocrystals and amorphous carbon in CFs has a strong EMW absorption capacity attributed from the boundary-type defects mechanism. Moreover, a new heterogeneous interface was formed between the CFs and the Fe₃O₄ nanocrystal particles existed on the surface of which, improving the electromagnetic wave absorption properties due to the strong magnetic loss and interfacial polarization of the composite (Figures 9J–9L). By taking advantages of multiple loss mechanisms, the RL_{min}

of -51.11 , -42.99 , and -55.98 dB at 9, 12 (X-band), and 17 GHz (Ku-band) are achieved, respectively, corresponding to the thicknesses of 2.0, 1.5, and 1.0 mm. In addition, the EAB is 3.3 GHz in frequency range of 14.7–18 GHz with the thickness of only 1.09 mm (Figures 9M–9P).

Although the application temperature of CF-based composite materials can reach 400°C , attention should be paid to the improved comprehensiveness properties of durability, oxidation resistance and EM wave absorption at high temperatures.^{176,177} In order to improve high-temperature resistance and EMW absorption capability, Ye et al.¹⁷⁸ prepared a three-layers EMW absorbing material (CFs/Fe₃O₄/BN) by depositing a Fe₃O₄ and boron nitride (BN) coating onto the surface of a CFs through *in situ* hybridization. SEM images show that Fe₃O₄ was distributed along the axial direction of the fiber, whereas BN was found in the outermost coating layer. Compared with the sample without outermost BN layer (CF/Fe₃O₄), the decomposition temperature (550°C) of the prepared CF/Fe₃O₄/BN increased by more than 200°C after soaking composites into the metal salt solution (20 g/100 mL), which is attributed to the excellent corrosion and oxidation resistance performances of NB layer. In addition, the prepared CFs/Fe₃O₄/BN had an absorption bandwidth of 9.2 GHz (8.8–18 GHz) with EMW loss of less than -5 dB, and its effective EMW absorbing bandwidth (RL < -10 dB) is 4.2 GHz (11.2–15.4 GHz).

The above-mentioned works increase the wave absorption performance of CFs/Fe₃O₄ composites, however, the EAB of the as-prepared CFs/Fe₃O₄ composites is narrow. Covering the surface of CFs/Fe₃O₄ composites with a layer of conductive material is an effective approach to broaden the EAB.¹⁷⁹ Alanagh et al.¹⁸⁰ fabricated CFs@nano-Fe₃O₄@PANI composites by firstly depositing Fe₃O₄ particles on CFs via a modified multi-step electrophoretic deposition (EPD) and then coating PANI layer on the surface of CFs@nano-Fe₃O₄ through *in situ* polymerization. With the reduction in the effective mass/volume percentage of nano-Fe₃O₄ particles in composites, the saturated magnetization (Ms) of the resultant CFs@nano-Fe₃O₄ and CFs@nano-Fe₃O₄@PANI are 8.934 emu/g and 0.191 emu/g, respectively. The composite containing 1 wt % CFs@nano-Fe₃O₄@PANI shows a RL_{min} of -11.11 dB with an EAB of about 6 GHz in the frequency range of 8.2–18 GHz under the thickness of 1.5 mm.

Fiber/cobalt derivatives

The impedance mismatching and low magnetic loss limit the pure carbonaceous materials practical applications in EM wave absorption. Ferrites are accepted as an excellent EMW absorbing materials owing to their magnetic loss, ease of synthesis, and low cost.^{181–183} However, because of the Snoek's limit, the natural resonance of traditional ferrites is usually in the range from megahertz frequency (MHz) to low gigahertz frequency (<3 GHz), which makes the complex permeability reduced quickly in the gigahertz range, hindering their practical applications.¹⁸⁴ Besides, high density and poor impedance matching also block their wide application as EMW absorbing materials. Therefore, hybridization of carbon-based fiber materials with ferromagnetic metal/alloy materials is a reasonable approach for designing absorbing fibers.^{174,185–190} In comparison, as significant ferromagnetic and alloy materials, cobalt, cobalt oxide, cobalt-based ferrites, and alloy generally have larger complex permeability, broader resonance frequency and bigger magnetic loss in the GHz frequency range owing to their larger Snoek's limit, which is more beneficial for absorbing microwaves in GHz range.^{191–193}

In previous study, the combination of carbonaceous fibrous structure and magnetic substances was confirmed to effectively improve the EM wave absorption capacity of composite materials.^{20,194,195} Li et al.¹⁹⁶ reported a nanofibrous membrane composed of flexible carbon nanofibers and magnetic cobalt oxide (Co₃O₄) nanoparticles by the combination of electrospinning, stabilization and carbonization process (Figures 10A–10D). The nanofiber membrane (PAN/AAc) was formed by electrospinning the precursor solution of polyacrylonitrile (PAN, Mw = 150 000) polymer with different concentrations of cobalt acetylacetonate (AAc, Co(acac)₃). Afterward, the obtained PAN/AAc membrane was stabilized in an oven with external tension and annealed in a tube furnace under N₂ flow at 800°C to complete the carbonization process for obtaining the black magnetic CNFs/Co₃O₄ nanofibrous membrane. The study of electromagnetic absorbing behavior of the CNFs/Co₃O₄ nanofibrous membranes in the frequency range of 2–18 GHz shows that the resultant samples exhibit improved absorbing performance toward higher frequencies with an increase in the cobalt nanoparticle concentration. Due to the reduction of magnetization and coercivity of cobalt nanoparticles by carbon nanofibers decreasing magnetic permeability of CNFs/Co₃O₄ nanofibrous membrane, the optimal RL is 36.27 dB with sample thickness of 2 mm in 13.76 GHz which is mainly considered as a result of the dielectric loss (Figures 10E–10J).

Generally, reasonably designing the chemical component of the hybrids to obtain high magnetic loss and dielectric loss is an efficient approach to constructing high-performance EMW absorbing materials.^{61,197,198} Besides, modifying the nano-micro structures of the composites to achieve multiple reflection can also effectively improve properties.^{60,199,200} Via electrospinning and *in situ* self-assembly strategy, a 3D hierarchical core-shell NC@Co/NC nanofiber network (NC@Co/NC-900) was fabricated by Che's team.²⁰¹ In order to enhance the polarization loss and magnetic loss, N-doped carbon fibers with diameter of ~ 250 nm built a 3D-conductive network, and Co@C nanoparticles (diameter of ~ 20 nm) embedded into N-doped Carbon (Co/NC) shell *in situ* assembles on the surface CFs network, as shown in Figures 11A–11D. More importantly, the size of Co@C nanoparticles with a narrow particle size distribution in the range of 15–25 nm are easily controlled by modulating the calcination temperature. The NC@Co/NC composites with optimal impedance matching and uniformly multiple reflection in core-shell structure enhances the EMW attenuation and displays RL_{min} of -55.82 dB at 11.60 GHz. Wide EAB of 7.44 GHz in a low filler loading of 15 wt % is achieved, which fully covers the whole X and Ku bands in different thickness of 4.0 and 3.0 mm (Figures 11E–11G).

Hierarchical nano-micro structures are beneficial for improving performance. However, if the granulometry of metal/alloy material larger than $2\ \mu\text{m}$, eddy current effect existed in the metal/alloy material may greatly decrease the complex permeability and degrade the microwave absorption efficiency at GHz frequency range.^{202–204} To solve this issue, Zheng et al.²⁰⁵ reduced the size of metal/alloy particles into nanoscale to weak the influence of eddy current effect and enhance the microwave absorption properties. In their work, one-dimensional FeCo/CFs difunctional magnetic/dielectric absorbers were fabricated by electrospinning method and subsequent anoxic annealing treatment (Figures 12A–12J). Due to the large aspect ratio of CFs, tiny magnetic FeCo nanocrystals are uniformly decorated in the amorphous dielectric

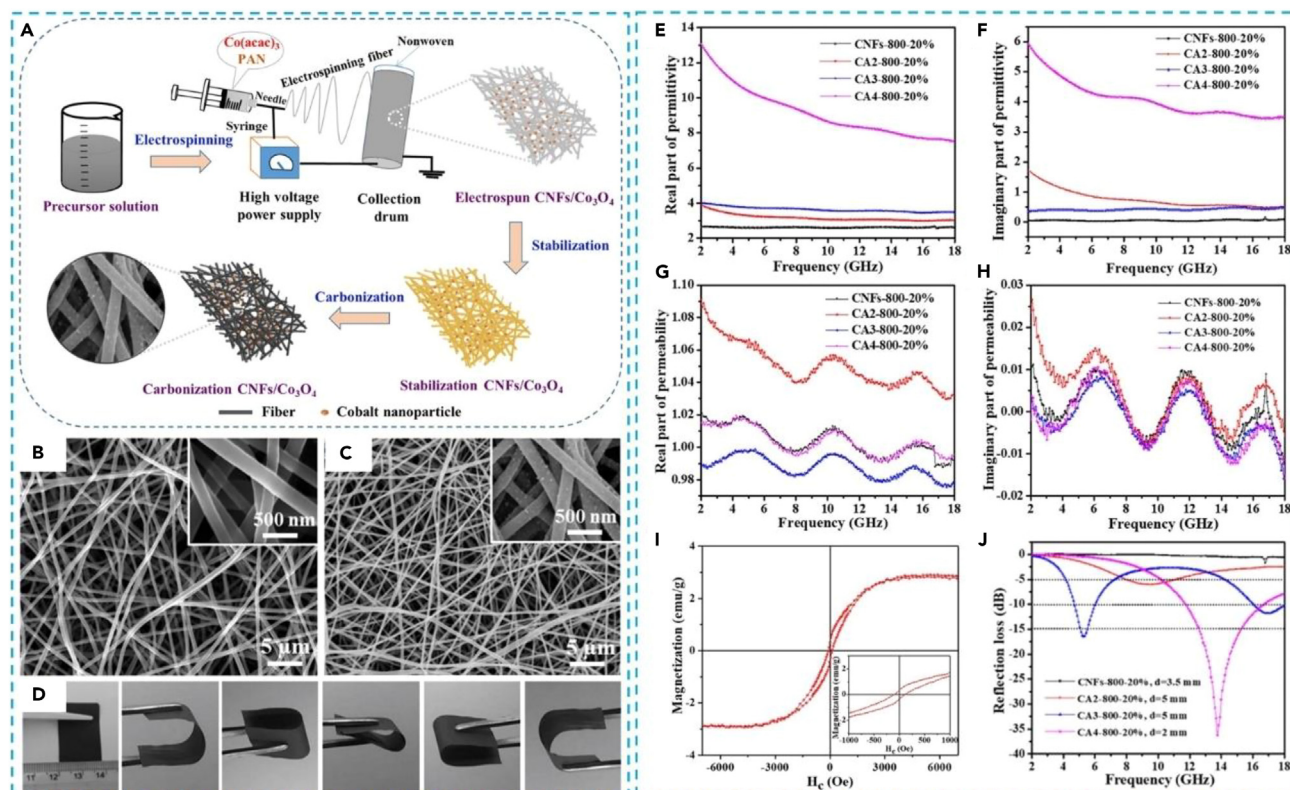


Figure 10. Fiber/cobalt derivates absorbing materials

(A) Schematic illustrating the preparation process of PAN/AAC nanofiber membrane.

(B and C) FE-SEM images of CNFs-800 (B) and CA4-800 (C).

(D) The digital images presenting the flexibility of CA4-800 samples.

(E–H) Frequency dependence of the real part (E), imaginary part (F) of the relative complex permittivity, the real part (G) and imaginary part (H) of relative complex permeability of the absorbers in the frequency range 2–18 GHz.

(I) Magnetization curve of CA4-800 sample measured at room temperature. Inset is the magnified image of the considered magnetic property.

(J) RL of various CNFs/Co₃O₄ composite samples. Reproduced with permission from Cai et al.,¹⁹⁶ Copyright 2018, Nature Publishing Group.

CFs. The as-prepared FeCo/CFs composites exhibit boosting microwave absorption performance benefited from the good impedance matching, and synergistic effect between ferromagnetic FeCo and dielectric CFs. The optimal FeCo/C/paraffin composites with 40 wt % of functional fillers show RL_{\min} value of -59.9 dB with EAB of 6.0 GHz at 13.2 GHz corresponding to thickness of 2.6 mm (Figures 12K–12Q). Moreover, the FeCo/C composites have a small density of only about 1.1 g/cm³, which is much smaller than that of the bulk FeCo (7.4 – 7.6 g/cm³).

Similar work was reported by Ye's group.¹⁹⁴ The reported CFs/FeCoNi hybrid fibers were prepared by impregnating polyacrylonitrile (PAN)-based pre-oxidized felt in the metal salt solution containing Fe, Co, and Ni then heating in high-temperature. These magnetic particles include Fe₃O₄, NiFe₂O₄, CoFe₂O₄, and Ni₃Fe on the surface of carbon fiber as the magnetic loss agents distribute uniformly along the axial direction. At the same time, the EM wave absorbing fiber is soft and can be bent arbitrarily. By tanking advantages of the synergistic effect of electric loss and magnetic loss, the as-prepared CFs/FeCoNi hybrid fibers exhibit excellent performances. The RL_{\min} at 11.74 GHz is -30.62 dB, and the absorption bandwidth is 7.4 GHz in frequency range of 8.7–16.1 GHz with 1 h of heat treatment at 650°C.

In addition to the reasonable combination of magnetic and dielectric components, the morphology is another factor for enhanced EM wave absorption properties.²⁰⁶ Luo et al.²⁰⁷ coated magnetic Fe–Co alloy on the surface of carbon fibers by a conventional and facile electrodeposition to prepare carbon fiber-based hybrid EMW absorption materials (FeCo@CFs). The different Fe–Co coating morphologies including of thin plate, irregular particle, and pyramid obtained at different plating temperatures of 25, 35, and 50°C, respectively, has significant impact on magnetic properties, complex permittivity, and microwave absorption properties of FeCo@CFs. The FeCo@CFs with plate-like Fe–Co coating obtained at 25°C plating temperature possesses lower complex permittivity and better microwave absorption properties in comparison to other FeCo@CFs hybrid composites. Due to plate-like morphology with larger surface-to-volume ratio and the existence of the special core/shell structure, the FeCo@CF-25-paraffin sample exhibits strong absorption ($RL < -10$ dB) over the whole frequency range of 2–18 GHz at all thicknesses. The absorption bandwidth (RL below -20 dB) is 7.9 GHz, as well as RL_{\min} at 9 GHz with a matching thickness of 1.8 mm is -37.7 dB.

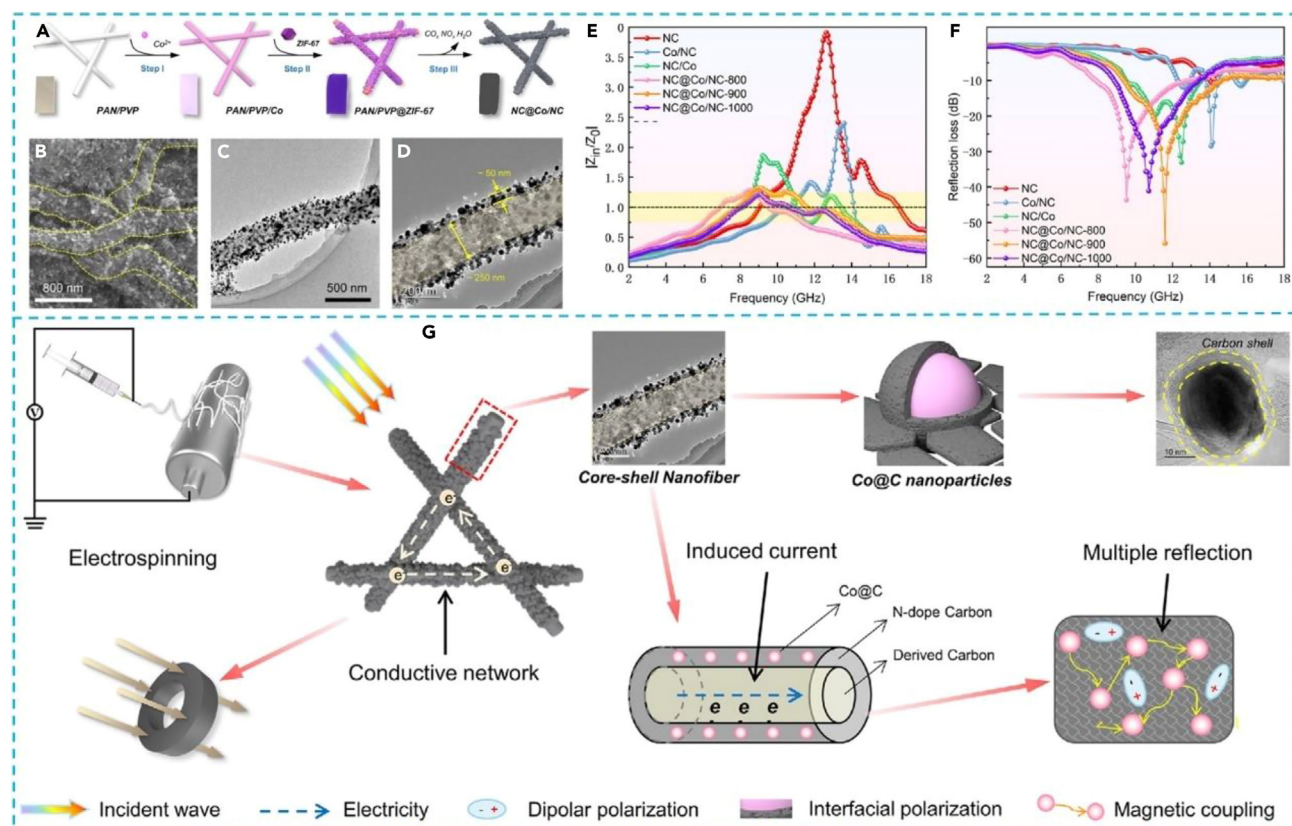


Figure 11. Hierarchical core-shell structured cobalt derivatives fibrous absorbing materials

(A) The illustrated synthesis route of NC@Co/NC composites.

(B–D) SEM, TEM and HR-TEM images of NC@Co/NC-900.

(E and F) The optimal $|Z_{in}/Z_0|$ values (E) and RL_{min} values (F) of various samples.

(G) Schematic diagram of the EMW absorption mechanisms for NC@Co/NC-900. Reproduced with permission from Che et al.,²⁰¹ Copyright 2022, ELSEVIER.

In a word, the high saturation magnetization, greater dielectric properties, high electrochemical performance of cobalt, cobalt oxide, cobalt-based ferrites and alloy make them an attractive candidate for excellent EM wave absorbers.^{185–187} At present, carbon fibers are usually surface modified using cobalt-based ferrites to improve the EMW absorbing properties.^{206,208–211}

Fiber/metal-organic frameworks derivatives

Metal-organic frameworks (MOFs) features large pore volume and periodic network and consist of metal ions or clusters as centers and organic ligands.²¹² The centers contain various metal ions such as main group, transition, lanthanide and rare earth metals, and the polyamines, carboxyl, pyridine, porphyrin, cyano, crown ethers and phosphoric acid usually work as the organic ligands.^{213–216} MOFs can be divided into imidazole zeolite frame works (ZIFs),²¹⁷ isorecticular MOFs (IRMOFs),²¹⁸ materials of institute lavoisier (MIL),²¹⁹ and so forth. In terms of EMW absorption, MOFs have attached more attentions as self-sacrificing precursors of microwave absorbers due to the regular porosity, ultra-high specific surface area, and tunable structural units resulted from the coexistence of metal and organic components. In addition, easy and mass production via hydrothermal or solvothermal methods followed by thermal decomposition are also their advantages.^{220–223} Compared with other absorbing materials, the absorption performance of MOFs-derived materials can be enhanced easily through *in situ* generated metal/metal oxide nanoparticles or clusters by improving impedance matching, magnetic and dielectric losses. For all the above reasons, combing MOFs derivatives with other fibrous materials is an effective way to fabricate composites with multiple absorption mechanisms and excellent properties.

ZIF series materials can be synthesized by the coordination reaction of Co^{2+} or Zn^{2+} with imidazole ligands based on aluminosilicate zeolite meshes. In terms of EMW absorption, ZIF materials are an important MOFs derivate because carbon-wrapped cobalt element and cobalt oxide exhibit shows great potential in wave absorption.²²⁴ Among them, ZIF-67 has attracted much interesting due to good structural stability and multiple active sites, as well as simple preparation method. According to the mechanisms of EMW absorption discussed above, compared with the physical mixing, the reasonably designed heterostructure is beneficial to improve the EMW absorbing properties. Among

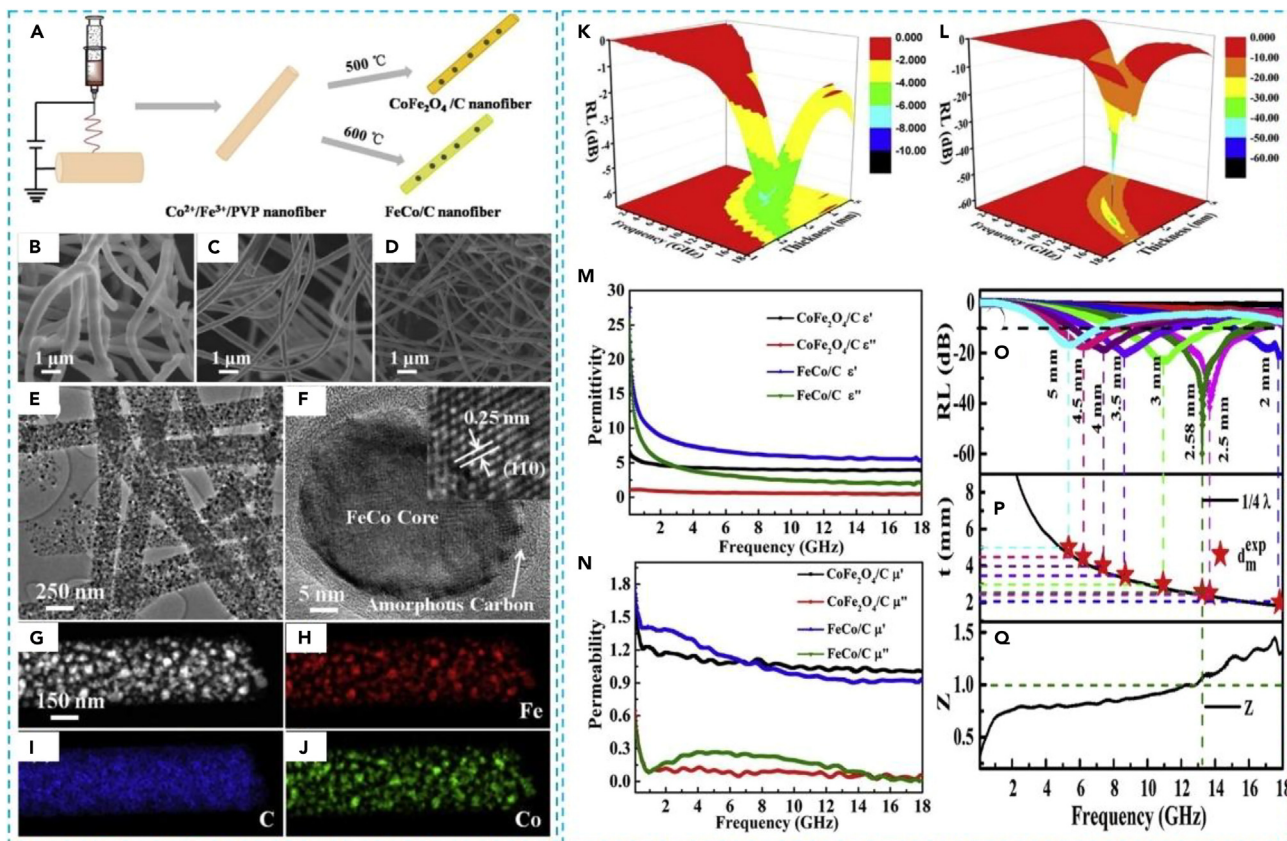


Figure 12. Hierarchical nano-micro structured cobalt derivatives fibrous absorbing materials

(A) Schematic illustration for the fabrication process of $\text{CoFe}_2\text{O}_4/\text{CFs}$ and FeCo/CFs .

(B–D) SEM images of $\text{Co}^{2+}/\text{Fe}^{3+}/\text{PVP}$ precursor (B), $\text{CoFe}_2\text{O}_4/\text{CFs}$ (C) and FeCo/CFs (D).

(E and F) TEM image of FeCo/CFs (E) and a single FeCo nanocrystal in the nanofibers (F), inset shows the HRTEM image of FeCo nanocrystal.

(G–J) HAADF-STEM image (G) and corresponding EDX elemental mapping (H–J) of FeCo/CFs .

(K and L) Three-dimensional RL representations of the paraffin-based microwave absorbers with 40 wt % functional fillers $\text{CoFe}_2\text{O}_4/\text{CFs}$ (K) and FeCo/CFs (L).

(M and N) Complex permittivity (M) and complex permeability (N) for $\text{CoFe}_2\text{O}_4/\text{CFs}$ and FeCo/CFs .

(O) Two-dimensional RL curves of FeCo/CFs absorber (40 wt %) with different thicknesses.

(P) Simulations of the relationship between thickness (t) and frequency of peak (f) under $\lambda/4$ condition.

(Q) Impedance matching condition (Z). Reproduced with permission from Zheng et al.,²⁰⁵ Copyright 2022, ELSEVIER.

the reported heterostructures, core-shell structure can not only realize the complementary advantages of components but also induce unique heterogeneous interface characteristics owing to close fit, especially in EMA absorbing materials.²²⁵ Li's group²²⁶ reported a series of core-shell $\text{CFs@C}/\text{Co}$ composites assembled by using CF as the core and cubic ZIF-67-derived C/Co as the shell with controllable structure and adjustable graphitization. The effects of shell coverage ratio and micro-morphology influenced by calcination temperature on the absorbing properties were analyzed. The roughness and thickness of the shell increase significantly with increasing coating number of MOFs, as shown in Figures 13A–13E. When the calcination temperature kept at 700°C , the obtained sample (A3-700) achieves RL_{\min} of -58.42 dB with thickness of 1.8 mm and reaches EAB of 4.24 GHz corresponding to the thickness of 1.91 mm (Figures 13F and 13G). However, the resultant composite with obvious multi-polarization effect prepared under the calcination temperature of 600°C exhibits super absorbing properties. RL_{\min} reaches up to -58.42 dB with the thickness of 1.78 mm, and EAB improves to 6.26 GHz at 1.71 mm (Figures 13H and 13I). The increased polarity difference in the heterogeneous interface between the core and shell, as well as the increased number of graphite/disordered interfaces in the shell are responsible to the perfect EMW absorption. This dual strategy of shell design and graphitization control may be an effective method to coordinate electromagnetic matching and construct multi-polarization.

It is generally recognized that the EW absorption performance is highly dependent on structure and morphology. Layered metal hydroxides (LDHs) have attracted more and more attentions because adjustable interlayer spacing allows them to flexibly tune the conductivity and the reduced layer spacing can effectively improve the conductivity by shortening the electron migration path with filling other materials (e.g., CFs).^{227–229} Cobalt-based layered hydroxides can take the advantages of layered structure, cobalt element, and interface polarization for enhancing absorption performance. In addition, ZIF-67, as a hard template, is a good source of Co element through slowly release Co

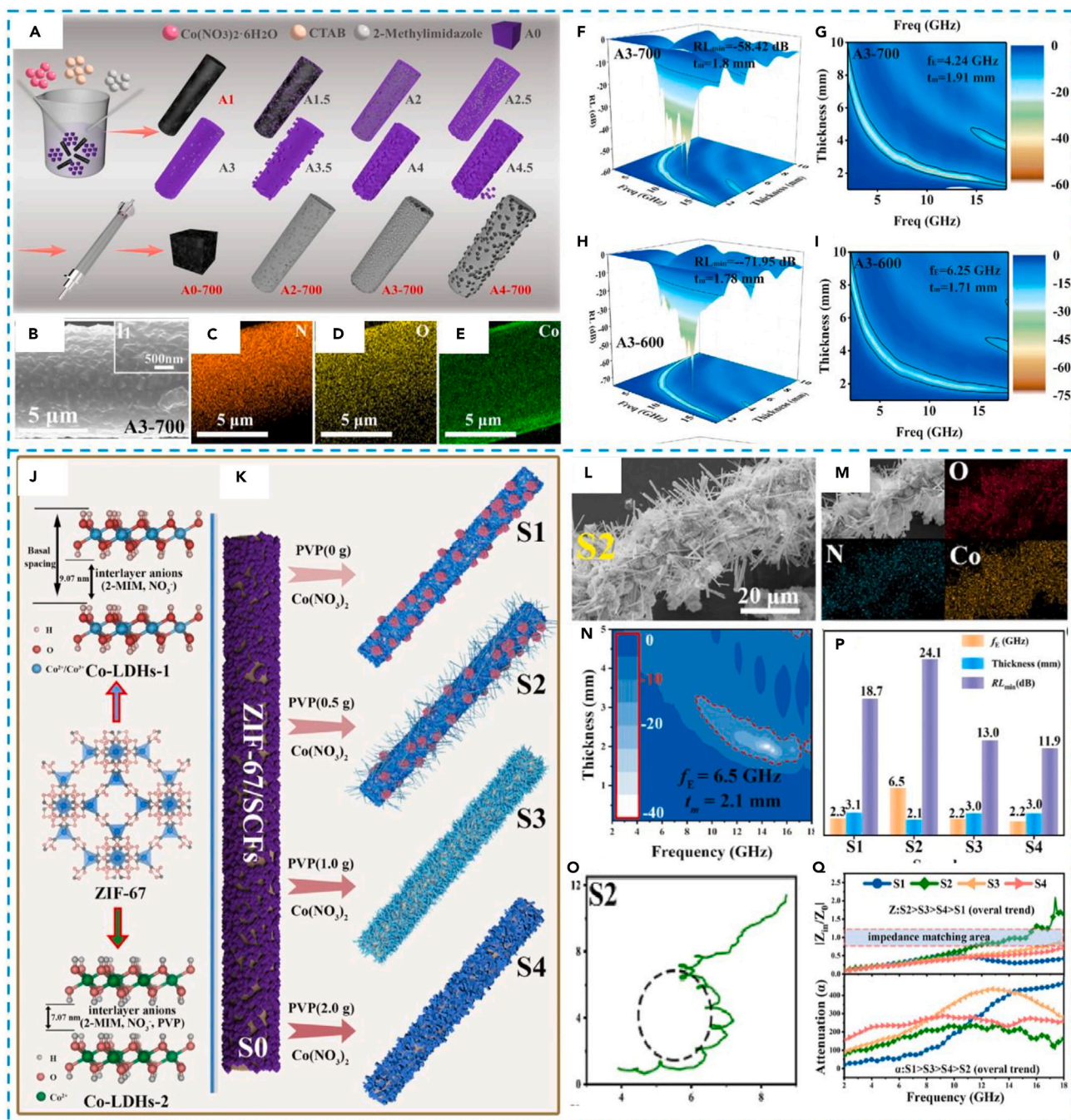


Figure 13. Fiber/MOFs derivatives absorbing materials

(A) Schematic diagram of synthesis of CF@ZIF-67 and CF@C/Co.

(B–E) SEM (B) and element mapping (C–E) of CF@C/Co composites carbonized at 700°C.

(F–H) Three-dimensional (F, H) and two-dimensional EMA absorption diagrams (G, I) of A3-700 and A3-600, respectively. Reproduced with permission from Li et al.,²²⁶ Copyright 2021, ELSEVIER.

(J) Crystal structure of Co-LDHs-1, ZIF-67 and Co-LDHs-2.

(K) Schematic illustration of the synthesis process of Co-LDHs/SCFs composites.

(L and M) SEM image and EDX mappings of S2.

(N–O) RL values and Cole-Cole plots of S2.

(P) The comparisons of sample performance.

(Q) Impedance matching (Z) at a thickness of 2.0 mm and attenuation constant (α) of S1-S4. Reproduced with permission from Wu et al.,²²⁴ Copyright 2021, ELSEVIER.

ions in an acidic environment to fabricate cobalt-based layered hydroxides. For example, Wu et al.²²⁴ prepared hydrangea-like Co-LDHs-1 and rod-like Co-LDHs-2 with different interlayer spacing grown Co *in situ* on surface of CFs by using ZIF-67 as template (Figures 13J–13M). Because of the strong coordination interaction between the cobalt ion sites in ZIF-67 and the C=O groups in PVP, hydrangea-like Co-LDHs-1 and rod-shaped Co-LDHs-2 were successfully synthesized by simply tuning the doping amount of PVP in ZIF-67 template. The mechanism analysis indicated that the Co-LDHs-1 and Co-LDHs-2 with different conductivities and morphologies are coordinated to optimize the excessively high complex permittivity of CFs, refining attenuation constant and impedance matching. As a result, the EAB of optimal electromagnetic reaches 6.5 GHz at 2.1 mm with low filling ratio (5 wt %) in paraffin matrix (Figures 13N and 13Q).

MOF-derived carbon fibers or bundles show perfect properties in EWM absorption. However, it is very difficult to combine simultaneously the properties of broad bandwidth and thin thickness for single dielectric material or magnetic material, this issue could be solved by prepared composites through hybridizing dielectric and magnetic materials by adjusting permittivity and permeability over a broad range. Zhang et al.²³⁰ synthesized firstly $Y_2Co_8Fe_9$ by an alloy smelting method, and then the MOF-derived carbon fiber bundles (MCFB) were fabricated via hydrothermal and catalytic carbonization. The composites (MCFB/ $Y_2Co_8Fe_9$) with various weight ratios of MCFB (0%, 0.1%, 0.3%, 0.5%) were prepared by mixing MCFB and $Y_2Co_8Fe_9$ with paraffin. For these as-prepared composites, the hierarchical porous structure of MCFB is beneficial to dissipate EM energy due to the multiple scattering and dipole polarization, and $Y_2Co_8Fe_9$ is responsible for the magnetic loss. Moreover, MOF-based hierarchical porous carbon was innovatively doped into the rare earth material with high magnetic permeability to achieve synergy effect, and the optimal impedance matching was also acquired by tuning doping amount, obtaining a broadband absorber with thin thickness. The resultant sample with 0.1% MCFB/ $Y_2Co_8Fe_9$ exhibited perfect EMA absorption performance with broaden band and thin thickness. RL_{min} of -64.79 dB and EAB of 5.02 GHz was obtained corresponding the thickness of 1.44 mm, increasing the thickness to 1.6 mm leads to EAB of 6.52 GHz.

Among the MOFs materials, Fe^{III} -MOF-5 derivative is usually used as a source for preparing magnetic metal particles and is composited with CFs for fabricating light weight absorbing materials with great EM wave attenuation characteristics. For example, Ji's group²³¹ prepared Fe^{III} -MOF-5 derived Fe magnetic particles modified CFs by using Fe^{III} -MOF-5 and PAN as the raw materials via electrospinning method followed with further heat-treatment. Based on the rational design strategy, the multiple attenuation mechanisms including of conductivity loss resulted from CFs, interface polarization loss between Fe particles and CFs, and magnetic loss because of Fe particles were introduced into the as-fabricated composites (FMCFs). Therefore, the reluctant FMCFs preformed excellent EM wave absorption performance with a RL_{min} of -39.2 dB at a bandwidth of 4.44 GHz under a small thickness of 1.4 mm. In addition, the calculation of the radar cross section (RCS) was conducted by applying ANSYS Electronics Desktop 2018 (HFSS), and the material coatings with FMCFs contribute to the RCS values with the strongest RCS reduction value up to 32 dBm.² So, combining simulation technology (HFSS) and material design is beneficial to evaluate absorbing materials for practical application.

In a word, by adjusting the morphology and composition of MOFs and MOF-based absorbers, the high absorption and loss of incident EMW can be achieved. Besides, the advantages of porosity, high specific surface area, simple preparation process, low cost and high thermal stability make MOF-derivates an attractive candidate in field of EMW absorption. Although the development of MOF-derived absorbing materials and some meaningful results have been obtained, several significant challenges such as new routes for the preparation, enhanced conductivity, morphology diversity and strict carbonization temperature control, and so forth. should be improved. MOF-derivates as a new star, is a very promising high-efficiency EMW absorption material at present and in the future.

CONCLUSIONS AND PROSPECTS

In recent decades, fibers or fibrous absorbers have continued to attract the increased interesting in electromagnetic wave absorption due to their advantages of simple preparation process, low cost, high thermal stability and high specific surface area. This work proposes recent development of CFs and SiC_f -based composites as a promising absorption candidate for providing a basis for the future study of fibrous microwave absorption materials. Adjusting the composition, structure and morphology can fabricate absorbing materials with suitable impedance matching, strong absorption and broadband (Table 1). In terms of the composition, pure CFs or SiC_f has poor impedance matching and absorption properties owing to the high conductivity. Compositing conductive fiber with other dielectric loss and/or magnetic loss materials into one is an efficient way to significantly improve the performance. For the microstructure, the crosslinked structure between fibers could provide abundant conductive pathway leading to much conduction loss. Porous and layered structure can effectively reduce the density of the resultant composites and increase the capability of EMW absorption through multiple reflection. Core-shell heterostructure and flower-like structure coated on the surface of fiber not only increase the specific surface area but enhance interfacial polarization for dissipating microwave energy. Different compositions and/or structures has their own unique advantages for attenuating microwave energy, the multi-dimension control strategy break the shackles and get more desirable performance.

Although some perfect results for the research and development of fibrous absorbing materials have been demonstrated, they still faced several significant challenges. Firstly, current fibrous materials tend to composite more and more other dielectric and/or magnetic loss materials, leading to fibrous composites with very complex composition, which pushed by the too much pursue of RL and EAB. On the one hand, many blind spots exist in the preparation of multicomponent composite fibrous absorbing materials because of the lack of detailed research on the significance of these materials combinations. On the other hand, the preparation of multicomponent MA materials is complicated and involves some toxic or polluting reagents, which goes against the requirements of practical application characterized with easy preparation, loss cost and friendly environment, and so forth. Due to the inherent characteristics, the structure of CFs and SiC_f obtained by direct carbonization has a single morphology and is not easily adjustable, and the carbonization process requires strict temperature control. Therefore, the parameters of various synthetic fibrous absorbing materials need to be further investigated. Secondly, multiple factors including of

Table 1. Summarized EMW absorption data for different fibrous materials

Absorber	Thickness (mm)	RL _{min} (dB)	EAB (RL < -10dB) (GHz)	Reference
CNT/CFs	2.5	-42.0	2.7	Singh et al. ²³²
CNT/PANI/CFs	2.0	-45.7	5.6	Wang et al. ²³³
CNT/Fe ₃ O ₄ /CFs	1.5	-59.9	/	Li et al. ⁶⁰
CNTs/Fe ₃ O ₄ /PANI/CFs	2	-22.4	6.9	Zhang et al. ²³⁴
CNT/CFs	3.0	-44.46	7.44	Zhan et al. ⁹⁵
CNTs/SiC _f	3.35	-37.6	1.5	Xie et al. ²³⁵
CNT/SiC _f	4.0	-62.5	8.8	Xu et al. ¹⁰⁰
SiOC/CFs	2.3	-47.9	4.6	Liu et al. ²³⁶
MWCNT/PPy/CFs	3.5	-17	6.12	Zhang et al. ²³⁷
MWCNTs/PEDOT/CFs	2	-39	4.5	Jiao et al. ²³⁸
rGO/SiC _f	3.7	-35	4.2	Han et al. ²³⁹
rGO-SiC _f /SiOC	1.4	-69.3	3.4	Han et al. ²⁴⁰
rGO/FeNi ₃ /CFs	4.8	-43.17	6.2	Ding et al. ²⁴¹
C/SiC _f	3.0	-36	4.1	Huo et al. ²⁴²
Graphite/SiC _f	1.7	-22.0	4.7	Wang et al. ²⁴³
Graphite/Si ₃ N ₄ /SiC _f	2.5	-32.3	6.4	Wang et al. ²⁴⁴
Ti ₃ C ₂ T _x /SiC _f	3.5	-55.7	4.2	Li et al. ²⁴⁵
Ti ₃ C ₂ T _x /NiCo ₂ O ₄ /CFs	/	-50.96	/	Li et al. ²⁴⁶
Ti ₃ C ₂ T _x /CNTs/CFs	1.55	-52.9	4.46	Li et al. ²⁴⁵
Ti ₃ C ₂ T _x /PPy/CFs	3.2	-49.2	4.9	Wei et al. ²⁴⁷
Ti ₃ C ₂ T _x /SiC _f	3.7	-55.7	4.2	Han et al. ²⁴⁸
Ti ₃ C ₂ T _x /CFs	1.8	-56.3	/	Wu et al. ²⁴⁹
Ti ₃ C ₂ T _x /Co-CZIF	2.7	-60.09	9.3	Wang et al. ²⁵⁰
Ti ₃ C ₂ T _x /CoNi/CNTs	1.6	-51.6	4.5	Qian et al. ¹⁵⁰
Ti ₃ C ₂ T _x /MoS ₂ /CFs	2.1	-61.51	7.6	Hua et al. ²⁵¹
Ti ₃ C ₂ T _x /CNFs	2.0	-44.9	5.7	Singh et al. ²³²
Al ₄ C ₃ @C _{NWs}	1.9	-47.1	5.5	Wang et al. ²³³

impedance matching, multiple reflections, dielectric and magnetic losses together effect the final absorbing capability, the quantitative estimation of the effect of various factors still lacks sufficient theoretical support. Therefore, the parameter contribution degree and absorption mechanism of fibrous absorbing materials need to be further clarified. Finally, the wide band feature of fibrous absorbing materials with are usually occurred in the high frequency region, while the study of how to control frequency band toward to low-frequency is still not enough. Besides, the materials can be broadly used in harsh environments such as strong acid, high humidity and high temperature.

In summary, fibrous materials have infinite possibilities in the field of microwave absorption, although there are still many problems and most of the research is still at the experimental development stage. Fibrous materials characterized with light weight, high mechanical properties and pore structure are a very promising high-efficiency EMW absorption material at present and in the future.

Limitations of the study

It should be noted that this review emphasized only the preparation, structure, morphology, and absorbing performance of the representative CFs and SiC_f-based EMW-absorbing fibrous materials, without any discussion for their practical applications. In addition, EMW absorbing performance need to be tested by diverse test methods according to distinct application scenarios, which should be taken into full consideration.

ACKNOWLEDGMENTS

The valuable comments of potential reviewers are acknowledged. This work was financially supported by the National Key Research and Development Program of China (2022YFB3807101/2022YFB3807102/2022YFB3807100), Key Research and Development Program of Shaanxi Province (2023-YBGY-193), Natural Science Foundation Project of Chongqing (CSTB2022NSCQ-MSX0565).

AUTHOR CONTRIBUTIONS

Conceptualization: Y.D. and J.K. Investigation, interpretation, and compilation: Y.D., Y.L., and A.W. Visualization: Y.D. and Y.L. Supervision: J.K. Writing-Original Draft: Y.D. Writing-Review and Editing: Y.D. and J.K. All authors have commented on and approved the final article.

DECLARATION OF INTERESTS

The authors declare that they have no known competing financial interests or personal relationships that could have appeared to influence the work reported in this article.

REFERENCES

- Song, Y., Zhu, R., Liu, Z., Dai, X., and Kong, J. (2023). Phase-transformation nanoparticles synchronously boosting mechanical and electromagnetic performance of sibcn ceramics. *ACS Appl. Mater. Interfaces* 15, 4234–4245. <https://doi.org/10.1021/acsami.2c20397>.
- Zhang, M., Ling, H., Wang, T., Jiang, Y., Song, G., Zhao, W., Zhao, L., Cheng, T., Xie, Y., Guo, Y., et al. (2022). An equivalent substitute strategy for constructing 3d ordered porous carbon foams and their electromagnetic attenuation mechanism. *Nanomicro Lett.* 14, 157. <https://doi.org/10.1007/s40820-022-00900-x>.
- Zhao, H., Wang, F., Cui, L., Xu, X., Han, X., and Du, Y. (2021). Composition optimization and microstructure design in mofs-derived magnetic carbon-based microwave absorbers: a review. *Nanomicro Lett.* 13, 208. <https://doi.org/10.1007/s40820-021-00734-z>.
- Liang, L., Yao, C., Yan, X., Feng, Y., Hao, X., Zhou, B., Wang, Y., Ma, J., Liu, C., and Shen, C. (2021). High-efficiency electromagnetic interference shielding capability of magnetic Ti₃C₂Tx MXene/CNT composite film. *J. Mater. Chem. A* 9, 24560–24570. <https://doi.org/10.1039/d1ta07781c>.
- Shu, R., Li, X., Tian, K., and Shi, J. (2022). Fabrication of bimetallic metal-organic frameworks derived Fe₃O₄/C decorated graphene composites as high-efficiency and broadband microwave absorbers. *Compos. Pt. B-Eng.* 228, 109423. <https://doi.org/10.1016/j.compositesb.2021.109423>.
- Guan, H., Wang, Q., Wu, X., Pang, J., Jiang, Z., Chen, G., Dong, C., Wang, L., and Gong, C. (2021). Biomass derived porous carbon (BPC) and their composites as lightweight and efficient microwave absorption materials. *Compos. Pt. B-Eng.* 207, 108562. <https://doi.org/10.1016/j.compositesb.2020.108562>.
- Zhang, M., Niu, Y.R., Liu, J.Y., Wei, X.S., Wang, X.R., Ye, L.L., Peng, W.B., Zhang, J.C., Tao, X.N., and Zhou, Q. (2019). Preparation and electromagnetic wave absorption performance of Fe₃Si/SiC@SiO₂ nanocomposites. *J. Mol. Med.* 97, 619–631. <https://doi.org/10.1016/j.cej.2019.01.039>.
- Liang, J., Li, C., Cao, X., Wang, Y., Li, Z., Gao, B., Tong, Z., Wang, B., Wan, S., and Kong, J. (2022). Hollow hydrangea-like nitrogen-doped NiO/Ni-carbon composites as lightweight and highly efficient electromagnetic wave absorbers. *Nano Res.* 15, 6831–6840. <https://doi.org/10.1007/s12274-022-4511-3>.
- Liao, Q., He, M., Zhou, Y., Nie, S., Wang, Y., Wang, B., Yang, X., Bu, X., and Wang, R. (2018). Rational construction of Ti₃C₂T_x/Co-MOF-derived laminated Co/TiO₂-C hybrids for enhanced electromagnetic wave absorption. *Langmuir* 34, 15854–15863. <https://doi.org/10.1021/acs.langmuir.8b03238>.
- Li, N., Xie, X., Lu, H., Fan, B., Wang, X., Zhao, B., Zhang, R., and Yang, R. (2019). Novel two-dimensional Ti₃C₂T_x/Ni-spheres hybrids with enhanced microwave absorption properties. *Ceram. Int.* 45, 22880–22888. <https://doi.org/10.1016/j.ceramint.2019.07.331>.
- Liu, P., Yao, Z., Ng, V.M.H., Zhou, J., Kong, L.B., and Yue, K. (2018). Facile synthesis of ultrasmall Fe₃O₄ nanoparticles on MXenes for high microwave absorption performance. *Compos. Appl. Sci. Manuf.* 115, 371–382. <https://doi.org/10.1016/j.compositesa.2018.10.014>.
- Zheng, M., Wei, Y., Ren, J., Dai, B., Luo, W., Ma, M., Li, T., and Ma, Y. (2021). 2-aminopyridine functionalized magnetic core-shell Fe₃O₄@polypyrrole composite for removal of Mn (VII) from aqueous solution by double-layer adsorption. *Sep. Purif. Technol.* 277, 119455. <https://doi.org/10.1016/j.seppur.2021.119455>.
- Li, Y., Xu, F., Lin, Z., Sun, X., Peng, Q., Yuan, Y., Wang, S., Yang, Z., He, X., and Li, Y. (2017). Electrically and thermally conductive underwater acoustically absorptive graphene/rubber nanocomposites for multifunctional applications. *Nanoscale* 9, 14476–14485. <https://doi.org/10.1039/c7nr05189a>.
- Xie, S., Ji, Z., Shui, Z., Li, B., Wang, J., Hou, G., and Wang, J. (2018). Design and manufacture of a dual-functional exterior wall structure for 1.1-5 GHz electromagnetic radiation absorption. *Compos. Struct.* 201, 608–615. <https://doi.org/10.1016/j.compstruct.2018.06.079>.
- Wang, Y., Chen, Y., Zhu, M., Wang, J., Feng, C., Lan, X., and He, Y. (2002). Development for silicon carbide fibers with trilobal cross section. *J. Mater. Sci. Lett.* 21, 349–350. <https://doi.org/10.1023/a:1017973214756>.
- Shen, Q., Li, H., Lin, H., Li, L., Li, W., and Song, Q. (2018). Simultaneously improving the mechanical strength and electromagnetic interference shielding of carbon/carbon composites by electrophoretic deposition of SiC nanowires. *J. Mater. Chem. C* 6, 5888–5899. <https://doi.org/10.1039/c8tc01313f>.
- Das, T.K., Ghosh, P., and Das, N.C. (2019). Preparation, development, outcomes, and application versatility of carbon fiber-based polymer composites: a review. *Adv. Compos. Hybrid Mater.* 2, 214–233. <https://doi.org/10.1007/s42114-018-0072-z>.
- Dai, B., Li, J., Wang, W., Liu, X., Qi, Y., and Qi, Y. (2020). Carbon fibers with eddy current loss characteristics exhibit different microwave absorption properties in different graphitization states. *Mater. Lett.* 281, 128667. <https://doi.org/10.1016/j.matlet.2020.128667>.
- Xie, W., Cheng, H., Chu, Z., Chen, Z., and Long, C. (2011). Effect of carbonization temperature on the structure and microwave absorbing properties of hollow carbon fibres. *Ceram. Int.* 37, 1947–1951. <https://doi.org/10.1016/j.ceramint.2011.02.017>.
- Sun, Q., Sun, L., Cai, Y., Ji, T., and Zhang, G. (2018). Activated carbon fiber/Fe₃O₄ composite with enhanced electromagnetic wave absorption properties. *RSC Adv.* 8, 35337–35342. <https://doi.org/10.1039/C8RA05872E>.
- Dai, B., Qi, Y., Song, M., Zhang, B., Wang, N., and Dai, Y. (2022). Facile synthesis of core-shell structured C/Fe₃O₄ composite fiber electromagnetic wave absorbing materials with multiple loss mechanisms. *J. Chem. Phys.* 157, 114705. <https://doi.org/10.1063/5.0121257>.
- Gholampoor, M., Movassagh-Alanagh, F., and Salimkhani, H. (2017). Fabrication of nano-Fe₃O₄ 3d structure on carbon fibers as a microwave absorber and EMI shielding composite by modified EPD method. *Solid State Sci.* 64, 51–61. <https://doi.org/10.1016/j.solidstsci.2016.12.005>.
- Qin, F., and Brosseau, C. (2012). A review and analysis of microwave absorption in polymer composites filled with carbonaceous particles. *J. Appl. Phys.* 111, 061301. <https://doi.org/10.1063/1.3688435>.
- Song, Y., Bae, J., Jin, S., Lee, H., Kang, S., Lee, J., Shin, J., Cho, S., and Cho, B.K. (2022). Single source precursor derived SiBCNHf ceramic with enhanced high-temperature microwave absorption and antioxidation. *Metab. Eng.* 72, 215–226. <https://doi.org/10.1016/j.jmst.2022.03.015>.
- Liu, Y., Fu, Y., Liu, L., Li, W., Guan, J., and Tong, G. (2018). Low-cost carbothermal reduction preparation of monodisperse Fe₃O₄/C core-shell nanosheets for improved microwave absorption. *ACS Appl. Mater. Interfaces* 10, 16511–16520. <https://doi.org/10.1021/acsami.8b02770>.
- Zhang, M., Han, C., Cao, W.-Q., Cao, M.-S., Yang, H.-J., and Yuan, J. (2020). A nano-micro engineering nanofiber for electromagnetic absorber, green shielding and sensor. *Nano-Micro Lett.* 13, 27. <https://doi.org/10.1007/s40820-020-00552-9>.
- Wei, J., Zhang, Y., Li, X., Zhang, H., Guo, Y., Wang, T., Qiao, X., and Lei, W. (2022). Recent progress in synthesis, growth mechanisms, and electromagnetic wave absorption properties of silicon carbide nanowires. *Ceram. Int.* 48, 35966–35985. <https://doi.org/10.1016/j.ceramint.2022.10.102>.
- Qin, M., Lan, D., Wu, G., Qiao, X., and Wu, H. (2020). Sodium citrate assisted hydrothermal synthesis of nickel cobaltate absorbers with tunable morphology and complex dielectric parameters toward

- efficient electromagnetic wave absorption. *Appl. Surf. Sci.* 504, 144480. <https://doi.org/10.1016/j.apsusc.2019.144480>.
29. Darvishzadeh, A., and Nasouri, K. (2021). Broadband and tunable high-performance microwave absorption properties by Ni-coated carbon fibers. *Mater. Chem. Phys.* 274, 125127. <https://doi.org/10.1016/j.matchemphys.2021.125127>.
30. Wang, J., Jia, Z., Liu, X., Dou, J., Xu, B., Wang, B., and Wu, G. (2021). Construction of 1d heterostructure NiCo@C/ZnO nanorod with enhanced microwave absorption. *Nanomicro Lett.* 13, 175. <https://doi.org/10.1007/s40820-021-00704-5>.
31. Lan, D., Gao, Z., Zhao, Z., Wu, G., Kou, K., and Wu, H. (2021). Double-shell hollow glass microspheres@Co₂SiO₄ for lightweight and efficient electromagnetic wave absorption. *Chem. Eng. J.* 408, 127313. <https://doi.org/10.1016/j.cej.2020.127313>.
32. Peymanfar, R., and Fazlalizadeh, F. (2020). Microwave absorption performance of ZnAl₂O₄. *Chem. Eng. J.* 402, 126089. <https://doi.org/10.1016/j.cej.2020.126089>.
33. Zhang, M., Li, R., Chen, H., Zhou, J., and Zhang, Y. (2018). Confinedly implanted NiFe₂O₄-rGO: cluster tailoring and highly tunable electromagnetic properties for selective-frequency microwave absorption. *Nano Res.* 23, 1426–1431. <https://doi.org/10.1007/s12274-017-1758-1>.
34. Liang, X., Man, Z., Quan, B., Zheng, J., Gu, W., Zhang, Z., and Ji, G. (2020). Environment-stable coxyni encapsulation in stacked porous carbon nanosheets for enhanced microwave absorption. *Nanomicro Lett.* 12, 102. <https://doi.org/10.1007/s40820-020-00432-2>.
35. Zhao, B., Li, Y., Zeng, Q., Wang, L., Ding, J., Zhang, R., and Che, R. (2020). Galvanic replacement reaction involving core-shell magnetic chains and orientation-tunable microwave absorption properties. *Small* 16, 2003502. <https://doi.org/10.1002/smll.202003502>.
36. Wu, Z., Pei, K., Xing, L., Yu, X., You, W., and Che, R. (2019). Enhanced microwave absorption performance from magnetic coupling of magnetic nanoparticles suspended within hierarchically tubular composite. *Adv. Funct. Mater.* 29, 1901448. <https://doi.org/10.1002/adfm.201901448>.
37. Kong, L.B., Li, Z.W., Liu, L., Huang, R., Abshinova, M., Yang, Z.H., Tang, C.B., Tan, P.K., Deng, C.R., and Matitsine, S. (2013). Recent progress in some composite materials and structures for specific electromagnetic applications. *Int. Mater. Rev.* 58, 203–259. <https://doi.org/10.1179/1743280412y.0000000011>.
38. Sankaran, S., Deshmukh, K., Ahamed, M.B., and Khadheer Pasha, S. (2018). Recent advances in electromagnetic interference shielding properties of metal and carbon filler reinforced flexible polymer composites: a review. *Compos. Appl. Sci. Manuf.* 114, 49–71. <https://doi.org/10.1016/j.compositesa.2018.08.006>.
39. Meng, F., Wang, H., Huang, F., Guo, Y., Wang, Z., Hui, D., and Zhou, Z. (2018). Graphene-based microwave absorbing composites: a review and prospective. *Compos. Pt. B-Eng.* 137, 260–277. <https://doi.org/10.1016/j.compositesb.2017.11.023>.
40. Jia, Z., Lan, D., Lin, K., Qin, M., Kou, K., Wu, G., and Wu, H. (2018). Progress in low-frequency microwave absorbing materials. *J. Mater. Sci. Mater. Electron.* 29, 17122–17136. <https://doi.org/10.1007/s10854-018-9909-z>.
41. Quan, B., Liang, X., Ji, G., Cheng, Y., Liu, W., Ma, J., Zhang, Y., Li, D., and Xu, G. (2017). Dielectric polarization in electromagnetic wave absorption: review and perspective. *J. Alloys Compd.* 728, 1065–1075. <https://doi.org/10.1016/j.jallcom.2017.09.082>.
42. Wang, C., Murugadoss, V., Kong, J., He, Z., Mai, X., Shao, Q., Chen, Y., Guo, L., Liu, C., Angaiah, S., and Guo, Z. (2018). Overview of carbon nanostructures and nanocomposites for electromagnetic wave shielding. *Carbon* 140, 696–733. <https://doi.org/10.1016/j.carbon.2018.09.006>.
43. Bliokh, K.Y., Smirnova, D., and Nori, F. (2015). Quantum spin hall effect of light. *Science* 348, 1448–1451. <https://doi.org/10.1126/science.aaa9519>.
44. Cornacchia, S., La Tegola, L., Maldera, A., Pierpaoli, E., Tupputi, U., Ricatti, G., Eusebi, L., Salerno, S., and Guglielmi, G. (2020). Radiation protection in non-ionizing and ionizing body composition assessment procedures. *Quant. Imag. Med. Surg.* 10, 1723–1738. <https://doi.org/10.21037/qims-19-1035>.
45. Yang, L., Jie, R., Jiang, H.T., Yong, S., and Hong, C. (2017). Quantum spin hall effect in metamaterials. *Acta Phys. Sin.* 66, 227803. <https://doi.org/10.7498/aps.66.227803>.
46. Nicolau, E.V. (1966). Relaxation properties of transmission lines. *High Perform. Dev. IEEE Cornell Conf.* 54, 1127–1133. <https://doi.org/10.1109/proc.1966.5052>.
47. Pipes, L.A. (1966). Direct computation of transmission matrices of electrical transmission lines. *J. Franklin Inst.* 281, 275–292. [https://doi.org/10.1016/0016-0032\(66\)90224-9](https://doi.org/10.1016/0016-0032(66)90224-9).
48. Wang, K.-J., and Wang, G.-D. (2021). Periodic solution of the (2+1)-dimensional nonlinear electrical transmission line equation via variational method. *Results Phys.* 20, 103666. <https://doi.org/10.1016/j.rinp.2020.103666>.
49. Hu, X., Li, S., and Peng, H. (2012). A comparative study of equivalent circuit models for Li-ion batteries. *J. Power Sources* 198, 359–367. <https://doi.org/10.1016/j.jpowsour.2011.10.013>.
50. Wang, G., Gao, Z., Tang, S., Chen, C., Duan, F., Zhao, S., Lin, S., Feng, Y., Zhou, L., and Qin, Y. (2012). Microwave absorption properties of carbon nanocoils coated with highly controlled magnetic materials by atomic layer deposition. *ACS Nano* 6, 11009–11017. <https://doi.org/10.1021/nn304630h>.
51. Zhang, J., Wang, K., Xu, Q., Zhou, Y., Cheng, F., and Guo, S. (2015). Beyond yolk-shell nanoparticles: Fe₃O₄@Fe₃C core@shell nanoparticles as yolks and carbon nanospindles as shells for efficient lithium ion storage. *ACS Nano* 9, 3369–3376. <https://doi.org/10.1021/acs.nano.5b00760>.
52. Du, Y., Wang, X., Dai, X., Lu, W., Tang, Y., and Kong, J. (2022). Ultraflexible, highly efficient electromagnetic interference shielding, and self-healable triboelectric nanogenerator based on Ti₃C₂T_x MXene for self-powered wearable electronics. *J. Mater. Sci. Technol.* 100, 1–11. <https://doi.org/10.1016/j.jmst.2021.04.078>.
53. Zhang, Y., Wang, X., and Cao, M. (2018). Confinedly implanted NiFe₂O₄-rGO: cluster tailoring and highly tunable electromagnetic properties for selective-frequency microwave absorption. *Nano Res.* 11, 1426–1436. <https://doi.org/10.1007/s12274-017-1758-1>.
54. Wang, J., Wu, F., Cui, Y., Zhang, A., Zhang, Q., and Zhang, B. (2021). Efficient synthesis of N-doped porous carbon nanoribbon composites with selective microwave absorption performance in common wavebands. *Carbon* 175, 164–175. <https://doi.org/10.1016/j.carbon.2021.01.005>.
55. Wu, Y., Shu, R., Zhang, J., Wan, Z., Shi, J., Liu, Y., Zhao, G., and Zheng, M. (2020). Oxygen vacancies regulated microwave absorption properties of reduced graphene oxide/multi-walled carbon nanotubes/ cerium oxide ternary nanocomposite. *J. Alloys Compd.* 819, 152944. <https://doi.org/10.1016/j.jallcom.2019.152944>.
56. Chang, Q., Liang, H., Shi, B., and Wu, H. (2021). Sodium oxalate-induced hydrothermal synthesis of wood-texture-column-like NiCo₂O₄ with broad bandwidth electromagnetic wave absorption performance. *J. Colloid Interface Sci.* 600, 49–57. <https://doi.org/10.1016/j.jcis.2021.05.019>.
57. Tao, F., Chen, W., Xu, W., Pan, J., and Du, S. (2011). Asymmetric energy flux in a transmission line based on frequency multiplication. *Phys. Rev. E* 83, 056605. <https://doi.org/10.1103/PhysRevE.83.056605>.
58. Zhu, H.-J., and Zhang, G.-F. (2014). Geometric quantum discord and berry phase between two charge qubits coupled by a quantum transmission line. *Chin. Phys. B* 23, 120306. <https://doi.org/10.1088/1674-1056/23/12/120306>.
59. Wang, L., Liu, H., Lv, X., Cui, G., and Gu, G. (2020). Facile synthesis 3d porous MXene Ti₃C₂T_x@RGO composite aerogel with excellent dielectric loss and electromagnetic wave absorption. *J. Alloys Compd.* 828, 154251. <https://doi.org/10.1016/j.jallcom.2020.154251>.
60. Li, Y., Liu, X., Nie, X., Yang, W., Wang, Y., Yu, R., and Shui, J. (2019). Multifunctional organic-inorganic hybrid aerogel for self-cleaning, heat-insulating, and highly efficient microwave absorbing material. *Adv. Funct. Mater.* 29, 1807624. <https://doi.org/10.1002/adfm.201807624>.
61. Ye, F., Song, Q., Zhang, Z., Li, W., Zhang, S., Yin, X., Zhou, Y., Tao, H., Liu, Y., Cheng, L., et al. (2018). Direct growth of edge-rich graphene with tunable dielectric properties in porous Si₃N₄ ceramic for broadband high-performance microwave absorption. *Adv. Funct. Mater.* 28, 1707205. <https://doi.org/10.1002/adfm.201707205>.
62. Zhong, G., Xu, S., Chen, C., Kline, D.J., Giroux, M., Pei, Y., Jiao, M., Liu, D., Mi, R., Xie, H., et al. (2019). Synthesis of metal oxide nanoparticles by rapid, high-temperature 3d microwave heating. *Adv. Funct. Mater.* 29, 1904282. <https://doi.org/10.1002/adfm.201904282>.
63. Zhu, H., Zhang, H., Chen, Y., Li, Z., Zhang, D., Zeng, G., Huang, Y., Wang, W., Wu, Q., and Zhi, C. (2016). The electromagnetic property and microwave absorption of wormhole-like mesoporous carbons with different surface areas. *J. Mater. Sci.* 51, 9723–9731. <https://doi.org/10.1007/s10853-016-0206-z>.
64. Xu, R., Xu, D., Zeng, Z., and Liu, D. (2022). CoFe₂O₄/porous carbon nanosheet composites for broadband microwave absorption. *Chem. Eng. J.* 427, 130796. <https://doi.org/10.1016/j.cej.2021.130796>.

65. Zeng, X., Zhu, L., Yang, B., and Yu, R. (2020). Necklace-like Fe₃O₄ nanoparticle beads on carbon nanotube threads for microwave absorption and supercapacitors. *Mater. Des.* 189, 108517. <https://doi.org/10.1016/j.matdes.2020.108517>.
66. Ren, F., Yu, H., Wang, L., Saleem, M., Tian, Z., and Ren, P. (2014). Current progress on the modification of carbon nanotubes and their application in electromagnetic wave absorption. *RSC Adv.* 4, 14419–14431. <https://doi.org/10.1039/c3ra46989a>.
67. Lu, M.-M., Cao, W.-Q., Shi, H.-L., Fang, X.-Y., Yang, J., Hou, Z.-L., Jin, H.-B., Wang, W.-Z., Yuan, J., and Cao, M.-S. (2014). Multi-wall carbon nanotubes decorated with ZnO nanocrystals: mild solution-process synthesis and highly efficient microwave absorption properties at elevated temperature. *J. Mater. Chem. A* 2, 10540–10547. <https://doi.org/10.1039/c4ta01715c>.
68. Wen, B., Cao, M.-S., Hou, Z.-L., Song, W.-L., Zhang, L., Lu, M.-M., Jin, H.-B., Fang, X.-Y., Wang, W.-Z., and Yuan, J. (2013). Temperature dependent microwave attenuation behavior for carbon-nanotube/silica composites. *Carbon* 65, 124–139. <https://doi.org/10.1016/j.carbon.2013.07.110>.
69. Liu, P., Zhu, C., Gao, S., Guan, C., Huang, Y., and He, W. (2020). N-doped porous carbon nanoplates embedded with CoS₂ vertically anchored on carbon cloths for flexible and ultrahigh microwave absorption. *Carbon* 163, 348–359. <https://doi.org/10.1016/j.carbon.2020.03.041>.
70. Chen, N., Zhou, J., Yao, Z., Lei, Y., Tan, R., Zuo, Y., Zheng, W., and Jiao, Z. (2021). Fabrication of Nd-doped Ni-Zn ferrite/multi-walled carbon nanotubes composites with effective microwave absorption properties. *Ceram. Int.* 47, 10545–10554. <https://doi.org/10.1016/j.ceramint.2020.11.137>.
71. Qin, M., Liang, H., Zhao, X., and Wu, H. (2020). Glycine-assisted solution combustion synthesis of NiCo₂O₄ electromagnetic wave absorber with wide absorption bandwidth. *Ceram. Int.* 46, 22313–22320. <https://doi.org/10.1016/j.ceramint.2020.05.311>.
72. Liu, J., Wang, M., Zhang, L., Zang, D., Liu, H., Francesca Liotta, L., and Wu, H. (2021). Tunable sulfur vacancies and hetero-interfaces of FeS₂-based composites for high-efficiency electromagnetic wave absorption. *J. Colloid Interface Sci.* 591, 148–160. <https://doi.org/10.1016/j.jcis.2021.01.110>.
73. Qin, M., Zhang, L., and Wu, H. (2022). Dielectric loss mechanism in electromagnetic wave absorbing materials. *Adv. Sci.* 9, 2105553. <https://doi.org/10.1002/advs.202105553>.
74. Zhou, P., Wang, X., Song, Z., Wang, M., Huang, W., Yu, M., Wang, L., and Zhang, Q. (2021). Multi-dimensional ordered mesoporous carbon/silica@Ni composite with hierarchical nanostructure for strong and broadband microwave absorption. *Carbon* 176, 209–218. <https://doi.org/10.1016/j.carbon.2021.01.125>.
75. Dong, S., Hu, P., Li, X., Hong, C., Zhang, X., and Han, J. (2020). NiCo₂S₄ nanosheets on 3d wood-derived carbon for microwave absorption. *Chem. Eng. J.* 398, 125588. <https://doi.org/10.1016/j.cej.2020.125588>.
76. Qu, B., Zhu, C., Li, C., Zhang, X., and Chen, Y. (2016). Coupling hollow Fe₃O₄-Fe nanoparticles with graphene sheets for high-performance electromagnetic wave absorbing material. *ACS Appl. Mater. Interfaces* 8, 3730–3735. <https://doi.org/10.1021/acsami.5b12789>.
77. Kim, S.S., Kim, S.T., Yoon, Y.C., and Lee, K.S. (2005). Magnetic, dielectric, and microwave absorbing properties of iron particles dispersed in rubber matrix in gigahertz frequencies. *J. Appl. Phys.* 97, 10f905. <https://doi.org/10.1063/1.1852371>.
78. Gao, B., Qiao, L., Wang, J., Liu, Q., Li, F., Feng, J., and Xue, D. (2008). Microwave absorption properties of the Ni nanowires composite. *J. Phys. D Appl. Phys.* 41, 235005. <https://doi.org/10.1088/0022-3727/41/23/235005>.
79. Gao, Y., and Wang, Z. (2021). Microwave absorption and electromagnetic interference shielding properties of Li-Zn ferrite-carbon nanotubes composite. *J. Magn. Magn. Mater.* 528, 167808. <https://doi.org/10.1016/j.jmmm.2021.167808>.
80. Wu, T., Liu, Y., Zeng, X., Cui, T., Zhao, Y., Li, Y., and Tong, G. (2016). Facile hydrothermal synthesis of Fe₃O₄/C core-shell nanorings for efficient low-frequency microwave absorption. *ACS Appl. Mater. Interfaces* 8, 7370–7380. <https://doi.org/10.1021/acsami.6b00264>.
81. Lu, B., Dong, X.L., Huang, H., Zhang, X.F., Zhu, X.G., Lei, J.P., and Sun, J.P. (2008). Microwave absorption properties of the core/shell-type iron and nickel nanoparticles. *J. Magn. Magn. Mater.* 320, 1106–1111. <https://doi.org/10.1016/j.jmmm.2007.10.030>.
82. Li, H., Cui, L., Chen, Z., and Chen, Y. (2019). Risk factors for early-onset seizures in patients with cerebral venous sinus thrombosis: a meta-analysis of observational studies. *Seizure* 72, 33–39. <https://doi.org/10.1016/j.seizure.2019.09.006>.
83. Li, X., You, W., Wang, L., Liu, J., Wu, Z., Pei, K., Li, Y., and Che, R. (2019). Self-assembly-magnetized MXene avoid dual-agglomeration with enhanced interfaces for strong microwave absorption through a tunable electromagnetic property. *ACS Appl. Mater. Interfaces* 11, 44536–44544. <https://doi.org/10.1021/acsami.9b11861>.
84. Kong, L., Yin, X., Han, M., Yuan, X., Hou, Z., Ye, F., Zhang, L., Cheng, L., Xu, Z., and Huang, J. (2017). Macroscopic bioinspired graphene sponge modified with in-situ grown carbon nanowires and its electromagnetic properties. *Carbon* 111, 94–102. <https://doi.org/10.1016/j.carbon.2016.09.066>.
85. Zhu, L., Zeng, X., Chen, M., and Yu, R. (2017). Controllable permittivity in 3d Fe₃O₄/CNTs network for remarkable microwave absorption performances. *RSC Adv.* 7, 26801–26808. <https://doi.org/10.1039/C7RA04456A>.
86. Song, Z., Liu, X., Sun, X., Li, Y., Nie, X., Tang, W., Yu, R., and Shui, J. (2019). Alginate-templated synthesis of CoFe/carbon fiber composite and the effect of hierarchically porous structure on electromagnetic wave absorption performance. *Carbon* 151, 36–45. <https://doi.org/10.1016/j.carbon.2019.05.025>.
87. Wang, X., Pan, F., Xiang, Z., Zeng, Q., Pei, K., Che, R., and Lu, W. (2020). Magnetic vortex core-shell Fe₃O₄@C nanorings with enhanced microwave absorption performance. *Carbon* 157, 130–139. <https://doi.org/10.1016/j.carbon.2019.10.030>.
88. ur Rehman, S., Wang, J., Luo, Q., Sun, M., Jiang, L., Han, Q., Liu, J., and Bi, H. (2019). Starfish-like C/CoNiO₂ heterostructure derived from ZIF-67 with tunable microwave absorption properties. *Chem. Eng. J.* 373, 122–130. <https://doi.org/10.1016/j.cej.2019.05.040>.
89. Ismail, R.A., Mohsin, M.H., Ali, A.K., Hassoon, K.I., and Erten-Ela, S. (2020). Preparation and characterization of carbon nanotubes by pulsed laser ablation in water for optoelectronic application. *Physica* 119, 113997. <https://doi.org/10.1016/j.physe.2020.113997>.
90. Mehrabi, M., Parvin, P., Reyhani, A., and Mortazavi, S.Z. (2018). Hybrid laser ablation and chemical reduction to synthesize Ni/Pd nanoparticles decorated multi-wall carbon nanotubes for effective enhancement of hydrogen storage. *Int. J. Hydrogen Energy* 43, 12211–12221. <https://doi.org/10.1016/j.ijhydene.2018.04.144>.
91. Mehrabi, M., Reyhani, A., Parvin, P., and Mortazavi, S.Z. (2019). Surface structural alteration of multi-walled carbon nanotubes decorated by nickel nanoparticles based on laser ablation/chemical reduction methods to enhance hydrogen storage properties. *Int. J. Hydrogen Energy* 44, 3812–3823. <https://doi.org/10.1016/j.ijhydene.2018.12.122>.
92. Atchudan, R., Jebakumar Immanuel Edison, T.N., Perumal, S., RanjithKumar, D., and Lee, Y.R. (2019). Direct growth of iron oxide nanoparticles filled multi-walled carbon nanotube via chemical vapour deposition method as high-performance supercapacitors. *Int. J. Hydrogen Energy* 44, 2349–2360. <https://doi.org/10.1016/j.ijhydene.2018.08.183>.
93. Chen, C.M., Dai, Y.M., Huang, J.G., and Jehng, J.M. (2006). Intermetallic catalyst for carbon nanotubes (CNTs) growth by thermal chemical vapor deposition method. *Carbon* 44, 1808–1820. <https://doi.org/10.1016/j.carbon.2005.12.043>.
94. Zhang, Q., Wang, D.G., Huang, J.Q., Zhou, W.P., Luo, G.H., Qian, W.Z., and Wei, F. (2010). Dry spinning yarns from vertically aligned carbon nanotube arrays produced by an improved floating catalyst chemical vapor deposition method. *Carbon* 48, 2855–2861. <https://doi.org/10.1016/j.carbon.2010.04.017>.
95. Zhan, Y., Xia, L., Yang, H., Zhou, N., Ma, G., Zhang, T., Huang, X., Xiong, L., Qin, C., and Guangwu, W. (2021). Tunable electromagnetic wave absorbing properties of carbon nanotubes/carbon fiber composites synthesized directly and rapidly via an innovative induction heating technique. *Carbon* 175, 101–111. <https://doi.org/10.1016/j.carbon.2020.12.080>.
96. Kong, L., Zhang, S., Liu, Y., Wu, H., Fan, X., Cao, Y., and Huang, J. (2023). Hierarchical architecture bioinspired CNTs/CNF electromagnetic wave absorbing materials. *Carbon* 207, 198–206. <https://doi.org/10.1016/j.carbon.2023.03.024>.
97. Qiu, J., and Qiu, T. (2015). Fabrication and microwave absorption properties of magnetite nanoparticle-carbon nanotube-hollow carbon fiber composites. *Carbon* 81, 20–28. <https://doi.org/10.1016/j.carbon.2014.09.011>.
98. Liu, P., Huang, Y., and Zhang, X. (2015). Cubic NiFe₂O₄ particles on

- graphene-polyaniline and their enhanced microwave absorption properties. *Compos. Sci. Technol.* 107, 54–60. <https://doi.org/10.1016/j.compscitech.2014.11.021>.
99. Lihua, Z., Jiahui, S., Zhenzhen, X., Fangtao, R., Yiping, Q., and Zhi, L. (2020). Electromagnetic wave absorbing properties of cotton fabric with carbon nanotubes coating. *Fibres Text. East. Eur.* 28, 82–90. <https://doi.org/10.5604/01.3001.0014.2390>.
100. Xu, J., Xia, L., Luo, J., Lu, S., Huang, X., Zhong, B., Zhang, T., Wen, G., Wu, X., Xiong, L., and Wang, G. (2020). High-performance electromagnetic wave absorbing cnt/sicf composites: synthesis, tuning, and mechanism. *ACS Appl. Mater. Interfaces* 12, 20775–20784. <https://doi.org/10.1021/acsami.9b19281>.
101. Yang, M., Yuan, Y., Li, Y., Sun, X., Wang, S., Liang, L., Ning, Y., Li, J., Yin, W., Che, R., and Li, Y. (2020). Dramatically enhanced electromagnetic wave absorption of hierarchical CNT/Co/C fiber derived from cotton and metal-organic-framework. *Carbon* 161, 517–527. <https://doi.org/10.1016/j.carbon.2020.01.073>.
102. Wang, C., Li, Y., He, X., Ding, Y., Peng, Q., Zhao, W., Shi, E., Wu, S., and Cao, A. (2015). Cotton-derived bulk and fiber aerogels grafted with nitrogen-doped graphene. *Nanoscale* 7, 7550–7558. <https://doi.org/10.1039/c5nr00996k>.
103. Yuan, Y., Sun, X., Yang, M., Xu, F., Lin, Z., Zhao, X., Ding, Y., Li, J., Yin, W., Peng, Q., et al. (2017). Stiff, thermally stable and highly anisotropic wood-derived carbon composite monoliths for electromagnetic interference shielding. *ACS Appl. Mater. Interfaces* 9, 21371–21381. <https://doi.org/10.1021/acsami.7b04523>.
104. Yuan, Y., Ding, Y., Wang, C., Xu, F., Lin, Z., Qin, Y., Li, Y., Yang, M., He, X., Peng, Q., and Li, Y. (2016). Multifunctional stiff carbon foam derived from bread. *ACS Appl. Mater. Interfaces* 8, 16852–16861. <https://doi.org/10.1021/acsami.6b03985>.
105. Liang, C., Wang, Z., Wu, L., Zhang, X., Wang, H., and Wang, Z. (2017). Light and strong hierarchical porous sic foam for efficient electromagnetic interference shielding and thermal insulation at elevated temperatures. *ACS Appl. Mater. Interfaces* 9, 29950–29957. <https://doi.org/10.1021/acsami.7b07735>.
106. Hu, B., Wang, K., Wu, L., Yu, S.H., Antonietti, M., and Titirici, M.M. (2010). Engineering carbon materials from the hydrothermal carbonization process of biomass. *Adv. Mater.* 22, 813–828. <https://doi.org/10.1002/adma.200902812>.
107. Song, S., Ma, F., Wu, G., Ma, D., Geng, W., and Wan, J. (2015). Facile self-templating large scale preparation of biomass-derived 3d hierarchical porous carbon for advanced supercapacitors. *J. Mater. Chem. A* 3, 18154–18162. <https://doi.org/10.1039/c5ta04721h>.
108. Borghei, M., Lehtonen, J., Liu, L., and Rojas, O.J. (2018). Advanced biomass-derived electrocatalysts for the oxygen reduction reaction. *Adv. Mater.* 30, 1703691. <https://doi.org/10.1002/adma.201703691>.
109. Zhang, Y., Liu, X., Wu, L., Dong, W., Xia, F., Chen, L., Zhou, N., Xia, L., Hu, Z.-Y., Liu, J., et al. (2020). A flexible, hierarchically porous PANI/MnO₂ network with fast channels and an extraordinary chemical process for stable fast-charging lithium–sulfur batteries. *J. Mater. Chem. A* 8, 2741–2751. <https://doi.org/10.1039/C9TA12135H>.
110. Zhuang, Z., Wang, W., Wei, Y., Li, T., Ma, M., and Ma, Y. (2021). Preparation of polyaniline nanorods/manganese dioxide nanoflowers core/shell nanostructure and investigation of electrochemical performances. *Adv. Compos. Hybrid Mater.* 4, 938–945. <https://doi.org/10.1007/s42114-021-00225-0>.
111. Yan, J., Huang, Y., Liu, X., Zhao, X., Li, T., Zhao, Y., and Liu, P. (2021). Polypyrrole-based composite materials for electromagnetic wave absorption. *Polym. Rev.* 61, 646–687. <https://doi.org/10.1080/15583724.2020.1870490>.
112. Guo, J., Li, X., Chen, Z., Zhu, J., Mai, X., Wei, R., Sun, K., Liu, H., Chen, Y., Naik, N., and Guo, Z. (2022). Magnetic NiFe₂O₄/Polypyrrole nanocomposites with enhanced electromagnetic wave absorption. *J. Mater. Sci. Technol.* 108, 64–72. <https://doi.org/10.1016/j.jmst.2021.08.049>.
113. Kruželák, J., Kvasničáková, A., Hložeková, K., and Hudec, I. (2021). Progress in polymers and polymer composites used as efficient materials for EMI shielding. *Nanoscale Adv.* 3, 123–172. <https://doi.org/10.1039/d0na00760a>.
114. Yu, Z., Yan, Z., Zhang, F., Wang, J., Shao, Q., Murugadoss, V., Alhadhrami, A., Mersal, G.A., Ibrahim, M.M., El-Bahy, Z.M., et al. (2022). Waterborne acrylic resin co-modified by itaconic acid and γ -methacryloxypropyl triisopropoxidesilane for improved mechanical properties, thermal stability, and corrosion resistance. *Prog. Org. Coating* 168, 106875. <https://doi.org/10.1016/j.porgcoat.2022.106875>.
115. Wang, Y., Du, Y., Xu, P., Qiang, R., and Han, X. (2017). Recent advances in conjugated polymer-based microwave absorbing materials. *Polymers* 9, 29. <https://doi.org/10.3390/polym9010029>.
116. Wei, Y., Luo, W., Zhuang, Z., Dai, B., Ding, J., Li, T., Ma, M., Yin, X., and Ma, Y. (2021). Fabrication of ternary MXene/MnO₂/ polyaniline nanostructure with good electrochemical performances. *Adv. Compos. Hybrid Mater.* 4, 1082–1091. <https://doi.org/10.1007/s42114-021-00323-z>.
117. Ma, Y., Hou, C., Zhang, H., Zhang, Q., Liu, H., Wu, S., and Guo, Z. (2019). Three-dimensional core-shell Fe₃O₄/Polyaniline coaxial heterogeneous nanonets: preparation and high performance supercapacitor electrodes. *Electrochim. Acta* 315, 114–123. <https://doi.org/10.1016/j.electacta.2019.05.073>.
118. Zhang, P., Han, X., Kang, L., Qiang, R., Liu, W., and Du, Y. (2013). Synthesis and characterization of polyaniline nanoparticles with enhanced microwave absorption. *RSC Adv.* 3, 12694–12701. <https://doi.org/10.1039/c3ra40973b>.
119. Jia, H., Xing, H., Ji, X., and Gao, S. (2021). Self-template and in-situ polymerization strategy to lightweight hollow MnO₂@polyaniline core-shell heterojunction with excellent microwave absorption properties. *Appl. Surf. Sci.* 537, 147857. <https://doi.org/10.1016/j.apsusc.2020.147857>.
120. Zhang, M., Ling, H., Ding, S., Xie, Y., Cheng, T., Zhao, L., Wang, T., Bian, H., Lin, H., Li, Z., and Meng, A. (2021). Synthesis of CF@PANI hybrid nanocomposites decorated with Fe₃O₄ nanoparticles towards excellent lightweight microwave absorber. *Carbon* 174, 248–259. <https://doi.org/10.1016/j.carbon.2020.12.005>.
121. Zhao, L., Guo, Y., Xie, Y., Cheng, T., Meng, A., Yuan, L., Zhao, W., Sun, C., Li, Z., and Zhang, M. (2022). Construction of SiCNWS@NiCo₂O₄@PANI 1d hierarchical nanocomposites toward high-efficiency microwave absorption. *Appl. Surf. Sci.* 592, 153324. <https://doi.org/10.1016/j.apsusc.2022.153324>.
122. Truong, V.T., Riddell, S.Z., and Muscat, R.F. (1998). Polypyrrole based microwave absorbers. *J. Mater. Sci.* 33, 4971–4976. <https://doi.org/10.1023/a:1004498705776>.
123. Asmatulu, R., Bollavaram, P.K., Patlolla, V.R., Alarifi, I.M., and Khan, W.S. (2020). Investigating the effects of metallic submicron and nanofilms on fiber-reinforced composites for lightning strike protection and EMI shielding. *Adv. Compos. Hybrid Mater.* 3, 66–83. <https://doi.org/10.1007/s42114-020-00135-7>.
124. Shi, Y., Yu, L., Li, K., Li, S., Dong, Y., Zhu, Y., Fu, Y., and Meng, F. (2020). Well-matched impedance of polypyrrole-loaded cotton non-woven fabric/polydimethylsiloxane composite for extraordinary microwave absorption. *Compos. Sci. Technol.* 197, 108246. <https://doi.org/10.1016/j.compscitech.2020.108246>.
125. Zhang, M., Zhao, L., Zhao, W., Wang, T., Yuan, L., Guo, Y., Xie, Y., Cheng, T., Meng, A., and Li, Z. (2022). Boosted electromagnetic wave absorption performance from synergistic induced polarization of SiCNWs@MnO₂@PPy heterostructures. *Nano Res.* 16, 3558–3569. <https://doi.org/10.1007/s12274-022-5289-z>.
126. Sultanov, F., Daulbayev, C., Bakbolat, B., and Daulbayev, O. (2020). Advances of 3d graphene and its composites in the field of microwave absorption. *Adv. Colloid Interface Sci.* 285, 102281. <https://doi.org/10.1016/j.cis.2020.102281>.
127. Zhao, W., Li, Y., Zhang, X., Zhang, R., Hu, Y., Boyer, C., and Xu, F.J. (2020). Graphitic carbon nitride: preparation, properties and applications in energy storage. *Eng. Sci.* 323, 24–35. <https://doi.org/10.30919/es8d1008>.
128. Zhao, Z., Zhao, R., Bai, P., Du, W., Guan, R., Tie, D., Naik, N., Huang, M., and Guo, Z. (2022). AZ91 alloy nanocomposites reinforced with Mg-coated graphene: phases distribution, interfacial microstructure, and property analysis. *J. Alloys Compd.* 902, 163484. <https://doi.org/10.1016/j.jallcom.2021.163484>.
129. Jing, C., Zhang, Y., Zheng, J., Ge, S., Lin, J., Pan, D., Naik, N., and Guo, Z. (2022). In-situ constructing visible light CdS/Cd-MOF photocatalyst with enhanced photodegradation of methylene blue. *Particuology* 69, 111–122. <https://doi.org/10.1016/j.partic.2021.11.013>.
130. Fan, Z., Wang, D., Yuan, Y., Wang, Y., Cheng, Z., Liu, Y., and Xie, Z. (2020). A lightweight and conductive MXene/graphene hybrid foam for superior electromagnetic interference shielding. *Chem. Eng. J.* 381, 122696. <https://doi.org/10.1016/j.cej.2019.122696>.
131. Hou, Y., Sheng, Z., Fu, C., Kong, J., and Zhang, X. (2022). Hygroscopic holey graphene aerogel fibers enable highly efficient moisture capture, heat allocation and microwave absorption. *Nat. Commun.* 13, 1227. <https://doi.org/10.1038/s41467-022-28906-4>.
132. Khazaei, M., Arai, M., Sasaki, T., Chung, C.Y., Venkataraman, N.S., Estili, M., Sakka, Y.,

- and Kawazoe, Y. (2013). Novel electronic and magnetic properties of two-dimensional transition metal carbides and nitrides. *Adv. Funct. Mater.* 23, 2185–2192. <https://doi.org/10.1002/adfm.201202502>.
133. Luo, W., Wei, Y., Zhuang, Z., Lin, Z., Li, X., Hou, C., Li, T., and Ma, Y. (2022). Fabrication of $\text{Ti}_3\text{C}_2\text{T}_x$ MXene/polyaniline composite films with adjustable thickness for high-performance flexible all-solid-state symmetric supercapacitors. *Electrochim. Acta* 406, 139871. <https://doi.org/10.1016/j.electacta.2022.139871>.
134. Naguib, M., Kurtoglu, M., Presser, V., Lu, J., Niu, J., Heon, M., Hultman, L., Gogotsi, Y., and Barsoum, M.W. (2011). Two-dimensional nanocrystals produced by exfoliation of Ti_3AlC_2 . *Adv. Mater.* 23, 4248–4253. <https://doi.org/10.1002/adma.201102306>.
135. Wang, J., Fan, Q., Yu, T., Zhang, Y., Xie, Z., Wang, Y., and Fan, Z. (2021). Super-fast fabrication of MXene film through a combination of ion induced gelation and vacuum-assisted filtration. *BMC Genom. Data* 22, 57–66.
136. Wang, Y., Liu, Y., Wang, C., Liu, H., Zhang, J., Lin, J., Fan, J., Ding, T., Ryu, J.E., and Guo, Z. (2020). Significantly enhanced ultrathin NiCo-based MOF nanosheet electrodes hybridized with $\text{Ti}_3\text{C}_2\text{T}_x$ MXene for high performance asymmetric supercapacitor. *Eng. Sci.* 9, 50–59. <https://doi.org/10.30919/es8d903>.
137. Wei, Y., Luo, W., Li, X., Lin, Z., Hou, C., Ma, M., Ding, J., Li, T., and Ma, Y. (2022). PANI-MnO₂ and $\text{Ti}_3\text{C}_2\text{T}_x$ (MXene) as electrodes for high-performance flexible asymmetric supercapacitors. *Electrochim. Acta* 406, 139874. <https://doi.org/10.1016/j.electacta.2022.139874>.
138. Yang, H., Dai, J., Liu, X., Lin, Y., Wang, J., Wang, L., and Wang, F. (2017). Layered PVB/ $\text{Ba}_3\text{Co}_2\text{Fe}_{24}\text{O}_{41}/\text{Ti}_3\text{C}_2$ MXene composite: enhanced electromagnetic wave absorption properties with high impedance match in a wide frequency range. *Mater. Chem. Phys.* 200, 179–186. <https://doi.org/10.1016/j.matchemphys.2017.05.057>.
139. Yan, S., Cao, C., He, J., He, L., and Qu, Z. (2019). Investigation on the electromagnetic and broadband microwave absorption properties of Ti_3C_2 MXene/flaky carbonyl iron composites. *J. Mater. Sci. Mater. Electron.* 30, 6537–6543. <https://doi.org/10.1007/s10854-019-00959-0>.
140. Guo, Y., Wang, D., Bai, T., Liu, H., Zheng, Y., Liu, C., and Shen, C. (2021). Electrostatic self-assembled $\text{NiFe}_2\text{O}_4/\text{Ti}_3\text{C}_2\text{T}_x$ MXene nanocomposites for efficient electromagnetic wave absorption at ultralow loading level. *Adv. Compos. Hybrid Mater.* 4, 602–613. <https://doi.org/10.1007/s42114-021-00279-0>.
141. Lan, D., Gao, Z., Zhao, Z., Kou, K., and Wu, H. (2021). Application progress of conductive conjugated polymers in electromagnetic wave absorbing composites. *Compos. Commun.* 26, 100767. <https://doi.org/10.1016/j.coco.2021.100767>.
142. Yan, J., Huang, Y., Liu, X., Zhao, X., Li, T., Zhao, Y., and Liu, P. (2021). Polypyrrole-based composite materials for electromagnetic wave absorption. *Polym. Rev.* 61, 646–687. <https://doi.org/10.1080/15583724.2020.1870490>.
143. Wang, S., Lin, L., and Wang, Z.L. (2015). Triboelectric nanogenerators as self-powered active sensors. *Nano Energy* 11, 436–462. <https://doi.org/10.1016/j.nanoen.2014.10.034>.
144. Ling, Z., Ren, C.E., Zhao, M.Q., Yang, J., Giammarco, J.M., Qiu, J., Barsoum, M.W., and Gogotsi, Y. (2014). Flexible and conductive MXene films and nanocomposites with high capacitance. *Proc. Natl. Acad. Sci. USA* 111, 16676–16681. <https://doi.org/10.1073/pnas.1414215111>.
145. Gogotsi, Y., and Anasori, B. (2019). The rise of MXenes. *ACS Nano* 13, 8491–8494. <https://doi.org/10.1021/acsnano.9b06394>.
146. Kojima, Y., Usuki, A., Kawasumi, M., Okada, A., Fukushima, Y., Kurauchi, T., and Kamigaito, O. (1993). Mechanical properties of nylon 6-clay hybrid. *J. Mater. Res.* 8, 1185–1189. <https://doi.org/10.1557/JMR.1993.1185>.
147. Messersmith, P.B., and Giannelis, E.P. (1995). Synthesis and barrier properties of poly(*ε*-caprolactone)-layered silicate nanocomposites. *J. Polym. Sci. A. Polym. Chem.* 33, 1047–1057. <https://doi.org/10.1002/pola.1995.080330707>.
148. Vaia, R.A., Vasudevan, S., Krawiec, W., Scanlon, L.G., and Giannelis, E.P. (1995). New polymer electrolyte nanocomposites-melt intercalation of poly(ethylene oxide) in mica-type silicates. *Adv. Mater.* 7, 154–156. <https://doi.org/10.1002/adma.19950070210>.
149. Mayerberger, E.A., Urbanek, O., McDaniel, R.M., Street, R.M., Barsoum, M.W., and Schauer, C.L. (2017). Preparation and characterization of polymer- $\text{Ti}_3\text{C}_2\text{T}_x$ (MXene) composite nanofibers produced via electrospinning. *J. Appl. Polym. Sci.* 134, 45295. <https://doi.org/10.1002/app.45295>.
150. Qian, S., Liu, G., Yan, M., and Wu, C. (2022). Flexible mxene/cellulose nanofiber aerogels for efficient electromagnetic absorption. *ACS Appl. Nano Mater.* 5, 9771–9779. <https://doi.org/10.1021/acsnanm.2c01983>.
151. Yin, G., Wang, Y., Wang, W., and Yu, D. (2020). Multilayer structured PANI/MXene/CF fabric for electromagnetic interference shielding constructed by layer-by-layer strategy. *Colloid Surf. A-Physicochem. Eng. Asp.* 601, 125047. <https://doi.org/10.1016/j.colsurfa.2020.125047>.
152. Xu, J., Cui, Y., Wang, J., Fan, Y., Shah, T., Ahmad, M., Zhang, Q., and Zhang, B. (2020). Fabrication of wrinkled carbon microspheres and the effect of surface roughness on the microwave absorbing properties. *Chem. Eng. J.* 401, 126027. <https://doi.org/10.1016/j.cej.2020.126027>.
153. Cui, Y., Wu, F., Wang, J., Wang, Y., Shah, T., Liu, P., Zhang, Q., and Zhang, B. (2021). Three dimensional porous MXene/CNTs microspheres: preparation, characterization and microwave absorbing properties. *Compos. Appl. Sci. Manuf.* 145, 106378. <https://doi.org/10.1016/j.compositesa.2021.106378>.
154. Jin, L., Wang, J., Wu, F., Yin, Y., and Zhang, B. (2021). MXene@ Fe_3O_4 microspheres/fibers composite microwave absorbing materials: Optimum composition and performance evaluation. *Carbon* 182, 770–780. <https://doi.org/10.1016/j.carbon.2021.06.073>.
155. Wang, X., Liao, M., Zhong, Y., Zheng, J.Y., Tian, W., Zhai, T., Zhi, C., Ma, Y., Yao, J., Bando, Y., and Golberg, D. (2012). ZnO hollow spheres with double-yolk egg structure for high-performance photocatalysts and photodetectors. *Adv. Mater.* 24, 3421–3425. <https://doi.org/10.1002/adma.201201139>.
156. Zhao, B., Ma, C., Liang, L., Guo, W., Fan, B., Guo, X., and Zhang, R. (2017). An impedance match method used to tune the electromagnetic wave absorption properties of hierarchical ZnO assembled by porous nanosheets. *CrystEngComm* 19, 3640–3648. <https://doi.org/10.1039/c7ce00883j>.
157. Cai, M., Shui, A., Wang, X., He, C., Qian, J., and Du, B. (2020). A facile fabrication and high-performance electromagnetic microwave absorption of ZnO nanoparticles. *J. Alloys Compd.* 842, 155638. <https://doi.org/10.1016/j.jallcom.2020.155638>.
158. Wang, L., Li, X., Li, Q., Yu, X., Zhao, Y., Zhang, J., Wang, M., and Che, R. (2019). Oriented polarization tuning broadband absorption from flexible hierarchical ZnO arrays vertically supported on carbon cloth. *Small* 15, 1900900. <https://doi.org/10.1002/sml.201900900>.
159. Qi, Y., Qi, L., Liu, L., Dai, B., Wei, D., Shi, G.M., and Qi, Y. (2019). Facile synthesis of lightweight carbonized hydrochars decorated with dispersed ZnO nanocrystals and enhanced microwave absorption properties. *Carbon* 150, 259–267. <https://doi.org/10.1016/j.carbon.2019.05.026>.
160. Wang, F., Sun, Y., Li, D., Zhong, B., Wu, Z., Zuo, S., Yan, D., Zhuo, R., Feng, J., and Yan, P. (2018). Microwave absorption properties of 3d cross-linked Fe/C porous nanofibers prepared by electrospinning. *Carbon* 134, 264–273. <https://doi.org/10.1016/j.carbon.2018.03.081>.
161. Yu, Z., Zhou, R., Ma, M., Zhu, R., Miao, P., Liu, P., and Kong, J. (2022). ZnO/nitrogen-doped carbon nanocomplex with controlled morphology for highly efficient electromagnetic wave absorption. *J. Mater. Sci. Technol.* 114, 206–214. <https://doi.org/10.1016/j.jmst.2021.11.021>.
162. Li, J., Dai, B., Qi, Y., Dai, Y., and Qi, Y. (2021). Enhanced electromagnetic wave absorption properties of carbon nanofibers embedded with ZnO nanocrystals. *J. Alloys Compd.* 877, 160132. <https://doi.org/10.1016/j.jallcom.2021.160132>.
163. Zhao, S., Yan, L., Tian, X., Liu, Y., Chen, C., Li, Y., Zhang, J., Song, Y., and Qin, Y. (2018). Flexible design of gradient multilayer nanofilms coated on carbon nanofibers by atomic layer deposition for enhanced microwave absorption performance. *Nano Res.* 11, 530–541. <https://doi.org/10.1007/s12274-017-1664-6>.
164. Kumar, M.R.A., Abebe, B., Nagaswarupa, H.P., Murthy, H.C.A., Ravikumar, C.R., and Sabir, F.K. (2020). Enhanced photocatalytic and electrochemical performance of TiO_2 - Fe_2O_3 nanocomposite: Its applications in dye decolorization and as supercapacitors. *Sci. Rep.* 10, 1249. <https://doi.org/10.1038/s41598-020-58110-7>.
165. Chakhtouna, H., Benzeid, H., Zari, N., Quaiss, A.E.K., and Bouhfid, R. (2021). Recent progress on Ag/ TiO_2 photocatalysts: photocatalytic and bactericidal behaviors. *Environ. Sci. Pollut. Res. Int.* 28, 44638–44666. <https://doi.org/10.1007/s11356-021-14996-y>.
166. Chen, Y., Tang, S., Li, L., Liu, X., and Liang, J. (2023). Selective photocatalytic conversion of methane induced by lewis acid-base pair on the surface of $\text{In}_2\text{O}_3/\text{TiO}_2$ heterojunction photocatalyst. *ACS Sustainable Chem. Eng.*

- 11, 3568–3575. <https://doi.org/10.1021/acsschemeng.2c05045>.
167. Seetharaman, A., Kandasamy, M., Manivannan, S., Jothivenkatachalam, K., Subramani, K., Pandikumar, A., Sathish, M., Rao Soma, V., Sivasubramanian, D., and Chakraborty, B. (2021). TiO₂/Carbon allotrope nanohybrids for supercapacitor application with theoretical insights from density functional theory. *Appl. Surf. Sci.* 563, 150259. <https://doi.org/10.1016/j.apsusc.2021.150259>.
168. Liang, H., Liu, J., Zhang, Y., Luo, L., and Wu, H. (2019). Ultra-thin broccoli-like SCFs@TiO₂ one-dimensional electromagnetic wave absorbing material. *Compos. Pt. B-Eng.* 178, 107507. <https://doi.org/10.1016/j.compositesb.2019.107507>.
169. Huo, Y., Zhao, K., Miao, P., Li, F., Lu, Z., Meng, Q., and Tang, Y. (2021). Construction of tunable and high-efficiency microwave absorber enabled by growing flower-like TiO₂ on the surface of SiC/C nanofibers. *J. Solid State Chem.* 304, 122553. <https://doi.org/10.1016/j.jssc.2021.122553>.
170. Ni, S., Sun, X., Wang, X., Zhou, G., Yang, F., Wang, J., and He, D. (2010). Low temperature synthesis of Fe₃O₄ microspheres and its microwave absorption properties. *Mater. Chem. Phys.* 124, 353–358. <https://doi.org/10.1016/j.matchemphys.2010.06.046>.
171. Wang, F., Liu, J., Kong, J., Zhang, Z., Wang, X., Itoh, M., and Machida, K.i. (2011). Template free synthesis and electromagnetic wave absorption properties of monodispersed hollow magnetite nano-spheres. *J. Mater. Chem.* 21, 4314–4320. <https://doi.org/10.1039/c0jm02894k>.
172. Jin, D., and Kim, H. (2015). Stretched exponential change of magnetic weight of magnetite ferrofluid: distribution of energy barrier for agglomeration of nanoparticles. *Bull. Kor. Chem. Soc.* 36, 424–426. <https://doi.org/10.1002/bkcs.10056>.
173. Osouli-Bostanabad, K., Hosseinzade, E., Kianvash, A., and Entezami, A. (2015). Modified nano-magnetite coated carbon fibers magnetic and microwave properties. *Appl. Surf. Sci.* 356, 1086–1095. <https://doi.org/10.1016/j.apsusc.2015.08.115>.
174. Meng, X., Wan, Y., Li, Q., Wang, J., and Luo, H. (2011). The electrochemical preparation and microwave absorption properties of magnetic carbon fibers coated with Fe₃O₄ films. *Appl. Surf. Sci.* 257, 10808–10814. <https://doi.org/10.1016/j.apsusc.2011.07.108>.
175. Dai, B., Qi, Y., Song, M., Zhang, B., Wang, N., and Dai, Y. (2022). Facile synthesis of core-shell structured C/Fe₃O₄ composite fiber electromagnetic wave absorbing materials with multiple loss mechanisms. *J. Chem. Phys.* 157, 114705. <https://doi.org/10.1063/5.0121257>.
176. Zhou, W., Xiao, P., Li, Y., Luo, H., and Zhou, L. (2013). Synthesis and microwave absorbing properties of Pyc/BN composite powders. *J. Inorg. Mater.* 28, 479–484. <https://doi.org/10.3724/sp.J.1077.2013.12349>.
177. Cofer, C.G., and Economy, J. (1995). Oxidative and hydrolytic stability of boron nitride—a new approach to improving the oxidation resistance of carbonaceous structures. *Carbon* 33, 389–395. [https://doi.org/10.1016/0008-6223\(94\)00163-t](https://doi.org/10.1016/0008-6223(94)00163-t).
178. Ye, W., Sun, Q., Long, X., and Cai, Y. (2020). Preparation and properties of CF-Fe₃O₄-BN composite electromagnetic wave-absorbing materials. *RSC Adv.* 10, 11121–11131. <https://doi.org/10.1039/D0RA00785D>.
179. Lu, K., Jiang, R., Gao, X., and Ma, H. (2014). Fe₃O₄/carbon nanotubes/polyaniline ternary composites with synergistic effects for high performance supercapacitors. *RSC Adv.* 4, 52393–52401. <https://doi.org/10.1039/c4ra11088a>.
180. Movassagh-Alanagh, F., Bordbar-Khiabani, A., and Ahangari-Asl, A. (2017). Three-phase PANI@nano-Fe₃O₄@CFs heterostructure: fabrication, characterization and investigation of microwave absorption and EMI shielding of PANI@nano-Fe₃O₄@CFs/epoxy hybrid composite. *Compos. Sci. Technol.* 150, 65–78. <https://doi.org/10.1016/j.compscitech.2017.07.010>.
181. Liu, Y., Cui, T., Wu, T., Li, Y., and Tong, G. (2016). Excellent microwave-absorbing properties of elliptical Fe₃O₄ nanorings made by a rapid microwave-assisted hydrothermal approach. *Nanotechnology* 27, 165707. <https://doi.org/10.1088/0957-4484/27/16/165707>.
182. Tong, G., Liu, Y., Cui, T., Li, Y., Zhao, Y., and Guan, J. (2016). Tunable dielectric properties and excellent microwave absorbing properties of elliptical Fe₃O₄ nanorings. *Appl. Phys. Lett.* 108, 072905. <https://doi.org/10.1063/1.4942095>.
183. Chen, X., Huang, Y., and Zhang, K. (2018). Cobalt nanofibers coated with layered nickel silicate coaxial core-shell composites as excellent anode materials for lithium ion batteries. *J. Colloid Interface Sci.* 513, 788–796. <https://doi.org/10.1016/j.jcis.2017.11.078>.
184. Sun, C., Lee, J.S.H., and Zhang, M. (2008). Magnetic nanoparticles in MR imaging and drug delivery. *Adv. Drug Deliv. Rev.* 60, 1252–1265. <https://doi.org/10.1016/j.addr.2008.03.018>.
185. Qiang, C., Xu, J., Zhang, Z., Tian, L., Xiao, S., Liu, Y., and Xu, P. (2010). Magnetic properties and microwave absorption properties of carbon fibers coated by Fe₃O₄ nanoparticles. *J. Alloys Compd.* 506, 93–97. <https://doi.org/10.1016/j.jallcom.2010.06.193>.
186. Chen, Y.H., Huang, Z.H., Lu, M.M., Cao, W.Q., Yuan, J., Zhang, D.Q., and Cao, M.S. (2015). 3d Fe₃O₄ nanocrystals decorating carbon nanotubes to tune electromagnetic properties and enhance microwave absorption capacity. *J. Mater. Chem. A* 3, 12621–12625. <https://doi.org/10.1039/c5ta02782a>.
187. Li, G., Sheng, L., Yu, L., An, K., Ren, W., and Zhao, X. (2015). Electromagnetic and microwave absorption properties of single-walled carbon nanotubes and CoFe₂O₄ nanocomposites. *Mater. Sci. Eng. B-Adv. Funct. Solid-State Mater.* 193, 153–159. <https://doi.org/10.1016/j.mseb.2014.12.008>.
188. Sutradhar, S., Das, S., Roychowdhury, A., Das, D., and Chakrabarti, P. (2015). Magnetic property, Mössbauer spectroscopy and microwave reflection loss of maghemite nanoparticles (γ-Fe₂O₃) encapsulated in carbon nanotubes. *Mater. Sci. Eng. B* 196, 44–52. <https://doi.org/10.1016/j.mseb.2015.02.008>.
189. Yuan, K., Che, R., Cao, Q., Sun, Z., Yue, Q., and Deng, Y. (2015). Designed fabrication and characterization of three-dimensionally ordered arrays of core-shell magnetic mesoporous carbon microspheres. *ACS Appl. Mater. Interfaces* 7, 5312–5319. <https://doi.org/10.1021/am508683p>.
190. Liu, Y., Zhang, Z., Xiao, S., Qiang, C., Tian, L., and Xu, J. (2011). Preparation and properties of cobalt oxides coated carbon fibers as microwave-absorbing materials. *Appl. Surf. Sci.* 257, 7678–7683. <https://doi.org/10.1016/j.apsusc.2011.04.007>.
191. Wang, K., Chen, Y., Tian, R., Li, H., Zhou, Y., Duan, H., and Liu, H. (2018). Porous Co-C Core-Shell nanocomposites derived from Co-MOF-74 with enhanced electromagnetic wave absorption performance. *ACS Appl. Mater. Interfaces* 10, 11333–11342. <https://doi.org/10.1021/acsami.8b00965>.
192. Xie, P., Li, H., He, B., Dang, F., Lin, J., Fan, R., Hou, C., Liu, H., Zhang, J., Ma, Y., and Guo, Z. (2018). Bio-gel derived nickel/carbon nanocomposites with enhanced microwave absorption. *J. Mater. Chem. C* 6, 8812–8822. <https://doi.org/10.1039/c8tc02127a>.
193. Feng, J., Zong, Y., Sun, Y., Zhang, Y., Yang, X., Long, G., Wang, Y., Li, X., and Zheng, X. (2018). Optimization of porous FeNi₂/N-GN composites with superior microwave absorption performance. *Chem. Eng. J.* 345, 441–451. <https://doi.org/10.1016/j.cej.2018.04.006>.
194. Ye, W., Sun, Q., and Zhang, G. (2019). Effect of heat treatment conditions on properties of carbon-fiber-based electromagnetic-wave-absorbing composites. *Ceram. Int.* 45, 5093–5099. <https://doi.org/10.1016/j.ceramint.2018.11.212>.
195. Ye, W., Li, W., Sun, Q., Yu, J., and Gao, Q. (2018). Microwave absorption properties of lightweight and flexible carbon fiber/magnetic particle composites. *RSC Adv.* 8, 24780–24786. <https://doi.org/10.1039/c8ra05065a>.
196. Abdalla, I., Shen, J., Yu, J., Li, Z., and Ding, B. (2018). Co₃O₄/carbon composite nanofibrous membrane enabled high-efficiency electromagnetic wave absorption. *Sci. Rep.* 8, 12402. <https://doi.org/10.1038/s41598-018-30871-2>.
197. Liu, J., Zhang, L., and Wu, H. (2022). Enhancing the low/middle-frequency electromagnetic wave absorption of metal sulfides through f-regulation engineering. *Adv. Funct. Mater.* 32, 2110496. <https://doi.org/10.1002/adfm.202110496>.
198. Ning, M., Jiang, P., Ding, W., Zhu, X., Tan, G., Man, Q., Li, J., and Li, R.W. (2021). Phase manipulating toward molybdenum disulfide for optimizing electromagnetic wave absorbing in gigahertz. *Adv. Funct. Mater.* 31, 2011229. <https://doi.org/10.1002/adfm.202011229>.
199. Iqbal, A., Sambaly, P., and Koo, C.M. (2020). 2d MXenes for electromagnetic shielding: a review. *Adv. Funct. Mater.* 30, 2000883. <https://doi.org/10.1002/adfm.202000883>.
200. Huang, W., Gao, W., Zuo, S., Zhang, L., Pei, K., Liu, P., Che, R., and Zhang, H. (2022). Hollow MoC/NC sphere for electromagnetic wave attenuation: direct observation of interfacial polarization on nanoscale hetero-interfaces. *J. Mater. Chem. A* 10, 1290–1298. <https://doi.org/10.1039/d1ta09357f>.
201. Huang, W., Wang, S., Yang, X., Zhang, X., Zhang, Y., Pei, K., and Che, R. (2022). Temperature induced transformation of Co@C nanoparticle in 3d hierarchical core-shell nanofiber network for enhanced electromagnetic wave adsorption. *Carbon*

- 195, 44–56. <https://doi.org/10.1016/j.carbon.2022.04.019>.
202. Toneguzzo, P., Viau, G., Acher, O., Fiévet-Vincent, F., and Fiévet, F. (1998). Monodisperse ferromagnetic particles for microwave applications. *Adv. Mater.* 10, 1032–1035. [https://doi.org/10.1002/\(sici\)1521-4095\(199809\)10:13<1032::Aid-adma1032>3.3.Co;2-d](https://doi.org/10.1002/(sici)1521-4095(199809)10:13<1032::Aid-adma1032>3.3.Co;2-d).
203. Viau, G., Ravel, F., Acher, O., Fiévet-Vincent, F., and Fiévet, F. (1995). Preparation and microwave characterization of spherical and monodisperse Co-Ni particles. *J. Magn. Magn. Mater.* 140–144, 377–378. [https://doi.org/10.1016/0304-8853\(94\)00792-6](https://doi.org/10.1016/0304-8853(94)00792-6).
204. Xi, L., Wang, Z., Zuo, Y., and Shi, X. (2011). The enhanced microwave absorption property of CoFe_2O_4 nanoparticles coated with a $\text{Co}_3\text{Fe}_2\text{-Co}$ nanoshell by thermal reduction. *Nanotechnology* 22, 045707. <https://doi.org/10.1088/0957-4484/22/4/045707>.
205. Wang, Y., Sun, Y., Zong, Y., Zhu, T., Zhang, L., Li, X., Xing, H., and Zheng, X. (2020). Carbon nanofibers supported by FeCo nanocrystals as difunctional magnetic/dielectric composites with broadband microwave absorption performance. *J. Alloys Compd.* 824, 153980. <https://doi.org/10.1016/j.jallcom.2020.153980>.
206. Jiang, L., Wang, Z., Li, D., Geng, D., Wang, Y., An, J., He, J., Liu, W., and Zhang, Z. (2015). Excellent microwave-absorption performances by matched magnetic-dielectric properties in double-shelled Co/C/polyaniline nanocomposites. *RSC Adv.* 5, 40384–40392. <https://doi.org/10.1039/c5ra06212h>.
207. Wan, Y., Xiao, J., Li, C., Xiong, G., Guo, R., Li, L., Han, M., and Luo, H. (2016). Microwave absorption properties of FeCo-coated carbon fibers with varying morphologies. *J. Magn. Magn. Mater.* 399, 252–259. <https://doi.org/10.1016/j.jmmm.2015.10.006>.
208. Li, J., Zhang, D., Qi, H., Wang, G., Tang, J., Tian, G., Liu, A., Yue, H., Yu, Y., and Feng, S. (2018). Economical synthesis of composites of FeNi alloy nanoparticles evenly dispersed in two-dimensional reduced graphene oxide as thin and effective electromagnetic wave absorbers. *RSC Adv.* 8, 8393–8401. <https://doi.org/10.1039/c7ra13737k>.
209. Zhang, K., Zhang, Q., Gao, X., Chen, X., Wang, Y., Li, W., and Wu, J. (2018). Effect of absorbers' composition on the microwave absorbing performance of hollow Fe_3O_4 nanoparticles decorated CNTs/graphene/C composites. *J. Alloys Compd.* 748, 706–716. <https://doi.org/10.1016/j.jallcom.2018.03.202>.
210. Shi, B., Liang, H., Xie, Z., Chang, Q., and Wu, H. (2023). Dielectric loss enhancement induced by the microstructure of CoFe_2O_4 foam to realize broadband electromagnetic wave absorption. *Int J Min Met Mater* 30, 1388–1397. <https://doi.org/10.1007/s12613-023-2599-4>.
211. Liu, Z., Xu, G., Zhang, M., Xiong, K., and Meng, P. (2016). Synthesis of CoFe_2O_4 /RGO nanocomposites by click chemistry and electromagnetic wave absorption properties. *J. Mater. Sci. Mater. Electron.* 27, 9278–9285. <https://doi.org/10.1007/s10854-016-4966-7>.
212. Miao, P., Qu, N., Chen, W., Wang, T., Zhao, W., and Kong, J. (2023). A two-dimensional semiconductive Cu-S metal-organic framework for broadband microwave absorption. *Chem. Eng. J.* 454, 140445. <https://doi.org/10.1016/j.cej.2022.140445>.
213. Shan, Z., Cheng, S., Wu, F., Pan, X., Li, W., Dong, W., Xie, A., and Zhang, G. (2022). Electrically conductive two-dimensional metal-organic frameworks for superior electromagnetic wave absorption. *Chem. Eng. J.* 446, 137409. <https://doi.org/10.1016/j.cej.2022.137409>.
214. Wang, L., Zhu, S., and Zhu, J. (2022). Constructing ordered macropores in hollow Co/C polyhedral nanocages shell toward superior microwave absorbing performance. *J. Colloid Interface Sci.* 624, 423–432. <https://doi.org/10.1016/j.jcis.2022.05.158>.
215. Luo, F., Liu, D., Cao, T., Cheng, H., Kuang, J., Deng, Y., and Xie, W. (2021). Study on broadband microwave absorbing performance of gradient porous structure. *Adv. Compos. Hybrid Mater.* 4, 591–601. <https://doi.org/10.1007/s42114-021-00275-4>.
216. Xie, P., Liu, Y., Feng, M., Niu, M., Liu, C., Wu, N., Sui, K., Patil, R.R., Pan, D., Guo, Z., and Fan, R. (2021). Hierarchically porous Co/C nanocomposites for ultralight high-performance microwave absorption. *Adv. Compos. Hybrid Mater.* 4, 173–185. <https://doi.org/10.1007/s42114-020-00202-z>.
217. Guo, Y., Liu, H., Wang, D., El-Bahy, Z.M., Althakafy, J.T., Abo-Dief, H.M., Guo, Z., Xu, B.B., Liu, C., and Shen, C. (2022). Engineering hierarchical heterostructure material based on metal-organic frameworks and cotton fiber for high-efficient microwave absorber. *Nano Res.* 15, 6841–6850. <https://doi.org/10.1007/s12274-022-4533-x>.
218. Chamanehpour, E., Sayadi, M.H., and Hajiani, M. (2022). A hierarchical graphitic carbon nitride supported by metal-organic framework and copper nanocomposite as a novel bifunctional catalyst with long-term stability for enhanced carbon dioxide photoreduction under solar light irradiation. *Adv. Compos. Hybrid Mater.* 5, 2461–2477. <https://doi.org/10.1007/s42114-022-00459-6>.
219. Sun, Z., Wang, M., Fan, J., Feng, R., Zhou, Y., and Zhang, L. (2021). TiO_2 @MIL-101(Cr) nanocomposites as an efficient photocatalyst for degradation of toluene. *Adv. Compos. Hybrid Mater.* 4, 1322–1329. <https://doi.org/10.1007/s42114-021-00337-7>.
220. Cao, W., Ma, C., Tan, S., Ma, M., Wan, P., and Chen, F. (2019). Ultrathin and flexible CNTs/MXene/Cellulose nanofibrils composite paper for electromagnetic interference shielding. *Nano-Micro Lett.* 11, 72. <https://doi.org/10.1007/s40820-019-0304-y>.
221. Zhang, Z., Cai, Z., Zhang, Y., Peng, Y., Wang, Z., Xia, L., Ma, S., Yin, Z., Wang, R., Cao, Y., et al. (2021). The recent progress of MXene-Based microwave absorption materials. *Carbon* 174, 484–499. <https://doi.org/10.1016/j.carbon.2020.12.060>.
222. Wang, X., Yu, M., Zhang, W., Zhang, B., and Dong, L. (2015). Synthesis and microwave absorption properties of graphene/nickel composite materials. *Appl. Phys.* 118, 1053–1058. <https://doi.org/10.1007/s00339-014-8873-6>.
223. Deng, R., Chen, B., Li, H., Zhang, K., Zhang, T., Yu, Y., and Song, L. (2019). MXene/ Co_3O_4 composite material: stable synthesis and its enhanced broadband microwave absorption. *Appl. Surf. Sci.* 488, 921–930. <https://doi.org/10.1016/j.apsusc.2019.05.058>.
224. Zhao, Z., Zhou, X., Kou, K., and Wu, H. (2021). PVP-assisted transformation of ZIF-67 into cobalt layered double hydroxide/carbon fiber as electromagnetic wave absorber. *Carbon* 173, 80–90. <https://doi.org/10.1016/j.carbon.2020.11.009>.
225. Chen, Z., Wu, R., Liu, M., Liu, Y., Xu, S., Ha, Y., Guo, Y., Yu, X., Sun, D., and Fang, F. (2018). Tunable electronic coupling of cobalt sulfide/carbon composites for optimizing oxygen evolution reaction activity. *J. Mater. Chem. A* 6, 10304–10312. <https://doi.org/10.1039/c8ta01244j>.
226. Tao, J., Jiao, Z., Xu, L., Yi, P., Yao, Z., Yang, F., Zhou, C., Chen, P., Zhou, J., and Li, Z. (2021). Construction of MOF-Derived Co/C shell on carbon fiber surface to enhance multi-polarization effect towards efficient broadband electromagnetic wave absorption. *Carbon* 184, 571–582. <https://doi.org/10.1016/j.carbon.2021.08.064>.
227. Ping, J., Wang, Y., Lu, Q., Chen, B., Chen, J., Huang, Y., Ma, Q., Tan, C., Yang, J., Cao, X., et al. (2016). Self-assembly of single-layer CoAl-layered double hydroxide nanosheets on 3d graphene network used as highly efficient electrocatalyst for oxygen evolution reaction. *Adv. Mater.* 28, 7640–7645. <https://doi.org/10.1002/adma.201601019>.
228. Song, F., and Hu, X. (2014). Exfoliation of layered double hydroxides for enhanced oxygen evolution catalysis. *Nat. Commun.* 5, 4477. <https://doi.org/10.1038/ncomms5477>.
229. Zhang, J., Hu, H., Li, Z., and Lou, X.W.D. (2016). Double-shelled nanocages with cobalt hydroxide inner shell and layered double hydroxides outer shell as high-efficiency polysulfide mediator for lithium-sulfur batteries. *Angew. Chem., Int. Ed. Engl.* 55, 3982–3986. <https://doi.org/10.1002/anie.201511632>.
230. Lou, Y., Zhang, Z., Tan, G., Man, Q., Chen, S., Kang, Y., Zhong, J., and Lei, Z. (2022). Metal-organic framework-derived hierarchical porous carbon fiber bundles/ $\text{Y}_2\text{Co}_9\text{Fe}_9$ composite as a thin and broadband electromagnetic wave absorber. *Mater. Res. Bull.* 152, 111838. <https://doi.org/10.1016/j.materresbull.2022.111838>.
231. Chen, J., Zheng, J., Wang, F., Huang, Q., and Ji, G. (2021). Carbon fibers embedded with Fe-III-MOF-5-derived composites for enhanced microwave absorption. *Carbon* 174, 509–517. <https://doi.org/10.1016/j.carbon.2020.12.077>.
232. Singh, S.K., Akhtar, M.J., and Kar, K.K. (2018). Hierarchical carbon nanotube-coated carbon fiber: ultra lightweight, thin, and highly efficient microwave absorber. *ACS Appl. Mater. Interfaces* 10, 24816–24828. <https://doi.org/10.1021/acsami.8b06673>.
233. Wang, H., Meng, F., Huang, F., Jing, C., Li, Y., Wei, W., and Zhou, Z. (2019). Interface modulating CNTs@PANi hybrids by controlled unzipping of the walls of CNTs to achieve tunable high-performance microwave absorption. *ACS Appl. Mater. Interfaces* 11, 12142–12153. <https://doi.org/10.1021/acsami.9b01122>.
234. Zhang, D., Cheng, J., Yang, X., Zhao, B., and Cao, M. (2014). Electromagnetic and microwave absorbing properties of magnetite nanoparticles decorated carbon nanotubes/polyaniline multiphase heterostructures. *J. Mater. Sci.* 49, 7221–

7230. <https://doi.org/10.1007/s10853-014-8429-3>.
235. Xie, S., Jin, G.Q., Meng, S., Wang, Y.W., Qin, Y., and Guo, X.Y. (2012). Microwave absorption properties of in situ grown CNTs/SiC composites. *J. Alloys Compd.* 520, 295–300. <https://doi.org/10.1016/j.jallcom.2012.01.050>.
236. Liu, Y., Zeng, S., Teng, Z., Feng, W., Zhang, H., and Peng, S. (2020). Carbon nanofibers propped hierarchical porous SiOC ceramics toward efficient microwave absorption. *Nanoscale Res. Lett.* 15, 28. <https://doi.org/10.1186/s11671-020-3253-y>.
237. Zhang, K., Xie, A., Wu, F., Jiang, W., Wang, M., and Dong, W. (2016). Carboxyl multiwalled carbon nanotubes modified polypyrrole (PPy) aerogel for enhanced electromagnetic absorption. *Mater. Res. Express* 3, 055008. <https://doi.org/10.1088/2053-1591/3/5/055008>.
238. Jiao, Z., and Qiu, J. (2018). Microwave absorption performance of iron oxide/multiwalled carbon nanotubes nanohybrids prepared by electrostatic attraction. *J. Mater. Sci.* 53, 3640–3646. <https://doi.org/10.1007/s10853-017-1770-6>.
239. Han, M., Yin, X., Hou, Z., Song, C., Li, X., Zhang, L., and Cheng, L. (2017). Flexible and thermostable graphene/SiC nanowire foam composites with tunable electromagnetic wave absorption properties. *ACS Appl. Mater. Interfaces* 9, 11803–11810. <https://doi.org/10.1021/acsami.7b00951>.
240. Han, M., Yin, X., Duan, W., Ren, S., Zhang, L., and Cheng, L. (2016). Hierarchical graphene/SiC nanowire networks in polymer-derived ceramics with enhanced electromagnetic wave absorbing capability. *J. Eur. Ceram. Soc.* 36, 2695–2703. <https://doi.org/10.1016/j.jeurceramsoc.2016.04.003>.
241. Ding, X., Huang, Y., Li, S., and Wang, J. (2016). Preparation and electromagnetic wave absorption properties of FeNi₃ nanoalloys generated on graphene-polyaniline nanosheets. *RSC Adv.* 6, 31440–31447. <https://doi.org/10.1039/c5ra27905d>.
242. Huo, Y., Zhao, K., Xu, Z., and Tang, Y. (2020). Electrospinning synthesis of SiC/Carbon hybrid nanofibers with satisfactory electromagnetic wave absorption performance. *J. Alloys Compd.* 815, 152458. <https://doi.org/10.1016/j.jallcom.2019.152458>.
243. Wang, P., Kankala, R.K., Fan, J., Long, R., Liu, Y., and Wang, S. (2018). Electrospinning of graphite/SiC hybrid nanowires with tunable dielectric and microwave absorption characteristics. *J. Mater. Sci. Mater. Med.* 29, 68–80. <https://doi.org/10.1016/j.compositesa.2017.10.012>.
244. Wang, P., Cheng, L., Zhang, Y., and Zhang, L. (2017). Flexible SiC/Si₃N₄ composite nanofibers with in situ embedded graphite for highly efficient electromagnetic wave absorption. *ACS Appl. Mater. Interfaces* 9, 28844–28858. <https://doi.org/10.1021/acsami.7b05382>.
245. Li, X., Yin, X., Xu, H., Han, M., Li, M., Liang, S., Cheng, L., and Zhang, L. (2018). Ultralight MXene-coated, interconnected sicwns three-dimensional lamellar foams for efficient microwave absorption in the x-band. *ACS Appl. Mater. Interfaces* 10, 34524–34533. <https://doi.org/10.1021/acsami.8b13658>.
246. Li, X., Yin, X., Han, M., Song, C., Xu, H., Hou, Z., Zhang, L., and Cheng, L. (2017). Ti₃C₂ MXenes modified with in situ grown carbon nanotubes for enhanced electromagnetic wave absorption properties. *J. Mater. Chem. C* 5, 4068–4074. <https://doi.org/10.1039/c6tc05226f>.
247. Wei, H., Dong, J., Fang, X., Zheng, W., Sun, Y., Qian, Y., Jiang, Z., and Huang, Y. (2019). Ti₃C₂T_x MXene/polyaniline (PANI) sandwich intercalation structure composites constructed for microwave absorption. *Compos. Sci. Technol.* 169, 52–59. <https://doi.org/10.1016/j.compscitech.2018.10.016>.
248. Han, X., Huang, Y., Ding, L., Song, Y., Li, T., and Liu, P. (2021). Ti₃C₂T_x MXene nanosheet/metal-organic framework composites for microwave absorption. *ACS Appl. Nano Mater.* 4, 691–701. <https://doi.org/10.1021/acsnm.0c02983>.
249. Wu, F., Liu, Z., Wang, J., Shah, T., Liu, P., Zhang, Q., and Zhang, B. (2021). Template-free self-assembly of MXene and CoNi-bimetal MOF into intertwined one-dimensional heterostructure and its microwave absorbing properties. *Chem. Eng. J.* 422, 130591. <https://doi.org/10.1016/j.cej.2021.130591>.
250. Wang, J., Liu, L., Jiao, S., Ma, K., Lv, J., and Yang, J. (2020). Hierarchical carbon Fiber@MXene@MoS₂core-sheath synergistic microstructure for tunable and efficient microwave absorption. *Adv. Funct. Mater.* 30, 2002595. <https://doi.org/10.1002/adfm.202002595>.
251. Hua, A., Li, Y., Pan, D., Luan, J., Wang, Y., He, J., Tang, S., Geng, D., Ma, S., Liu, W., and Zhang, Z. (2020). Enhanced wideband microwave absorption of hollow carbon nanowires derived from a template of Al₄C₃@C nanowires. *Carbon* 161, 252–258. <https://doi.org/10.1016/j.carbon.2020.01.081>.